

UCSF

UC San Francisco Electronic Theses and Dissertations

Title

Function of Macromolecular Serine Protease Inhibitors in the Human Blood Fluke
Schistosoma mansoni

Permalink

<https://escholarship.org/uc/item/4zc5x2dg>

Author

Lopez Quezada, Landys Angela

Publication Date

2011

Peer reviewed|Thesis/dissertation

FUNCTION OF MACROMOLECULAR SERINE PROTEASE
INHIBITORS IN THE HUMAN BLOOD FLUKE
SCHISTOSOMA MANSONI

by

Landys A. Lopez Quezada

DISSERTATION

Submitted in partial satisfaction of the requirements for the degree of

DOCTOR OF PHILOSOPHY

in

Biomedical Sciences

in the

GRADUATE DIVISION

of the

UNIVERSITY OF CALIFORNIA, SAN FRANCISCO

**Copyright 2011
by
Landys A. Lopez Quezada**

Dedication

“...¡*Libertad!* Que aún se yergue serena
La victoria en su carro triunfal,
Y el clarín de la guerra aún resuena
Pregonando su gloria inmortal.
¡*Libertad!* Que los ecos se agiten
Mientras llenos de noble ansiedad
Nuestros campos de gloria repiten
¡*Libertad!* ¡*Libertad!* ¡*Libertad!*”

-Himno Nacional Dominicano escrito por Emilio Prud'Homme

Para mi familia. Con todo mi amor. Landy.

Acknowledgments

This work was made possible by the generosity of the UCSF National Institute of General Medical Science training program, the UCSF Microbial Pathogenesis Host Defense training program, and the Sandler Foundation.


My eternal gratitude goes out to my advisor Dr. James H. McKerrow and the McKerrow Lab. I would like to acknowledge the scientific and spiritual guidance of Dr. Mohammed Sajid and Dr. Arthur Baca, without whom I would not have seen this through with my sanity. To K.C. Lim, Zachary Mackey, Juan Engel, Christopher Franklyn, Jan Dvorak, and Anjan Debnath, my sincere thank you for all your assistance and advice.

Certain text and figures from the introduction and chapter 1 are reprinted as they appear in the *Anais da Academia Brasileira de Ciências* 83(2): 663-72, 2011. Permission granted for reproduction.

**FUNCTION OF MACROMOLECULAR SERINE PROTEASE
INHIBITORS IN THE HUMAN BLOOD FLUKE
*SCHISTOSOMA MANSONI***

by
Landys A. Lopez Quezada

under the supervision of


James H. McKerrow, MD/PhD

Abstract

Serine protease inhibitors (serpins) are a superfamily of structurally conserved proteins that are key regulators of proteolysis in plants, animals, and certain viruses. The *S. mansoni* genome contains eight full-length serpins. Semi-quantitative PCRs performed on *S. mansoni* cDNA samples verified the transcription of these eight putative serpins. All identified serpin sequences had homology to other members of the serpin family and contained all the structural components needed for functionality. Some schistosome serpins are predicted to be non-inhibitory while others showed clear tryptic or chymotryptic protease specificity. Two of these serpins, SmSrpQ and SmSerp_C, were of particular interest owing to their secretion by the infective larva of *S. mansoni*. Little published data exists examining the function of SmSrpQ, SmSerp_C, or any other of the schistosome serpin.

SmSrpQ and SmSerp_C are only expressed during larval development and, in the case of SmSrpQ, in the early stages of mammalian infection. ³⁵S-SmSrpQ was able to form an SDS-stable complex with a component of the larval lysate but no complex was detected

with several mammalian host proteases. Formation of a complex was sensitive to the protease active site inhibitors PMSF, Z-AAPF-CMK, and Z-AAPL-CMK. Similar experiments were carried out with ^{35}S -SmSerp_C, which formed a complex with trypsin, human plasma kallikrein, and a molluscan protease, most likely the tryptases found in the intermediate host of *S. mansoni*, *Biomphalaria glabrata*.

Invasion by *S. mansoni* larvae is facilitated by cercarial elastase (SmCE), a serine protease. The band detected between ^{35}S -SmSrpQ and a protease in cercarial lysates was also detected in western blot analysis of parasite lysates. These blots showed that when active SmCE was present, a complex of comparable size to SmCE bound to SmSrpQ was observed. This data together with the results from immunolocalization of these proteins in the parasite and in simulated infections suggest that SmCE degradation of skin tissue is carefully regulated by SmSrpQ during larval invasion.

SmSrpQ inhibition of SmCE and SmSerp_C inhibition of kallikrein and a snail protease confirm the inhibitory nature of these serpins and suggests a role in the pathogenesis/biology of the parasite.

Table of Contents

Introduction: Schistosomiasis and Serine Protease Inhibitors

| | |
|--|----|
| I. Schistosomiasis | |
| <i>Disease and global distribution</i> | 2 |
| <i>Life cycle</i> | 3 |
| <i>Architecture of human skin</i> | 5 |
| <i>Cutaneous immunology</i> | 6 |
| <i>Cercarial invasion</i> | 8 |
| II. Serine protease inhibitors (serpins) | |
| <i>Structure/ function</i> | 9 |
| <i>The biological role of serpins</i> | 10 |
| <i>Serpins in human disease and microbial pathogenesis</i> | 12 |
| Figures for introduction | 14 |

Chapter 1: Schistosome Serine Protease Inhibitors

| | |
|---|----|
| Abstract | 23 |
| Introduction | 23 |
| Experimental procedures | |
| <i>Genome search and phylogenetic analysis</i> | 26 |
| <i>BLAST and target protease prediction</i> | 26 |
| <i>RNA isolation and semi-quantitative PCR</i> | 27 |
| <i>Cloning and sequencing</i> | 28 |
| Results and discussion | |
| <i>Schistosome serpins and developmental stage distribution</i> | 28 |
| <i>Phylogeny of schistosome serpins</i> | 30 |
| <i>Validation of theoretical sequences of Sm1a, Sm1b, Sm1c</i> | 32 |
| <i>Putative protease targets of schistosome serpins</i> | 33 |
| Concluding remarks | 35 |
| Figures and tables for Chapter 1 | 36 |

Chapter 2: SmSrpQ: An Endogenous Inhibitor of Cercarial Elastase

| | |
|--------------------------------|----|
| Abstract | 46 |
| Introduction | 46 |
| Experimental procedures | |
| <i>Parasite material</i> | 47 |
| <i>Northern blots and qPCR</i> | 48 |

| | |
|---|-----|
| <i>Recombinant protein expression and antibody production</i> | 49 |
| <i>Western blots</i> | 50 |
| <i>Collection of material from newly transformed schistosomula</i> | 50 |
| <i>Confocal imaging</i> | 51 |
| <i>Ex vivo invasion and immunohistochemistry</i> | 51 |
| <i>³⁵S-labeled in vitro cell free SmSrpQ expression and inhibitor assays</i> | 52 |
| <i>Transverse urea gels (TUGs)</i> | 52 |
| Results | |
| <i>qPCR and northern blot analysis of SmSrpQ transcript levels</i> | 53 |
| <i>Functional expression of SmSrpQ</i> | 53 |
| <i>Western blots of SmSrpQ and SmCE during early life stages</i> | 55 |
| <i>Localization of SmSrpQ within the parasite</i> | 56 |
| <i>SmSrpQ and SmCE release and ex vivo skin co-localization</i> | 57 |
| Discussion | 57 |
| Figures for Chapter 2 | 62 |
| | |
| <u>Chapter 3: Expression and Purification of rSmSrpQ and rSmSerp_C</u> | |
| Abstract | 72 |
| Introduction | 72 |
| Experimental procedures | |
| <i>Construction of S. cerevisiae expression plasmids</i> | 73 |
| <i>Yeast transformations</i> | 75 |
| <i>Expression of SmSrpQ</i> | 75 |
| <i>Purification of SmSrpQ</i> | 76 |
| <i>Cloning and expression of SmSerp_C</i> | 76 |
| <i>Ion exchange and nickel purification of SmSerp_C</i> | 77 |
| <i>In vitro translation of ³⁵S-SmSerp_C and complex formation assays</i> | 78 |
| Results | |
| <i>Expression and purification of rSmSrpQ</i> | 78 |
| <i>Expression and purification of rSmSerp_C</i> | 80 |
| <i>SmSerp_C complex formation assays</i> | 80 |
| Discussion | 81 |
| Figures for Chapter 3 | 85 |
| | |
| <u>Chapter 4: Concluding Remarks</u> | |
| | |
| <u>Abbreviations and References</u> | |
| Library Agreement | 107 |

List of Figures

Introduction: Schistosomiasis and Serine Protease Inhibitors

| | |
|---|----|
| Figure I. 1: <i>Schistosome life cycle</i> | 14 |
| Figure I. 2: <i>Skin architecture and immune effector cells</i> | 15 |
| Figure I. 3: <i>Schistosoma mansoni cercarial secretory glands</i> | 16 |
| Figure I. 4: <i>Invasion of human skin by S. mansoni</i> | 17 |
| Figure I. 5: <i>Structure of α1-antitrypsin</i> | 18 |
| Figure I. 6: <i>Mechanism of serpin inhibition</i> | 19 |
| Figure I. 7: <i>Serine protease active site with catalytic triad & substrate binding pocket</i> | 20 |
| Figure I. 8: <i>Complex formation between granzyme B and CrmA</i> | 21 |

Chapter 1: Schistosome serine protease inhibitors

| | |
|--|----|
| Figure 1. 1: <i>Primary amino acid sequence alignment</i> | 36 |
| Figure 1. 2: <i>Semi-quantitative PCRs of S. mansoni serpins</i> | 37 |
| Figure 1. 3: <i>Phylogenetic analysis of schistosome serpins</i> | 38 |
| Figure 1. 4: <i>Alignment of the reactive center loops of schistosome serpins</i> | 39 |
| Figure 1. 5: <i>Alignment of the theoretical translation of Sm1a, Sm1b, and Sm1c</i> | 40 |

Chapter 2: SmSrpQ: An Endogenous Inhibitor of Cercarial Elastase

| | |
|---|----|
| Figure 2. 1. <i>³⁵S-SmSrpQ translation and conformation</i> | 62 |
| Figure 2. 2. <i>SmSrpQ mRNA levels during S. mansoni developmental life cycle</i> | 63 |
| Figure 2. 3. <i>³⁵S-SmSrpQ complex</i> | 64 |
| Figure 2. 4. <i>Effect of active site inhibitor PMSF on complex formation</i> | 65 |
| Figure 2. 5. <i>Effect of chloromethyl ketone inhibitors on complex formation</i> | 66 |
| Figure 2. 6. <i>Life cycle western blot analysis</i> | 67 |
| Figure 2. 7. <i>Confocal images localizing SmSrpQ and SmCE</i> | 68 |
| Figure 2. 8. <i>Secretion of SmSrpQ and SmCE by schistosomula</i> | 69 |
| Figure 2. 9. <i>Immunolocalization of SmSrpQ and SmCE during a mock infection</i> | 70 |

Chapter 3: Expression and Purification of rSmSrpQ and rSmSerp_C

| | |
|--|----|
| Figure 3. 1: <i>Expression vector constructs</i> | 85 |
| Figure 3. 2: <i>Codon usage of SmSrpQ2</i> | 86 |
| Figure 3. 3: <i>Comparison of SmSrpQ and SmSerp_C</i> | 87 |
| Figure 3. 4: <i>Comparison of non-fermentable carbon sources</i> | 88 |
| Figure 3. 5: <i>rSmSrpQ purification</i> | 89 |
| Figure 3. 6: <i>Ubiquitin-SmSrpQ expression using ADH2p and GAPDHp</i> | 90 |
| Figure 3. 7: <i>rSmSrpQ2 purification</i> | 91 |
| Figure 3. 8: <i>rSmSerp_C colony screening</i> | 92 |
| Figure 3. 9: <i>rSmSerp_C purification</i> | 93 |
| Figure 3. 10: <i>³⁵S-SmSerp_C complex formation assay</i> | 94 |

List of Tables

Chapter 1: Schistosome serine protease inhibitors

| | |
|---|----|
| Table 1. 1: <i>Primers used for semi-quantitative PCR</i> | 41 |
| Table 1. 2: <i>Serine protease inhibitor of Schistosoma mansoni, S. japonicum, and S. haematobium</i> | 42 |
| Table 1. 3: <i>Number of clones of Sm1a, Sm1b, and Sm1c</i> | 43 |
| Table 1.4: <i>Comparison the amino acid variability of Sm1a, Sm1b, and Sm1c</i> | 44 |

Introduction

Schistosomiasis & Serine Protease Inhibitors

I. Schistosomiasis

Disease and global distribution. The blood flukes *Schistosoma mansoni*, *S. japonicum*, and *S. haematobium* are the three main etiological agents of human schistosomiasis, also called bilharziasis. These parasitic worms infect approximately 235 million individuals, and 732 million are at risk of infection worldwide due to exposure to infested waters [1]. Given the high degree of misdiagnosis, it is likely that the true number of infections is closer to 391 to 587 million [2]. The parasites are endemic to 74 developing countries and are found throughout the tropical world with 80% of cases in sub-Saharan Africa [1, 3]. Of the three species, *S. mansoni* is the most widely distributed, affecting people in Africa, the Middle East, South America, and the Caribbean. *S. japonicum* is confined to China, the Philippines, and Indonesia and *S. haematobium* is found in Africa and the Middle East.

Largely a chronic disease of the poor who have inadequate access to a safe water supply, schistosomiasis can affect children's physical, sexual, and mental development. It can impair people's ability to work due to chronic fatigue [4] leading to poor school and job performance, exercise intolerance, and an increase use of health-care facilities. These health problems may arise from the anemia caused by hemoglobin feeding juvenile and adult worms [4]. The high morbidity account for the 1.7 million DALYs (disability adjusted life years) attributed to this disease [5]. DALYs are a measure of disease burden on a population; they are a time based measure that counts the number of years of life lost due to premature death or life with less than full health caused by disease. Severe schistosomiasis can lead to liver fibrosis, hepatosplenomegaly, and portal hypertension.

Urinary schistosomiasis can produce hematuria, cystitis, bladder calcification, kidney damage, and can increase the risk for squamous cell carcinoma of the bladder. The severe consequences of long term infection has been attributed to the formation of granulomas around schistosome eggs trapped in the liver, spleen, lung, bladder, and sometimes the central nervous system [6].

While research to expand treatment options is ongoing [7], praziquantel is, at present, the sole chemotherapeutic treatment recommended for schistosomiasis. The mechanism of drug killing remains unknown despite over 20 years of use as a chemotherapeutic agent. Praziquantel is only effective against adult worms and young larva but is not active against juvenile worms. No anti-schistosome vaccine currently exists but efforts are underway to develop such a vaccine [8]. Currently, interest is focused on the tetraspanin tegumental proteins to which resistant individuals from endemic areas have been shown to produce protective IgG1 and IgG3 [9-11].

Life cycle. Mammalian schistosomes are digenetic flatworms that spend part of their lifecycle in a freshwater mollusk host and part in a vertebrate host (Figure I. 1). While *S. mansoni* and *S. haematobium* largely infect only humans, *S. japonicum* has a wide range of vertebrate hosts such as domestic animals, field rodents, dogs, and cats. These serve as important reservoirs of disease [12]. There are schistosome species that do not infect humans, such as *Schistosomatium douthitti* that infect a wide range of rodents and *Trichobilharzia* species that infect several types of birds. These species can cause

cercarial dermatitis or “swimmer’s itch” in humans but are unable to mature into adulthood and egg production in humans [13-15].

The life cycle of schistosomes begins with the infected snails releasing free-swimming cercariae (larvae) into fresh water where humans fish, bathe, wash clothing, and play. When the cercariae come in contact with the skin of the vertebrate host, they are stimulated by the lipids on the surface of skin to invade and release the content of their secretion glands [16]. Once in the skin, cercariae transform into schistosomula. They degrade the host extracellular matrix by secreting proteolytic enzymes to facilitate entry into the host dermal blood vessels [17]. The schistosomula reach the lungs and later migrate to the portal venous system where they mature into adult worms. While male maturation is independent of the female adult, the female does not complete its physical and reproductive growth until it has situated itself inside the gynaecophoric canal of the male worm [18].

Mating pairs migrate either to the mesenteric venules (*S. mansoni* and *S. japonicum*) or the venous plexus of the bladder (*S. haematobium*) where the female worms begin egg production. In a mouse model of infection, a mature *S. mansoni* pair can produce on average a total of 340 eggs/day and a mature *S. japonicum* pair can produce approximately 1000 eggs/day [19]. The eggs enter the lumen of the intestine or bladder and are then deposited into fresh water where they hatch into another larval stage: the miracidium. Miracidia find and penetrate the snail intermediate host. *Biomphalaria* species are the molluscan hosts of *S. mansoni*, several species from the *Oncomelania*

genera act as the *S. japonicum* intermediate host, and *S. haematobium* develops in *Bulinus* species. After entry into the snail foot, miracidia mature into mother sporocysts. These mother sporocysts migrate to the hepatopancreas of the mollusk and after several rounds of asexual reproduction transform into daughter sporocysts. The daughter sporocysts then give rise to the free-swimming cercariae (Figure I. 1).

Architecture of the skin. The skin is often referred to as the first line of defense against infection. It covers an average area of 1.7 m² and accounts for approximately 15% of the total weight of a human [20]. A schistosome cercariae/ schistosomula must traverse multiple layers of skin cells and extracellular matrix (ECM), evade the sentinel innate and adaptive immune cells that inhabit the skin, and then penetrate the endothelial blood vessel wall before reaching its desired destination: the host blood stream.

Skin sits atop a subcutaneous layer of adipose tissue and is divided into two principal parts: the epidermis and the dermis (Figure I. 2). The epidermis, due to its lack of blood vessels, depends wholly on the underlying dermis for nutrients. Composed of 95% keratinocytes [20], the epidermis is divided into four distinct layers each varying in the level and type of keratin content. The lowest layer, the stratum basale, is the only layer capable of cell division thus it is responsible for the continual renewal and wound healing of the epidermis. These basal keratinocytes contain the lowest level of keratin. Hemidesmosomes connect the basal layer to the underlying basement membrane. The basement membrane spans the dermo-epidermal interface. It consists of a layer of laminin and a layer of collagen type IV.

As epidermal cells differentiate and mature, they migrate up the epidermis and form the next layer of cells called the stratum spinosum. Cells of this layer lose the columnar structure and increase their keratin content. They even change the type of keratin they produce. These cells maintain close cell-cell contact via desmosomes. The next layer, the stratum granulosum, derives its name from the dense granules of keratin fibrils and adhesion proteins that cement the cells of the stratum corneum. Tight junctions maintain the stratum granulosum's integrity and the fluid impermeability of the epidermis [21]. The stratum corneum is the terminal maturation step of epidermal keratinocytes. It is composed of anucleated dead cells called corneocytes. Filled with keratin and held firm by a lipid rich cement, the stratum corneum can be 15-25 corneocyte layers thick [20].

The dermis, contains a more heterogeneous cellular and ECM composition (Figure I. 2). The interstitial matrix of the dermis, produced by resident fibroblasts, is composed of mostly collagen fibers (type I and III), which provide mechanical support, elastin fibers that give elastic recoil to the dermis, and “ground” substances such as glycoaminoglycans that aid in water absorption and protect against compressive forces. It is in this layer where the cutaneous lymphatic and blood vessels reside. Most of the cells involved in skin immunobiology are located in the dermis.

Cutaneous immunology. The immunobiology of the skin was first described in detail in 1983 by Streilein [22] in which the skin was recognized as possessing its own unique immunological system. The keratinocytes of the epidermis contain receptors, for

example Toll-like receptors, that recognize conserved microbial components often called pathogen-associated-molecular patterns (PAMPs). Activation of these receptors leads to a predominantly pro-inflammatory response, which can include the production of type I interferon, tumor necrosis factor- α (TNF- α), as well as neutrophil chemokine, IL-8 [23]. Keratinocytes can themselves release any number of cytokines, chemokines, and antimicrobial peptides thus they can actively recruit effector cells and modulate an immune response [24]. Additionally, keratinocytes can detect irritants, allergens, and toxins. Activation of these receptors leads to an inflammasome mediated pro-inflammatory response including allergic contact dermatitis [25]. The epidermal layer also contains specialized dendritic cells (DCs) called Langerhans cells and several populations of T cells [26, 27]. Langerhans cells have long been thought to be involved in antigen presentation and priming naïve T-cells [28], however, recent data suggests cross-presentation is actually carried out by a subset of DCs from the dermis [29]. Activated dermal DCs play an active role during inflammation whether allergic [30] or pathogenic [31] in origin by quickly migrating to the lymph nodes where they can prime and activate T-cells [32].

The dermis, in addition to several populations of DCs [24], is also home to a diverse population of immune cells including macrophages and mast cells. In some circumstances neutrophils, CD8⁺ and CD4⁺ T-cells, and $\gamma\delta$ T-cells may also be found. Dermal sentinels of the innate immune system such as macrophages, mast cells, and immature dendritic cells are particularly important in response to the initial infection of the skin. Mast cells have an extensive repertoire of proteases. Human mast cell granules

contain up to four tryptases (α I, β I, δ , and γ I), chymase, and cathepsin G. Similar to neutrophil proteases, these mast cell proteases appear to play multiple roles in inflammation [33]. Neutrophil granular proteases (cathepsin G, neutrophil elastase, proteinase-3) are released into the extracellular environment following activation during an inflammatory response. Recent studies have revealed that these proteases are involved not only in bacterial killing but also in proteolytic activation of chemokines and cytokines, activation of receptors PAR-2 (proteinase-3) and TLR4 (neutrophil elastase), and cleavage of ICAM1 and VCAM1 [34].

Cercarial invasion. In order for schistosome larvae to reach the host circulatory system and establish a long-term infection, they must breach the normally impermeable barriers of the epithelium and the dermis as well as circumvent the skin immune sentinels. To accomplish this, each cercaria and schistosomula possess secretory cells (Figure I. 3) whose contents are released into the skin. The secreted material contains proteases involved in ECM and cell junction degradation and proteins thought to aid in immune evasion [35-37]. The secretory cells or “glands” consist of the pre-acetabular glands (two sets of cells located anterior to the acetabulum sucker), the post-acetabular glands (three sets of cells located posterior to the acetabulum sucker), and the head gland. While the head gland is located close to the oral aperture of the larva, the post and pre-acetabular glands have elongated processes, called ducts, that extend from the body of the cell to the aperture (Figure I. 3).

Studies on the migration of *S. mansoni* through skin tissue have identified several factors important for successful infection. The larvae release a serine protease, cercarial elastase, that has been shown to degrade dermal extracellular matrix [38] and has been implicated in the degradation of desmosomes. Invading larva produce a zone of tissue degradation as they travel through the layers of the skin (Figure I. 4). The larvae also release eicosanoids along with other factors upon entry into the host that are thought to be important in subverting the host immune system. Of these, prostaglandin (PG) E₂, seems to play a role in inhibiting TNF-dependent migration of Langerhans cells out of the epidermis [39] and PGE₂ also promotes the production of IL-10 by epithelial cells [40]. Mice deficient in IL-10 show a significant delay in larval penetration due to enhancement of dermal immune response [40]. When examining the skin ultrastructure, *S. mansoni* infection induces a thickening of the epidermis and dermis as well as an influx of neutrophils and mast cells [41]. It has been shown that cercarial secretion products can induce mast cell degranulation *in vitro* [42].

II. Serine protease *inhibitors* (serpins)

Structure/function. Serpins are a structurally conserved family of macromolecular protein inhibitors found in virtually all biological systems (reviewed in [43], [44], [45]). The mechanism employed by serpins to inhibit proteases is also highly conserved. Serpins are suicide hemi-substrate inhibitors that are approximately 40-50 kDa in size. The conserved metastable tertiary structure of a serpin features 7 to 9 α -helices and 3 β -sheets (Figure I. 5). Key to the inhibitory activity of the serpin is the reactive center loop (RCL) [46]. In the native, active form, it lies outside the main body of the serpin between

β -sheets A and C and serves as the protease ‘bait’ but in its inactive or “latent” state the RCL is partially inserted into the body of the serpin [47, 48] thus unavailable for cleavage. The RCL is composed of approximately 20 amino acid residues (P17-P4) with the P1 side chain fitting into the S1 specificity pocket of the target protease (Figure I. 7). Following proteolytic cleavage and formation of the acyl-enzyme intermediate, the RCL inserts into the body of the serpin, completing the antiparallel organization of β -sheet A (Figure I. 6). The crystal structure of the trypsin- α 1-antitrypsin complex reveals that once the complex forms, translocation distorts the structure of the protease by 37%, while the serpin itself remains largely unchanged [49]. The crystal structure confirms that translocation of the protease dislocates the active site serine, takes it out of productive alignment with the rest of the catalytic triad, and results in the destruction of the oxyanion hole. This complex between a protease and serpin can be visualized in several manners. In one method the serpin is radiolabeled and incubated with the cognate protease. The complex can be detected on SDS-PAGE as a shift in molecular weight (Figure I. 8).

The biological role of serpins. Serpins are found in animals, viruses, plants, archea, and bacteria. They can fulfill both inhibitory and non-inhibitory roles. Based on their genomes, *C. elegans*, *D. melanogaster*, and *A. thaliana* contain 9, 32, and 13 serpins respectively [45]. Thirty-seven serpins have been isolated in humans [45]. While some mammalian serpins are well characterized, the function of many of these serpins remains a mystery. A recent study on *C. elegans* serpin SRP-6, examined the role this intracellular serpin plays in survival of the worm during osmotic shock. SRP-6 is proven to inhibit both cytosolic calpain and lysosomal peptidase and, thus, allow the worm to

maintain cellular integrity during stressful stimulation [50]. Serpins also play an important role in the immune response of insects. In *D. melanogaster* Spn43Ac regulates the immune response to fungal infection by inhibiting the cleavage of the Toll ligand spaeztle [51]. There is evidence that SRPN6 of the malaria mosquito vector *Anopheles gambiae* is important for parasite clearance and/or lysis [52].

The mammalian serpins are involved in the regulation of proteases in blood coagulation, fibrinolysis, apoptosis, development, and inflammation as well as non-inhibitory functions. Maspin (mammary serine protease inhibitor), for example, is normally found in mammary epithelial cells where it is involved in mammary gland development [53]. Its expression is markedly reduced in breast cell carcinomas [54] and while the exact mechanism by which maspin acts as tumor suppressor is still under investigation, it has been shown to inhibit the motility of carcinoma cells in cultures [55].

Antithrombin is a classic example of a mammalian inhibitory serpin. This 58 kDa serpin is considered the most important inhibitor of blood coagulation [56]. It can reach plasma levels of 150 µg/ml [56]. In combination with its cofactor heparin it is the most effective inhibitor of Factor Xa, Factor IXa, and thrombin. Mice with a gene deletion of antithrombin die at 16.5 gestational days of substantial liver and myocardial hemorrhages [57]. Humans with inherited antithrombin deficiencies suffer from a predisposition to venous thrombosis [58].

Serpins in human disease and microbial pathogenesis. Serpins have been implicated in different human diseases. Many of these diseases arise from mutations within the body of the serpin that lead to misfolding and subsequent polymerization. Serpinopathies, as they are called, include early onset dementia, non-smoking related emphysema, and liver cirrhosis. Crystallographic studies have indicated that these polymers could arise from domain swapping between serpins [59]. Other diseases arise from deficiencies in the production of certain serpins. For example, deficiency in C1-inhibitor leads to increased vascular permeability resulting in angioedema [60].

In terms of infectious diseases, several poxvirus serpins have received attention due to their ability to inhibit apoptosis and modulate the immune response. One of these viral serpins, CrmA (cytokine response modifier A), has been shown to effectively inhibit both interleukin 1 β converting enzyme [61] and granzyme B [62]. These enzymes lie upstream of the pro-apoptotic response to viral infection. Research on these cowpox viral serpins can provide valuable insight into the pathogenesis of human poxviral infection.

Data on the function of serpins in parasitic diseases, on the other hand, has been limited. Two serpins have been cloned from the lymphatic filariasis agent *Brugia malayi*: BmSpn-1 [63] for which there is little functional data, and BmSpn-2 [64]. BmSpn-2 was originally thought to aid in microfilarial immune evasion by inhibiting neutrophil elastase and cathepsin G [64], but a follow-up study showed that it is unable to form a stable complex with either of these proteases [65]. However, BmSpn-2 is released into the blood of the host by microfilariae, suggesting that it plays some role in host-parasite

interactions (2003). Investigation of the *Onchocerca volvulus* serpins Ov-spi-1 and Ov-spi-2 by RNAi showed that knockdown of these serpins led to impaired L3 molting and viability. However, the endogenous targets have not been identified [66].

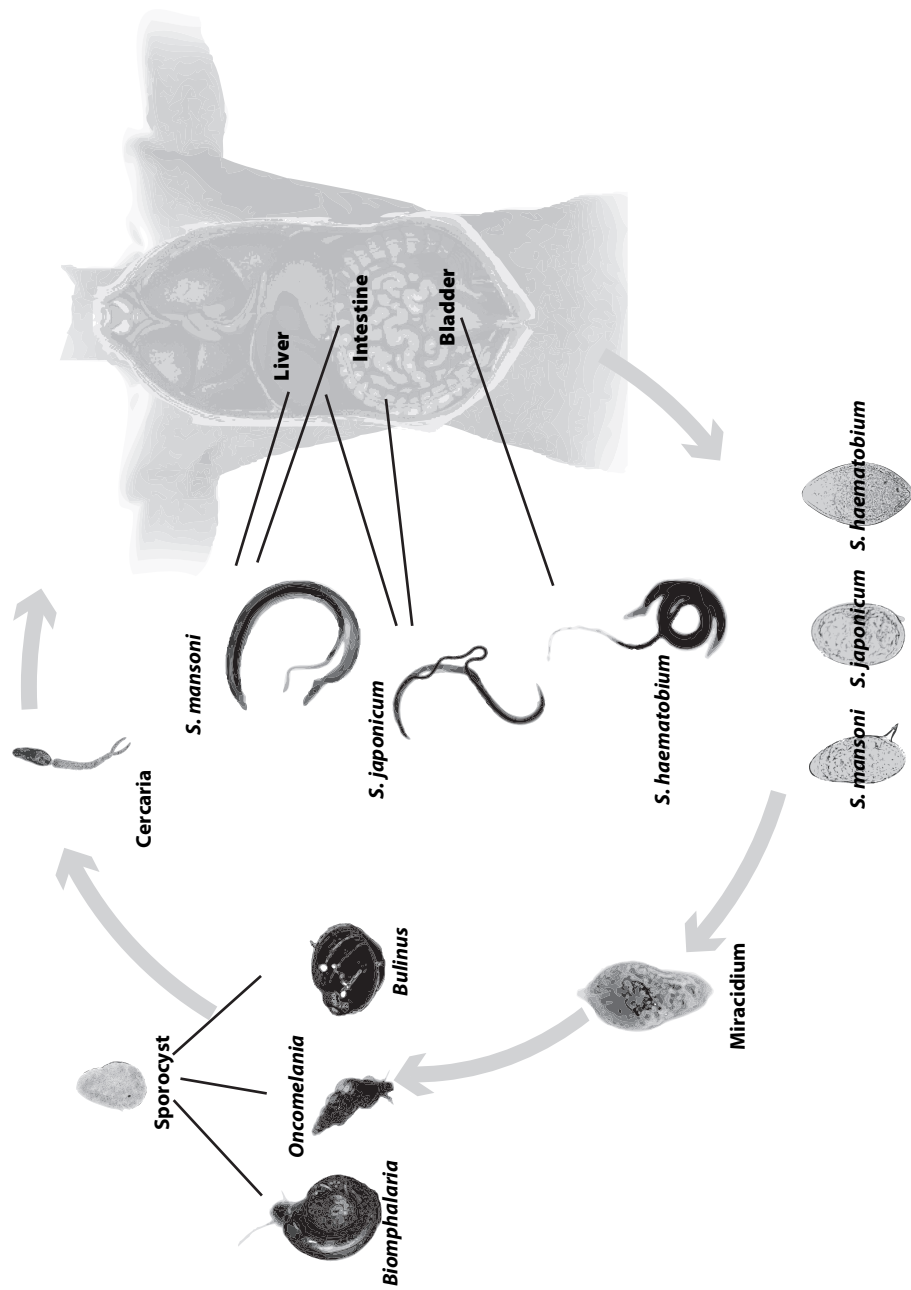


Figure I. 1: Schistosome life cycle. The main developmental stages of schistosomes as they cycle from fresh water mollusks and humans. The intermediate hosts of the parasites are *Biomphalaria* sp (*S. mansoni*), *Oncomelania* sp (*S. japonicum*), and *Bulinus* sp (*S. haematobium*). Shown are the mollusk stage of the parasites (sporocysts), the free swimming cercaria and miracidium, as well as the adults in the human circulatory system. Mating pairs of *S. mansoni* and *S. japonicum* migrate to the mesenteric blood vessels. *S. haematobium* mating pairs are found in the venous plexus of the bladder.

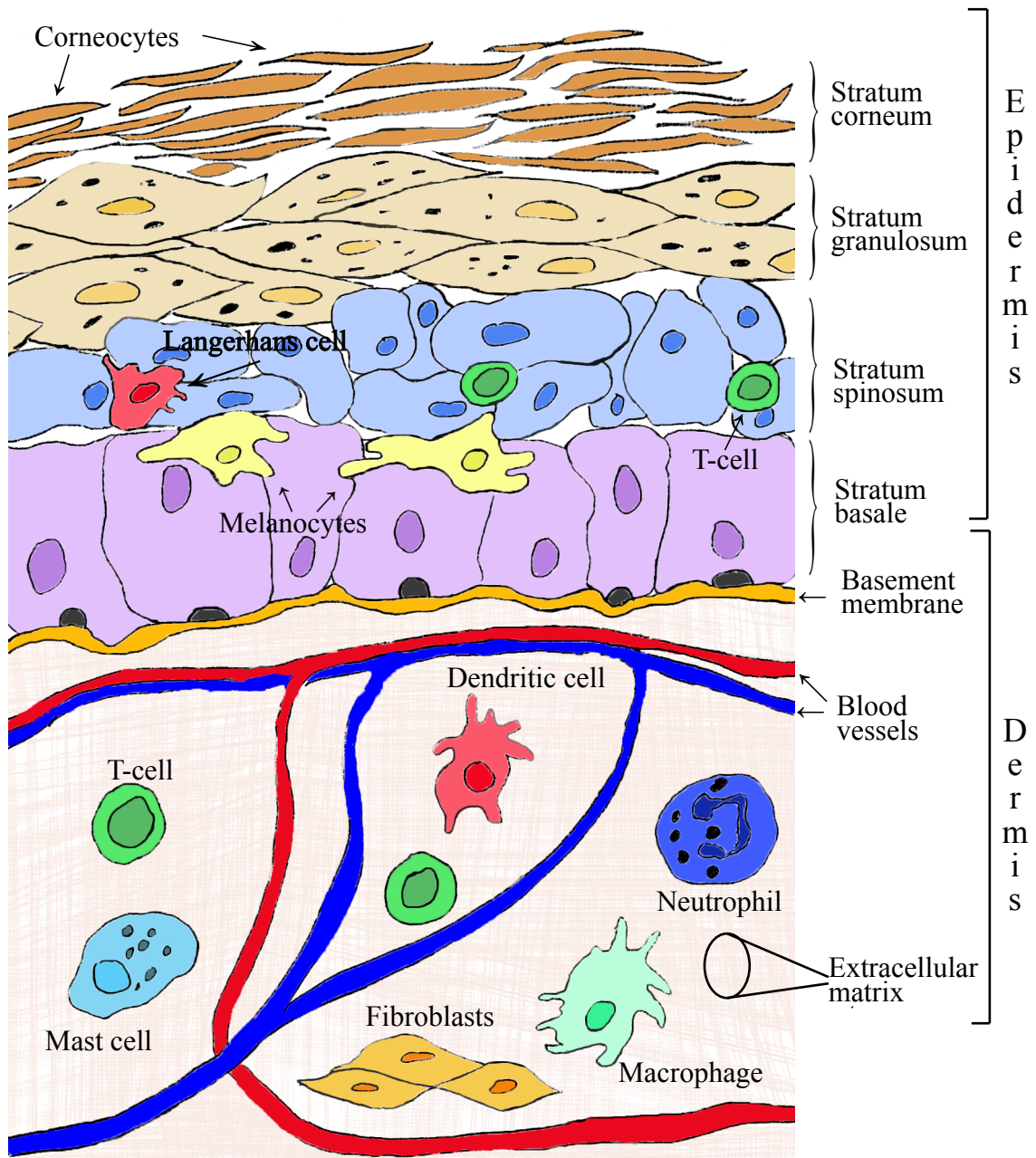


Figure I. 2: Skin architecture and immune effector cells. The protective barrier of the skin is divided into two sections: the epidermis (divided into four layers: the stratum basale, the stratum spinosum, the stratum granulosum, and the stratum corneum) and the dermis. The dermis is largely composed of a fibrous network of collagen and elastin which give the skin its strength and elasticity. Most immune effector cells are located in the dermis. Adapted from [24].

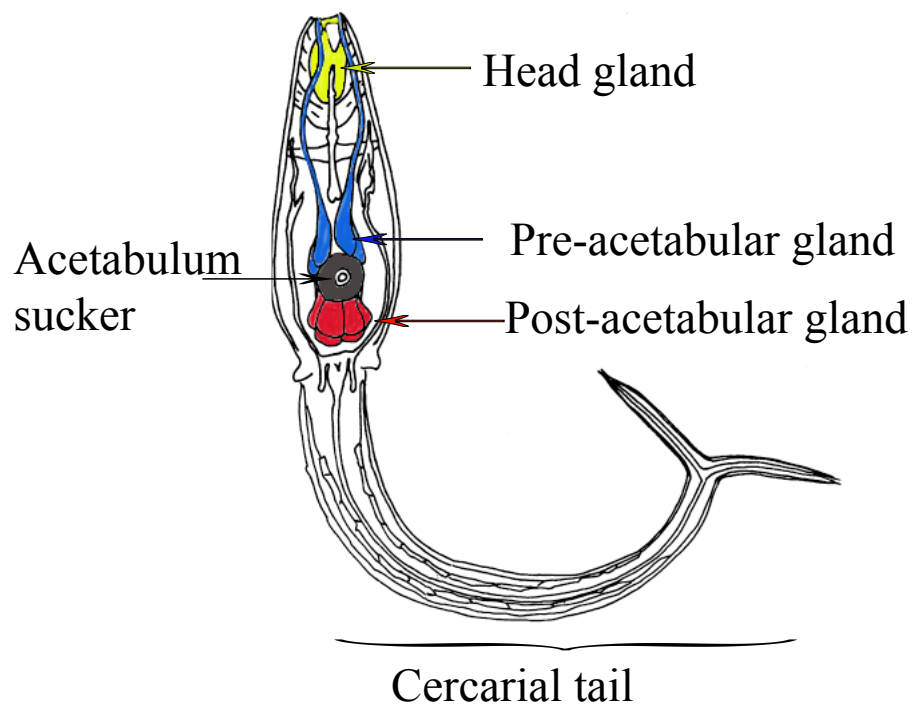


Figure I. 3: *Schistosoma mansoni* cercarial secretory glands. Schematic drawing of a cercaria highlighting the secretion glands: head gland (yellow), pre-acetabular gland (blue), post-acetabular glands (red). In dark grey is the acetabulum sucker. The secretory glands occupy close to 40% of the parasite. Adapted from [76].

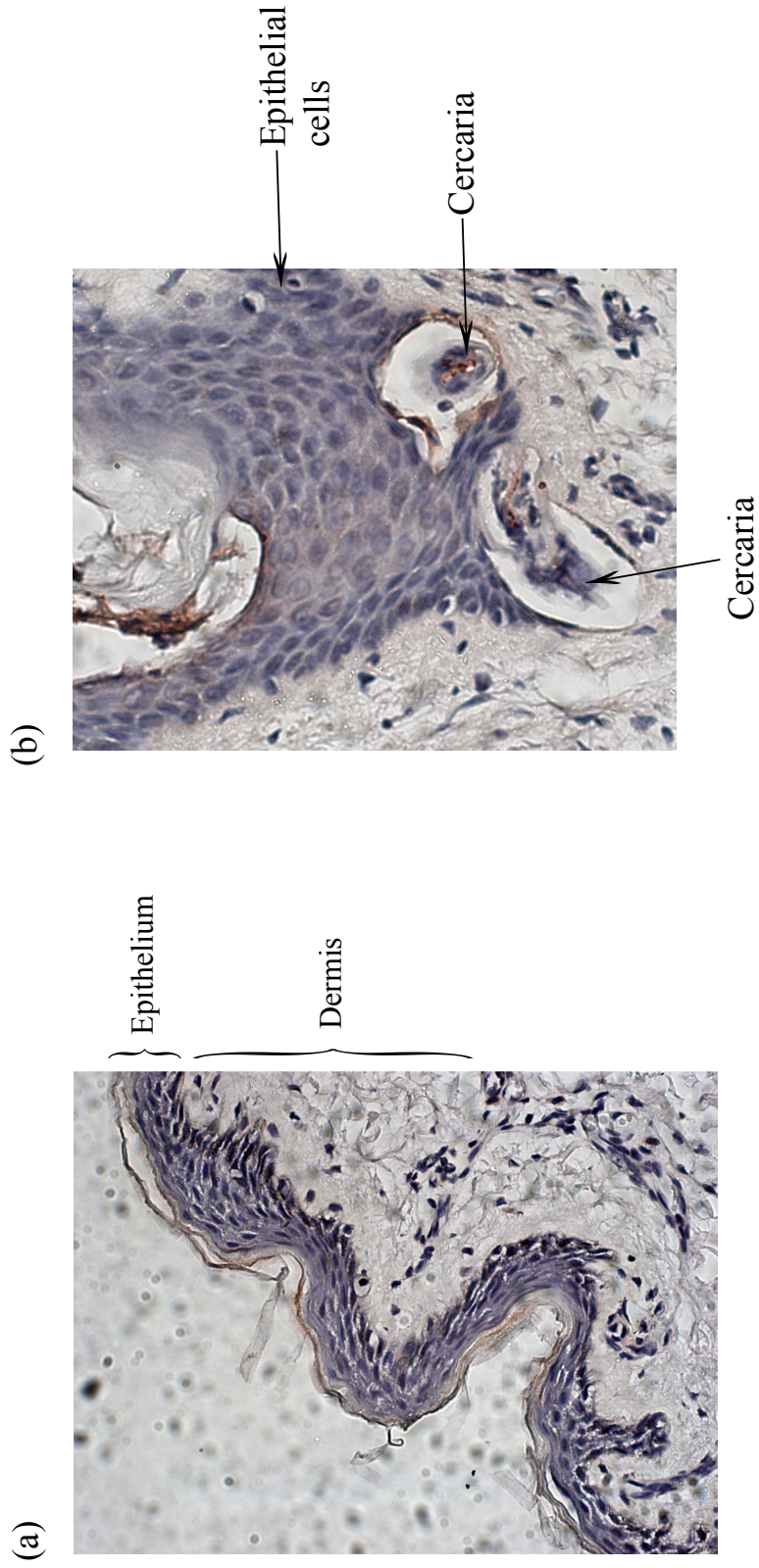


Figure I. 4: Invasion of human skin by *S. mansoni*. *S. mansoni* cercariae were placed on human cadaverous skin sections and incubated for four hours at 37°C over RPMI. Tissue samples were fixed in formalin and paraffin embedded. Sections were stained according to Vector Lab Elite ABC system instructions and counter stained with hematoxylin. Dark brown staining represents peroxidase activity denoting *S. mansoni* cercarial elastase protein localization. (a) Control uninfected skin. (b) Infected skin. Note the zone of tissue degradation around the larva.

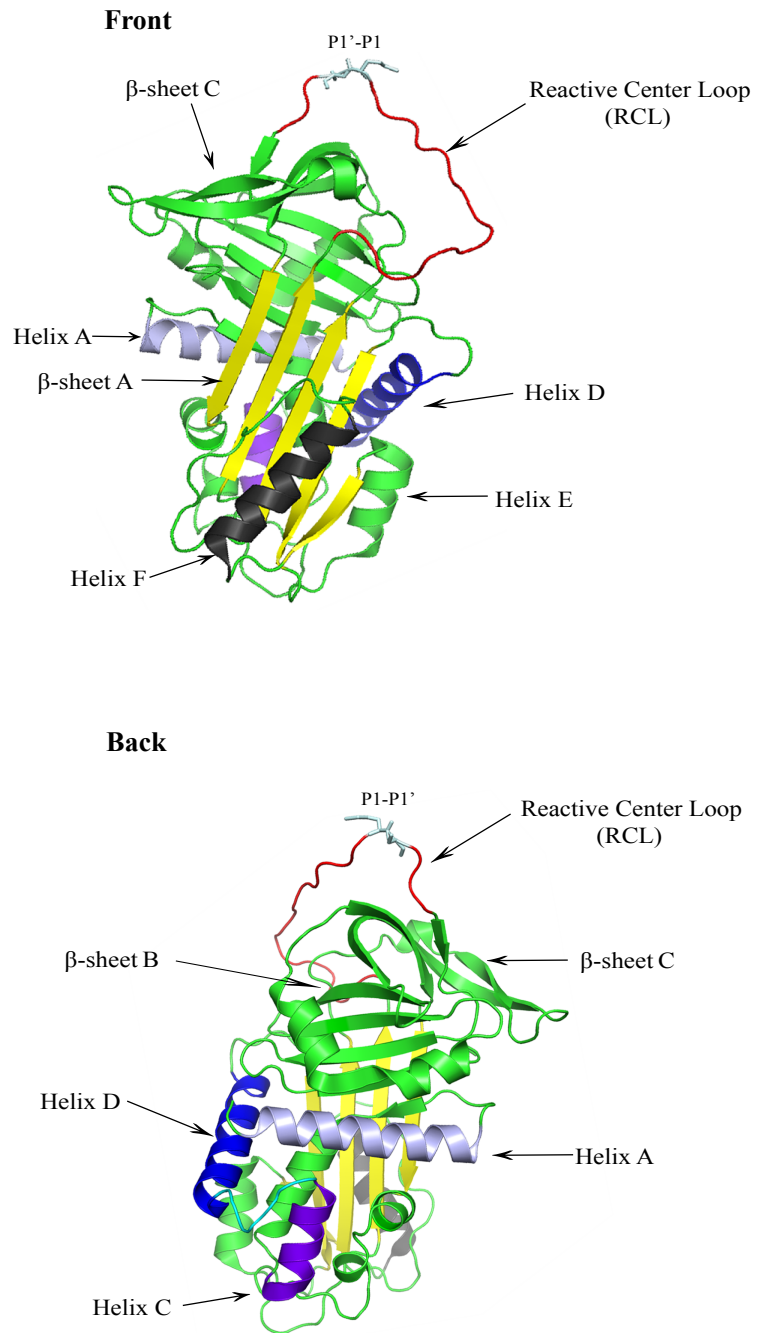


Figure I. 5: Structure of $\alpha 1$ -antitrypsin (adapted from PDB 2QUG) viewed from two angles. The RCL is highlighted in red and β -sheet A is in yellow. The P1-P1' site of the RCL notes the location of the peptide bond cleaved by the cognate protease before inhibition.

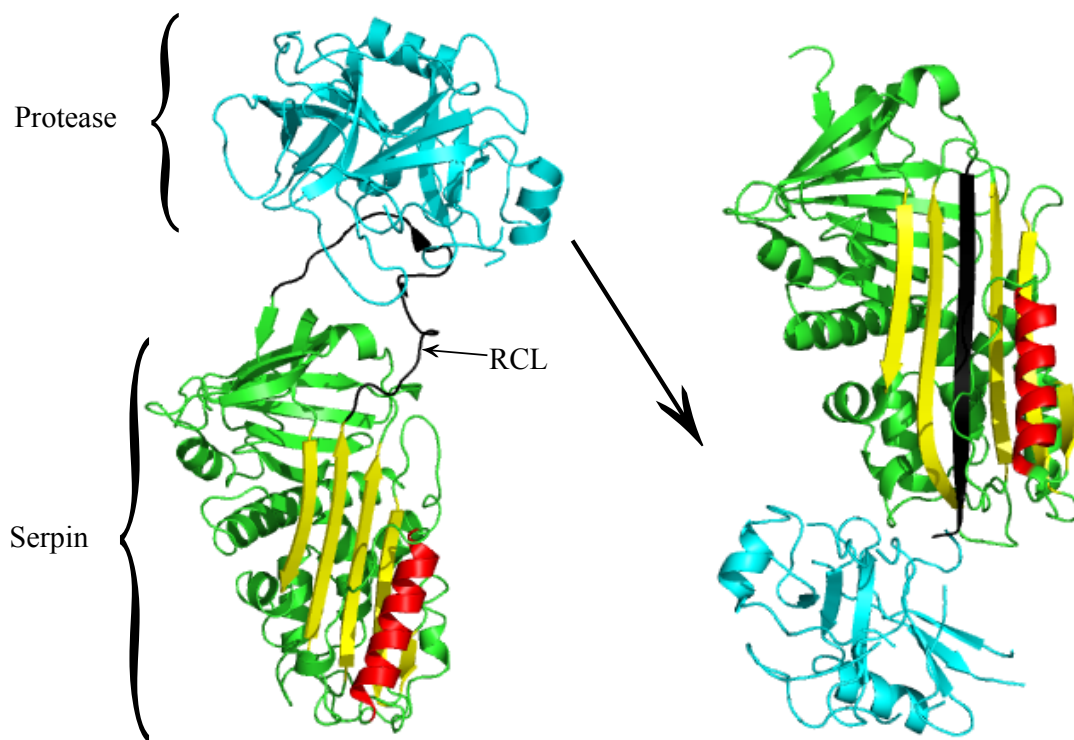


Figure I. 6: Mechanism of serpin inhibition. The initial trypsin (protease) and serpin Michaelis complex (adapted from PDB 1K9O). Upon cleavage of the RCL (black), the loop inserts into the β -sheet A of the serpin (PDB 1E2X).

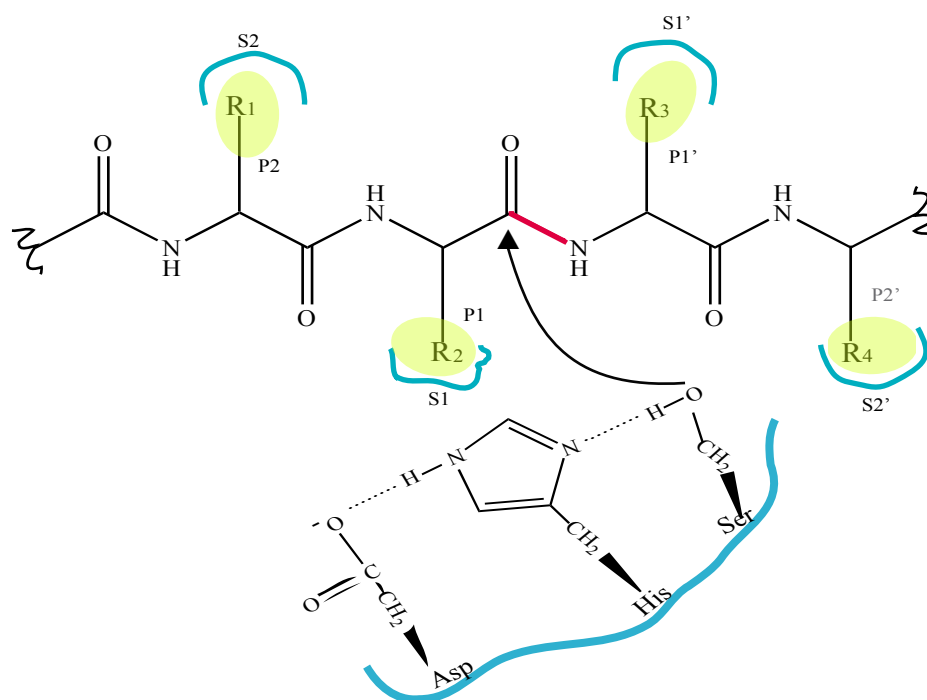


Figure I. 7: Serine protease active site with catalytic triad and substrate binding pocket. The active site serine, activated by the nearby base (His) acts as the nucleophile, attacking the carbonyl carbon of the substrate. R, amino acid side chains of substrate; S, protease subsite pocket; P substrate amino acid residue. The scissile bond is depicted by a bold red line.

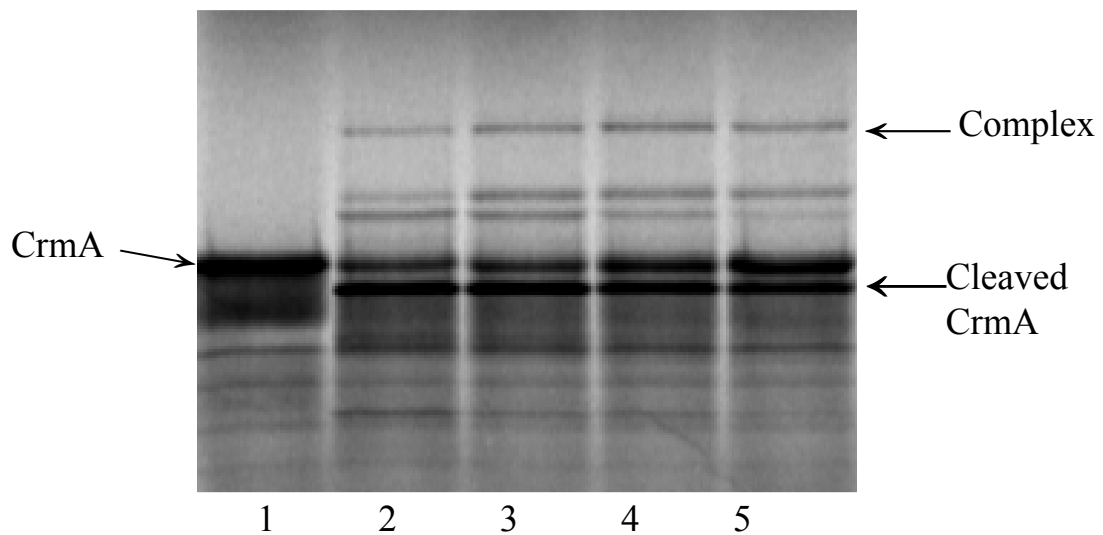


Figure I. 8: Complex formation between granzyme B and CrmA. An SDS-PAGE gel of radio-labeled viral serpin CrmA (cytokine response modifier A) and human granzyme B. Lane 1 is CrmA alone (triangle); lane 2-4 is CrmA incubated with decreasing amounts of hGraB for 30 minutes at 37°C. Complex between CrmA and hGraB was observed along with cleaved CrmA. The middle doublets could be degradation products.

Chapter 1

Schistosome Serine Protease Inhibitors

Abstract

Serpins are a structurally conserved family of macromolecular inhibitors found in numerous biological systems. The completion and annotation of the genomes of *Schistosoma mansoni* and *Schistosoma japonicum* has enabled the identification by phylogenetic analysis of two major clades. *S. mansoni* shows a greater multiplicity of serpin genes, perhaps reflecting more specific adaptation to infection of a human host versus the zoonotic *S. japonicum*. The *S. japonicum* genome contained one partial and three complete serpin sequences. In contrast, *S. mansoni* contained eight serpins. The active transcription of the eight *S. mansoni* serpins was verified using semi-quantitative PCRs. Of the eight *S. mansoni* serpins, Sm1a, Sm1b, and Sm1c were nearly identical except at a few loci, most notably in the reactive center loop (RCL) region. However, the transcription of these serpins was differentially regulated throughout the life cycle of *S. mansoni*.

Introduction

It is estimated that over 10% of the world population is affected by helminth-induced disease with sub-Saharan Africa bearing most of the burden [1]. Helminths are a diverse group of parasitic worms divided into two phyla: nematodes (roundworms) and platyhelminths (flatworms). *Ascaris lumbricoides*, *Strongyloides stercoralis*, *Trichuris trichiura*, and *Enterobius vermicularis* are example of roundworms known to infect humans. *Ascaris* infection rates are estimated as 1.5 billion infected individuals while trichuriasis affects 1.1 billion people [1]. The platyhelminths include the cestodes (e.g. *Taenia* sp and *Echinococcus* sp) as well as the trematodes (e.g. *Clonorchis sinensis* and

Fasciola hepatica). *Schistosoma* sp belong to the latter group of platyhelminths.

Although the infection rates do not number in the billion, platyhelminths represent a significant burden of disease; approximately 77 million people suffer from infection with *Taenia saginata* [1] and over 200 million individual are afflicted with schistosomiasis [2].

Helminth evolution and the development of the human immune system are thought to be deeply intertwined. Historical records can place the scourge of helminthes on human health as far back as ancient Egypt, China, Greece, and India [3]. In fact, fossilized helminth eggs have been found in pre-Colombian human coprolites [4] and in the remains of Egyptian mummies [5]. Epidemiological data has indicated an inverse relationship between the de-worming of a population and the rise in immunological dysfunction. From such data arose the hygiene hypothesis, originally proposed in 1989 by Stanchan [6] which postulates that lack of early exposure to infectious agents {especially parasitic worms} increases the susceptibility to develop allergies and autoimmune diseases. This hypothesis has gained a great deal of supporting evidence to the extent where helminth infections have been proposed as treatment (and perhaps a cure) for several immune-mediated maladies [7]. Understanding their biology and how helminths interact with their human hosts could prove invaluable to not only treating infections in developing world, but also to broaden our understanding of autoimmune and allergic diseases in industrialized countries.

Schistosomes are dioecious and not hermaphroditic, a unique feature among the platyhelminths. It consists of 8 pairs of chromosomes, seven autosomal pairs and one sex determining pair. The recent completion and annotation of the *S. mansoni* and *S. japonicum* genome has facilitated greatly the study of these unique trematodes. By current estimates, the 363 megabase genome of *S. mansoni* contains 11,809 genes encoding 13,197 transcripts [8]. All five classes of proteolytic enzymes were present and account for 2.5% of the genome [8]. *S. mansoni* has one third the number of putative protease sequences found in their human host (335 sequences vs. 945 sequences). Endogenous inhibitors of proteolytic activity are not as abundant as the proteases with only 34 genes in the nuclear genome [8]. Although only two cystatins (cysteine protease inhibitors) were originally reported, an in-depth search has revealed three. Of the 21 serine protease inhibitors found in the annotated genome database, 13 were of the I2 Kunitz-type family of inhibitors and eight were of the I4 serpin family.

The *S. japonicum* genome is slightly larger than that of *S. mansoni*. It is approximately 397 megabase pairs with a total of 13,469 genes [9]. The genome contains 314 putative proteases which include 108 metalloproteases, 102 cysteine proteases, and 65 serine proteases [9]. It was noted that both schistosome genomes, in a variety of cases, shared more orthologues with vertebrates than nematode worms [8, 9]. Indicating adaptation to survival with in their mammalian host. Unfortunately no mention has been made on the number and class of inhibitors found in the *S. japonicum* genome.

This study presents a comprehensive examination of the schistosome serpin family of inhibitors in the literature and schistosome genomes. Their possible roles in the biology of the parasite are explored.

Experimental Procedures

Genome search and phylogenetic analysis. The genome databases of both *S. japonicum* and *S. mansoni* are partially annotated but to ensure no potential serpin sequences were missed, the database search utilized the protein sequence of canonical serpin α 1-antitrypsin as the query sequence in order to find predicted protein sequences with serpin-like domains. The schistosome sequences obtained were then used as the query sequences to find any remaining putative serpins in the genome database. These findings were then compared to previously published putative serpins sequences. Multiple protein sequence alignments were carried out using Clustal W v1.8 as previously described [10] and the phylogenetic tree was carried out using the Phylogeny.fr platform [11]. The structure of α 1-antitrypsin has been published [12] and was used to predict the location of conserved tertiary structures along the schistosome serpin sequences. To predict the location of the reactive center loop of the sequences, each predicted serpin was aligned with α 1-antitrypsin, C1-inhibitor, and/or ovalbumin.

BLAST and target protease prediction. Each predicted serpin was queried against the NCBI BLASTp non-redundant database in order to find similar mammalian serpins. The peptidase database MEROPS was used to predict mammalian proteases that could potentially bind to the RCL and cleave at the P1-P1' position. The P3 and P2 positions

were also taken into consideration when selecting candidate proteases. In the case of Smp_155550 (Sm1b), Smp_155560 (Sm1c), and Smp_062120 (Sm1a) the position of the predicted P1 amino acid of Cys or Tyr is highly unusual thus the Arg in the P2 position was also considered as the possible P1 position.

RNA isolation and semi-quantitative PCR. *S. mansoni* (Puerto Rican isolate) cercariae were harvested from *B. glabrata* by light induction and washed with water. Approximately, a 250 ml cercarial pellet, a 350 ml adult worm pellet, and four snail hepatopancreases were used to isolate total RNA. RNA samples were collected by homogenizing and sonicating tissue in Trizol (Invitrogen) according to manufacturer's recommendation. RNA pellets were resuspended in water and treated with DNase I (New England Biolabs). Samples were then heat-treated and cleaned using RNeasy Mini Kit (Qiagen). Concentrations of final total RNA samples were determined using NanoDrop 3300 (Thermo Scientific). cDNA was synthesized using SuperScript III Kit (Invitrogen) according to manufacturer's instruction using an 18-mer oligo-dT primer. A control reaction containing no reverse transcriptase was also carried out. The amplification program was as follows: 10 cycles of 94°C for 30 seconds, 50°C for 30 seconds, 72°C for 1 minute and 30 seconds, followed by 20 cycles of 94°C for 30 seconds, 50°C for 30 seconds, 72°C for 1 minute and 30 seconds with 5 seconds added to the extension time after each cycle. PCRs were conducted using an in-house Phusion polymerase.

Cloning and sequencing. For the cloning of Sm1a, Sm1b, and Sm1c cDNA from late sporocysts, cercaria, schistosomula, and adults was used as template for PCR reactions. Primers were designed to span the whole transcript and add a *SacI* at the 5' end and *SmaI* at the 3' end for future cloning. PCRs were carried out using the High Fidelity PCR Kit (Roche) using forward primer: 5'-GGC CAG TTT ACC CCA CCT AAA GTC ACG AG-3' and reverse primer: 5'-CGA ACC ATC TGT GTT GCT GTA GCT GCA GC-3'. The amplification program was as follows: 10 cycles of 94°C for 30 seconds, 55°C for 30 seconds, 72°C for 1 minute and 30 seconds, followed by 20 cycles of 94°C for 30 seconds, 58°C for 30 seconds, 72°C for 1 minute and 30 seconds with 5 seconds added to the extension time after each cycle. PCR products were gel purified and cloned into pCR2.1 TOPO plasmid (Invitrogen). Eight *E. coli* colonies were isolated from each life stage. The procedure was repeated to select eight more colonies. Plasmids were retrieved using Qiagen Miniprep columns (USA) according to the manufacturer's recommended protocol. Sequencing was carried out by Elim Biopharmaceuticals (USA).

Results and Discussion

Schistosome serpins and developmental stage distribution. The completion of the *S. mansoni* and *S. japonicum* genomes has made it possible to explore the proteome of both parasites for proteins key to survival and pathogenesis. By searching the parasite databases for proteins homologous to the canonical serpin α 1-antitrypsin, eight complete serpin sequences were identified in the *S. mansoni* gene database. The *S. japonicum* database has one partial and three complete serpin sequences (Figure 1. 1). The *S.*

haematobium genome is incomplete as of the writing of this study, but a GenBank search identified one serpin in the organism.

Semi-quantitative PCRs were carried out to verify the expression of the *S. mansoni* serpins uncovered in our search (Figure 1. 2). Neither the expression profile nor the relative abundance of these serpins was identical. SmSerp_C was only found in the early and late sporocysts, a pattern also observed with Smp_090090. SmSerp_C was initially identified in a proteomic analysis of the secreted products of cercariae [13]. Release of this serpin into the host was validated by another study that analyzed the proteins released by cercariae invading human skin using mass spectrometry [14]. It is not surprising then that the SmSerp_C transcripts are found in the snail hepatopancreatic stage of the parasite since it is at this stage that proteins released by mature cercariae are synthesized [13]. Transcripts for SmSrpQ, also identified in the secretion products of invading larva [15, 16], were detected in the early and late sporocysts, and in cercarial RNA samples. This suggests that SmSrpQ is utilized for a longer period of time during invasion than SmSerp_C, and therefore is transcribed beyond the hepatopancreatic life stage. Smp_055330 is present in the early and late sporocysts but it is also present in egg/miracidia. Miracidia are the snail infective stage and Smp_055330 seems to be associated with the life stages involving the molluscan host. Attempts to amplify Smp_055330 from its predicted start site were unsuccessful but amplification was achieved from the preceding Met, eliminating the long N-terminal extension.

The sequences of Sm1a, Sm1b, and Sm1c were very closely related (Figure 1. 5) such that they could not be differentiated by simple PCR. Sequencing of whole transcripts revealed differences in relative abundances of each gene during the life cycle of the parasite (Table 1. 3). Sm1a was most abundant in schistosomula (8/10 clones) while Sm1c transcripts were predominantly found in cercariae (16/34 clones). Neither Sm1a nor Sm1b were found in cercariae. Transcripts of Sm1b were the least abundant overall (6/50 clones) and Sm1c transcripts were ubiquitous and most abundant out of the three genes (34/50 clones).

Phylogeny of schistosome serpins. Phylogenetic analysis of the *Schistosoma* serpins assigns two major branches to the group (Figure 1. 3a, blue). Branch 1 consists of Smp_090080, ShSPI, and Sjp_0085750 clustered closely together, with Smp_090090, Sjp_0113720, and SmSerp_C more distantly related. The remaining serpins form the second major branch (Figure 1. 3a, yellow). With Sm1c, Sm1b, and Sm1a, most of the variation occurred at the RCL region (Figure 1. 4). Considering the chromosomal arrangement of *S. mansoni* serpins (Figure 1. 3b) and the clustering pattern of the phylogenetic tree, the multiplicity of *S. mansoni* serpin genes compared to those of *S. japonicum* has likely arisen through several gene duplication events. This is not surprising, given recent findings that *S. japonicum* appears to be a more ancestral species among mammalian parasites [17]. *S. mansoni* and *S. haematobium* are more human-directed parasites than *S. japonicum*, leading to speculation that serpin gene duplications in *S. mansoni* reflect adaptations to the human host. It will be interesting to see if *S. haematobium* also exhibits similar gene duplication events when its genome is published.

With the exception of Sjp_0113720, alignment of the *Schistosoma* serpins with α 1-antitrypsin and the superimposition of the structural components of α 1-antitrypsin, show that these proteins contain all elements necessary for functionality (Figure 1. 2). Their predicted structures reveal the interesting phenomenon of elongation of the regions surrounding helix D. Branch 1 sequences (Figure 1. 3a) indicate a 9-16 amino acid extension of the helix D region across all three species. This could indicate either an elongation of helix D or an extension of the region connecting helix C to helix D. In either case, this extension could have ramifications on the biochemical properties and functionality of these serpins. Previous work on helix D has suggested it is involved in the allosteric control of the binding and release of glucocorticoids by corticoid-binding globulin, a non-inhibitory serpin [18]. Heparin activation of antithrombin is mediated through its binding site on helix D [19]. On the other hand, MENT, a serpin important in heterochromatin formation, contains an extension in the region between helix C and D that forms a loop outside the body of the serpin [20]. The authors speculate it may be involved in DNA binding.

ShSPI was discovered using a lgt11 cDNA library from adult worms [21].

Immunolocalization suggested ShSPI was on the surface of adult worms. Although one study indicated that ShSPI could bind to trypsin but not elastase or chymotrypsin [22], there was no corroborating evidence to validate active site binding. Closely related to ShSPI, Sjp_0085750 was the subject of another study. Transcripts of the Sjp_0085750 gene were found in male and female adult worms, and to a lesser extent in cercariae [23].

Yan et al. showed that this serpin localized to the surface of the adult worms, much like ShSPI, as well as the gut epithelium of the worm. When the authors evaluated the immune response to Sjp_0085750, they noted a Th2-type humoral response in mice. Protection studies with the serpin antigen showed a decrease in worm burden, suggesting a potential use of this parasite serpin as a vaccine candidate [23].

Fewer studies have been conducted on the serpins clustered in the second phylogenetic branch (Figure 1. 2a). An antisera screen against cercarial secreted products from a cercarial cDNA library identified a partial gene product, clone 8, with homology to serpin MNEI [16]. The authors found the protein product in cercarial and lung stage parasite lysates but not in adult worms. Based on the sequence, clone 8 is SmSrpQ. A proteomic study of skin lipid-induced cercarial secretion products also found a unique peptide belonging to clone 8/ SmSrpQ [15].

Validation of theoretical sequences Sm1a, Sm1b, Sm1c. The gene duplication event that gave rise to these three serpins afforded the opportunity to compare recent changes that have evolved in each gene. Because differences between the three serpins are so minimal (Figure 1. 4), primers could not be designed to individually amplify each transcript. This required sequencing of randomly selected clones from cDNA samples from each life stage of *S. mansoni*. Of the 64 clones sequenced, 50 yielded full-length sequences.

Once aligned, several differences from the predicted amino acid sequence were apparent (Table 1. 4). The predicted variation in the RCL region was confirmed. The gate region of a serpin, located primarily in β -sheet C stand 3 (s3C) and s4C, has been shown to be important in the latency to inhibitory state transition of PAI-1 [24]. In Sm1a-c (Table 1. 4) position 197 & 200 lie within s3C. The changing of a Leu for Met may not be of consequence but there is a biochemically significant difference between a basic residue like Lys and an acidic residue like Glu. Such a change can affect how the gate region functions in controlling the inhibitory fold of the RCL.

The transition of the RCL of a serpin into the main body of the protein requires movement of helix F (hF) and opening of β -sheet A stand 3 and 5 (s3A and s5A) in order for insertion to take place [25]. The initial opening of s3A and s5A occurs at the breach region between the two stands and the shutter region lies at the center of sA3 and 5. Both are important for accepting the hinge region of the RCL and stabilizing the new sA4 (formerly the RCL). Position 152 and 154 are predicted to lie in the breach region. At position 154 the sequence contains either a Pro or Cys (several clones contained His). These side chains have vastly different hydrogen bonding abilities. Changes in the breach regions have been shown to lead to an increase in serpin polymerization [26]. The shutter region appears unchanged in all three serpins.

Putative protease targets of schistosome serpins. To predict protease targets, the RCL of all the serpins were aligned with known serpins: inhibitory serpins α 1-antitrypsin and C1inh and non-inhibitory serpin ovalbumin (ovalb) (Figure 1. 5a). The predicted P1

positions (Figure 1. 5a, black triangle) as well as the P2 and P3 positions were used to predict possible proteases that could cleave the RCL scissile bond (Table 1. 2). In the case of Sm1a-c, C1inh, which has a shorter RCL than other mammalian serpins [27], was used to predict the P1 region (Figure 1. 5c, black triangle).

The RCLs of ShSPI, Smp_090080 and Smp_090090 contain a feature unusual for inhibitory serpins (Figure 1. 5b). The P12-P9 region of the RCLs of most inhibitory serpins is characterized by amino acids with short side-chains (Ala, Gly, Ser) [28], but this feature is not present in ShSPI, Smp_090080 and Smp_090090 (Figure 1. 4b, blue line). Whether the unusual RCL amino acid sequence signifies a non-inhibitory function is a subject for future study.

The predicted RCL sequence of Sjp_0113080 has a Leu-Ser at the P1-P1' specificity determining region. This corresponds to the predicted substrate specificity of the cercarial elastase [29]. The *S. japonicum* genome contains only one cercarial elastase gene. *S. japonicum* cercarial elastase antibodies were reported to localize in infected mouse skin [9], neither a protein corresponding to the putative protease, nor enzymatic activity was found in the cercarial secretions of *S. japonicum* [30]. Less is known about the *S. haematobium* cercarial elastase (ShCE). ShCE transcripts can be found in the sporocysts and it is closely related to SmCE [29]. ShSPI, Smp_090090, SmSrpQ, and Sjp_0113080 could be involved in the regulation of these elastases, although host proteases cannot be ruled out as potential targets.

A putative serpin, Smpi56, was partially purified from extracts of adult *S. mansoni* [31]. Smpi56 was able to form an SDS-stable complex with neutrophil elastase, pancreatic elastase, and an endogenous cercarial protease. Because the sequence of Smpi56 is not known, the authors were unable to positively identify it as a serpin. It did exhibit the biochemical characteristics of an inhibitory serpin and could therefore be Smp_090090 which has a Leu-Ser P1-P1' motif (Table 1. 2). However, the unconventional RCL of Smp_090090 makes it difficult predict its ability to form an inhibitory complex with a protease and no Smp_090090 transcripts were found in adult worms (Figure 1. 2)

Serp_C contains an Arg at the P1 position, making it a good candidate for trypsin-like protease inhibition. Considering its release into the host during invasion, thrombin, coagulation factors, and kallikrein-related peptidases are all potential targets (Table 1. 2).

Concluding Remarks

The role of serpins in schistosomiasis was last reviewed 14 years ago [32]. Although there are caveats and limitations to using of the RCL sequence as an accurate predictor of protease specificity (the existence of exosites in and outside the RCL region [33] and the differing binding specificities of protease substrate binding pockets beyond the S1-S1' sites) RCL-based specificity predictions can still lead to testable hypotheses about the function of serpins in these parasites. With 102 cysteine proteases and 65 serine proteases identified in the *S. japonicum* genome [9] and 97 cysteine and 78 serine proteases in the *S. mansoni* genome [8], the 12 predicted full-length schistosome serpins may perform specific, focused functions in these organisms.

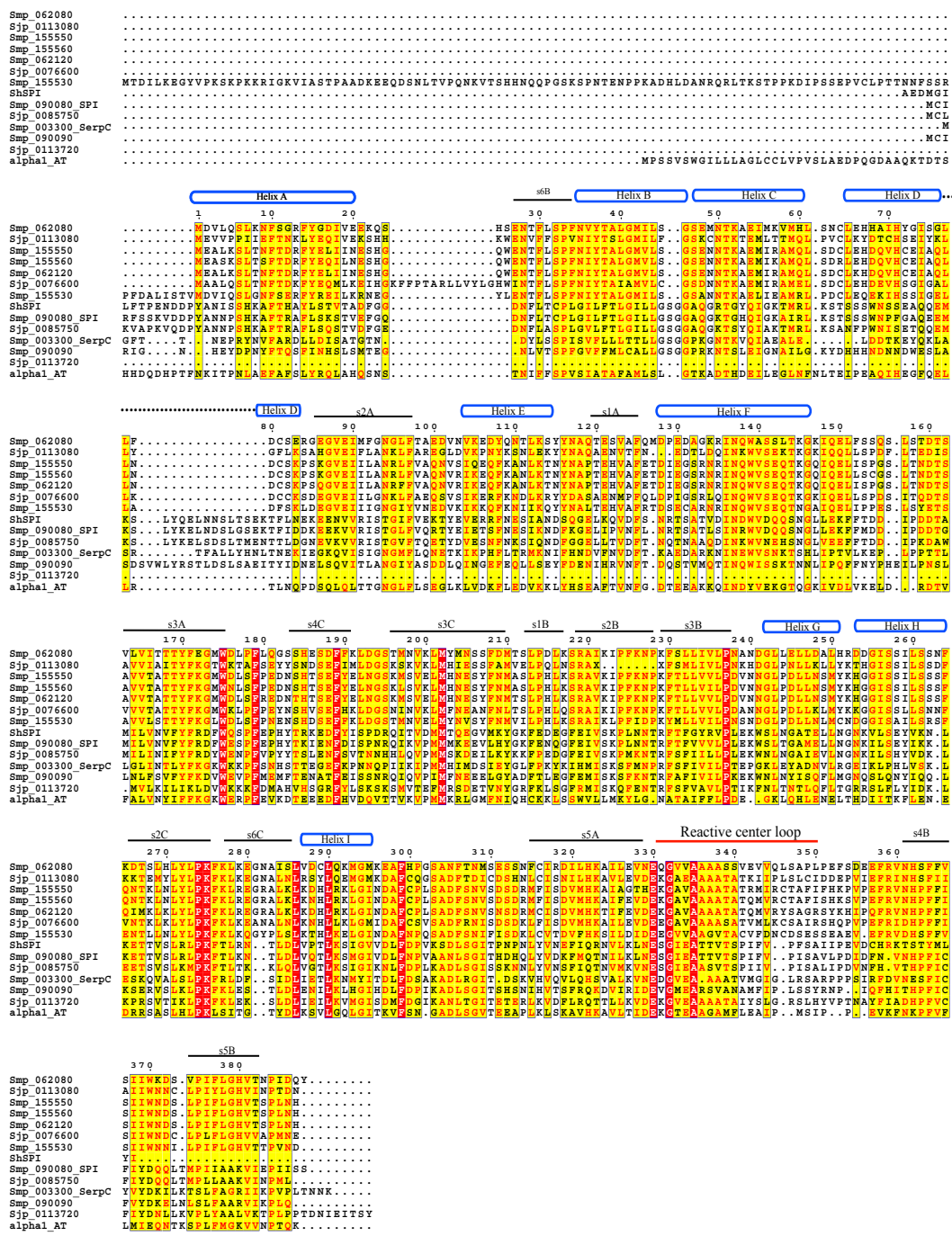


Figure 1. Primary amino acid sequence alignment. The predicted or known sequences were aligned with α 1-antitrypsin using Clustal W v1.8. Highlighted regions show at least a 50% sequence identity. The location of the helices (cylinders), β -sheets (black lines), and RCL (bold red line) were approximated using the known α 1-antitrypsin structure.

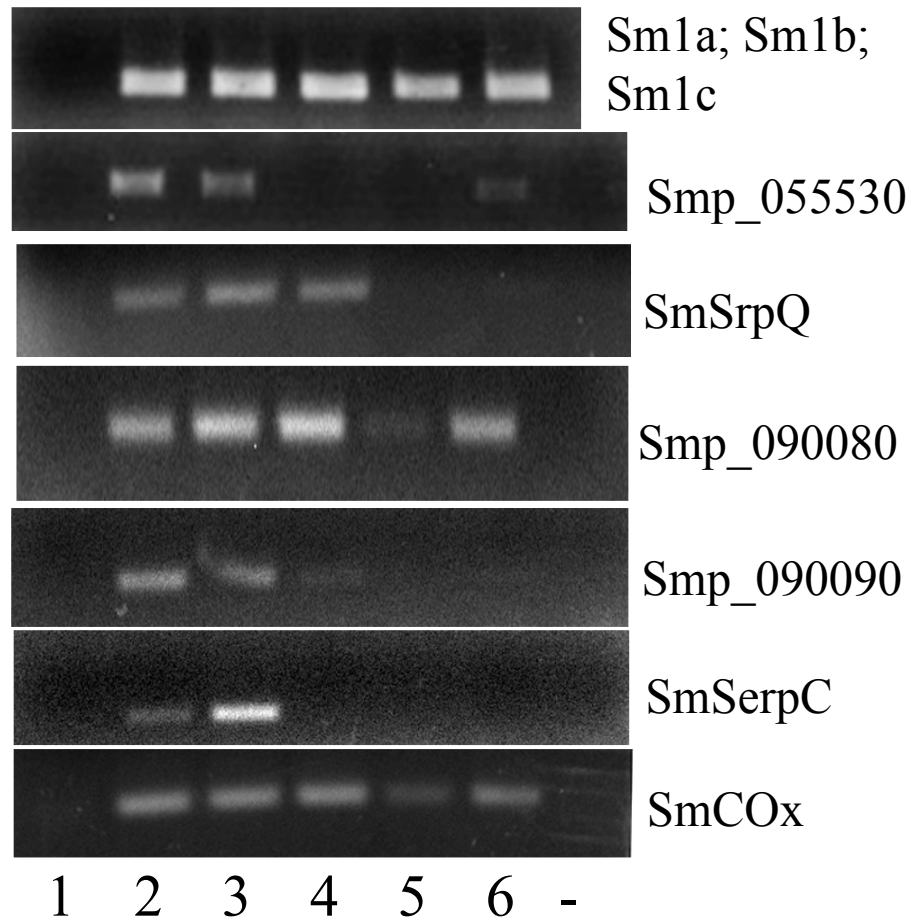


Figure 1. 2: Semi-quantitative PCRs of *S. mansoni* serpines. Equal amounts of cDNA from the developmental life stage of the parasite were used to determine active transcription of the eight putative *S. mansoni* serpines. Lane 1: uninfected *B. glabrata*; lane 2: early/daughter sporocysts; lane 3: late sporocysts; lane 4: cercaria; lane 5: adult worms; lane 6: egg/miracidia; (-) blank control. The cytochrome oxidase (SmCOx) gene was used as cDNA loading control.

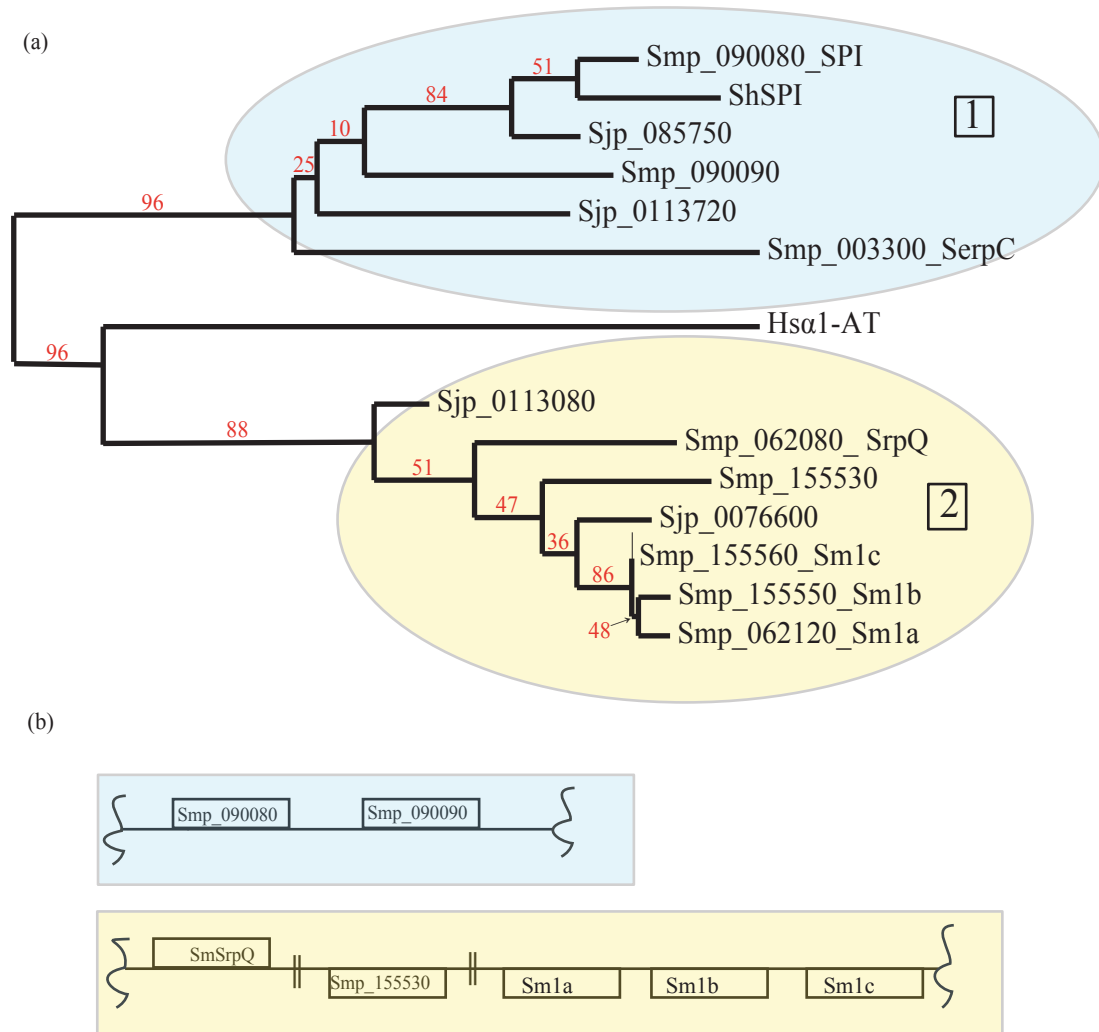


Figure 1. 3: (a) *Phylogenetic analysis of schistosome serpins*. The thirteen serpins were aligned using MUSCLE and a bootstrapped maximum likelihood tree was generated using PhyML 3.0. The percentage branch bootstrap support values are shown on branch splits. Method of analysis is fully described in [11]. (b) *Serpine gene arrangement in S. mansoni*. The location of each gene in their respective supercontig. Double lines denote the location of an unrelated gene.

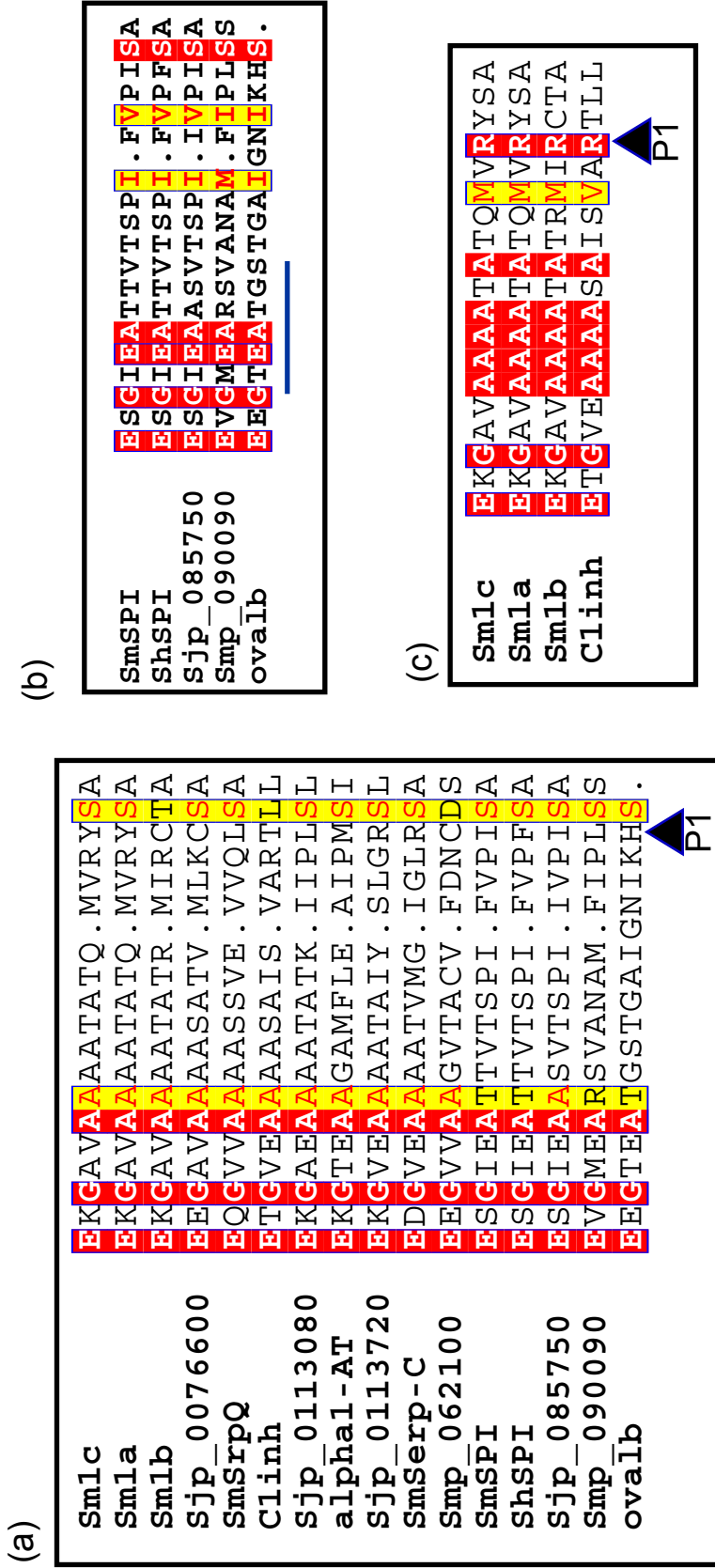


Figure 1. 4: (a) *Alignment of the reactive center loops of schistosome serpins*. The regions corresponding to P17-P2' of the serpin was aligned with the RCL of human α 1-antitrypsin, C1inh, and ovalbumin. The putative P1 site (black triangle) was deduced based on its alignment with the known serpins. (b) *Non-inhibitory RCL alignment*. The RCL sequences of ShSPI, SmSPI, Sjp_085750, and Smp_090090 bore a resemblance to the RCL of non-inhibitory serpin ovalbumin. The hinge region of the RCL (blue line) lacks the small side-chained amino acids observed in inhibitory serpins. (c) *RCL of Sm1a, Sm1b, and Sm1c*. The RCL sequences of these three serpins was aligned with C1inh. The Arg of all four serpins (black triangle) align at the new putative P1 position. Red amino acids are exact matches and yellow are similar amino acids. Alignments were conducted using Clustal W v1.8.

```

1      10      20      30      40      50      60
Sm1b MEALKSLTNFTDRFYELIINESHGQWENTFLSPFNIIYTAGMVLSGSENNTKAEMIRAMQLSDCLE
Sm1c MEASKSLTSFTDRFYEQIILNESHGQWENTFLSPFNIIYTAGMVLSGSENNTKAEMIKAMQLSDRLE
Sm1a MEALKSLTNFTDRFYELIINESHGQWENTFLSPFNIIYTAGMVLSGSENNTKAEMIRAMQLSDCLK

70     80     90     100    110    120    130
Sm1b HDQVHCEIAQLLNDCKPSKGV E I I L A N R L F V A Q N V S I O E Q F K A N L K T N Y N A P T E H V A F E T D I E G S
Sm1c HDQVHCEIAQLLNDCKPSKGV E I I L A N R L F V A Q N V R I K E Q F K A N L K T N Y N A P T E H V A F E T D I E G S
Sm1a HDQVHCEIAQLLNDCKPSQGV E I I L A N R F F V A Q N V R I K E Q F K A N L K T N Y N A P T E H V A F E T D I E G S

140    150    160    170    180    190
Sm1b RNRINQWVSEQTKGOIQELIISPGSLTNDTSAVV TATTYFKGMWDLSPEDNSHTSEFYELNGSKMS
Sm1c RNRINQWVSEQTKGOIQELIISCGSLTNDTSAVV TATTYFKGMWNLSPEDNSHTSEFYELNGSKLS
Sm1a RNRINQWVSEQTKGOIQELIISPGSLTNDTSAVV TATTYFKGMWDLSPREDNTHHTSEFYELNGSKMS

200    210    220    230    240    250    260
Sm1b VELMHNESYFNMAASLPHLKSRAVKIPFKNPKFTLLVVLDPDVNNGLPDLLNSMYKHGGISSILSSSF
Sm1c VKLMHNESYFNMAASLPHLKSRAVKIPFKNPKFTLLVVLDPDVNNGLPDLLNSMYKHGGISSILSSSF
Sm1a VELMHNESYFNMTLSLPHLKSRAVKIPFKNPKFTLLVVLDPDVNNGLPDLLNSMYKHGGISSILSSSF

270    280    290    300    310    320    330
Sm1b QNTKLNLYLPKFKLREGRALKLLKDH L R K L G I N D A F C P L S A D F S N V S D S D R M F I S D V M H K A I A G T H E
Sm1c QNTKLNLYLPKFKLREGRALKLLK N H L R K L G I N D A F C P L S A D F S N V S D S D R M F I S D V M H K A I F E V D E
Sm1a QIMKLNLYLPKFKLREGRALKLLK D H L R K L G I N D A F C P L S A D F S N V S N S D R M C I S D V M H K T I F E V D E

340    350    360    370    380
Sm1b KGAVAAAAATATRMIRCTAFIFHKPVPEFRVNHPFFISIIWNDLPIFLGHVTSPLNH
Sm1c KGAVAAAAATATQMVRC TAFISHKSVPEFRVNHPFFISIIWNDLPIFLGHVTSPLNH
Sm1a KGAVAAAAATATQMVRYSAGRSYKHIPQFRVNHPFFISIIWNDLPIFLGHVTSPLNH

```

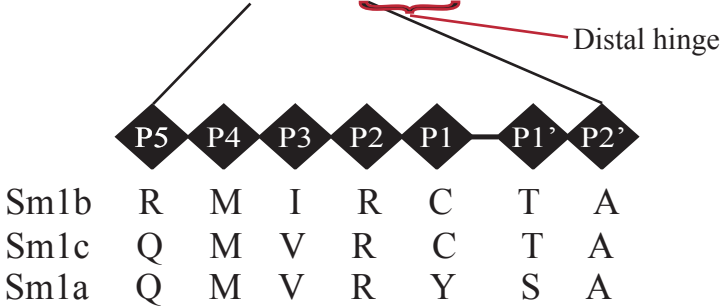


Figure 1. 5: Alignment of the theoretical translation of Sm1a, Sm1b, and Sm1c. The predicted sequences of Sm1a, Sm1b, and Sm1c. Identical amino acids are in black. A region of high divergence is the RCL region particularly the protease specificity-determining region of the RCL (P4-P1') and the distal hinge region of the RCL (red bracket).

Table 1. 1: Primers used for semi-quantitative PCR.

| Gene | Alias | Reverse 5' -> 3' | Forward 5' -> 3' | Product Size |
|--------------|--------------|------------------------------------|-----------------------------------|-------------------------|
| Smp_062080 | SmSrpQ | GTTGATAGTGATTGAGACGAAAAAGAGTCTTG | GGAGATATAGTAGAAAGAAAAACAGAGTCATTC | 431 |
| Smp_062120 | Sm1a | | | 415 |
| Smp_155550 | Sm1b | GTATTGAAGAAAATTCCACCATGTTTTATACATC | GATCAAAACTGAGTGTGAAGTTGATGCATAACG | |
| Smp_155560 | Sm1c | | | |
| Smp_003300 | Serp_C | GGAAATCAAAATGGCTTGTTTTATTACTGAC | TGGGTTTCACAACTAAATGAACCAAGATAT | 455 |
| Smp_155530 | - | GTTTCCAAAGTGATTGTAATTACATCCATC | CTGATATTTTGAAAAGAGGGTTATGTTCC | 360 |
| Smp_090090 | - | CATCTTTTTTGTGCGAAAAAGAAAGTAACATGG | TGGAAATGTTCCACAGAAAAATGCAAC | 426 |
| Smp_090080 | SPI | CCACATATAATTGATGATCATGGGTG | GCCTCATTACACTAAGATAGAGAATTTTGA | 405 |
| CyCr-Oxidase | COx | ACGGCCATCACCATACTAGC | TACGGTTGGTGTGCACAG | 250 |

Table 1. 2. Serine protease inhibitors of *Schistosoma mansoni*, *S. japonicum*, and *S. haematobium*.

| Database gene name | Alias | Size (kDa) | Reactive Center Loop (RCL) P17-P2' (P1-P1') | Similar mammalian serpin | Potential protease target | Ref. |
|--------------------|---------------|------------|---|----------------------------------|--|---------------------|
| Smp_003300 | Serp_C | 43.7 | EDGVEAAAAATVMGIGLR-SA | α_1 -AT (<i>Bos</i> 53%) | SmC12, Thrm, CF, KRPs | Curwen et al, 2006 |
| Smp_090080 | AAA29938 SPI | 46.0 | ESGIEATTVTSPIFVPL-SA | Neuroserpin (<i>Mus</i> 48%) | Elastase-2 (Non-inhibitory) | |
| Smp_090090 | | 46.3 | EVGMEARSVANAMFIPL-SS | Neuroserpin (<i>Homo</i> 52%) | CT, Cat G, CE (Non-inhibitory) | |
| Smp_062080 | AAB86571 SrpQ | 43.3 | EQGVVAAAAASSVEVQL-SA | SCCA-2 (<i>Mus</i> 53%) | NE, Cat G, CT, CE | Harrop et al, 2000 |
| Smp_155530 | | 51.0 | EEGVVAAGVTACVFDNC-DS | SCCA-2 (<i>Mus</i> 55%) | Sig. Peptidase complex(SPC) | |
| Smp_155550 | Smlb | 43.5 | EKGAVAAAAATATRMIRC-TA | PAI-2 (<i>Rattus</i> 53%) | Thrm, SPC | |
| Smp_155560 | Smlc | 43.6 | EKGAVAAAAATATQMVR-C-TA | SCCA2/SCCA1 (<i>Bos</i> 52%) | Thrm, CF, SPC | |
| Smp_062120 | Smla | 43.8 | EKGAVAAAAATATQMVR-Y-SA | PAI-2 (<i>Mus</i> 54%) | DPPIII, Thrm | |
| Sjp_0113080 | AAW25282 | 43.0 | EKGAEAAAAATATKIIPL-SL | PI-6 (<i>Rattus</i> 53%) | CT, Cat G, KRPs, CE | Liu et al, 2006 |
| Sjp_0076600 | | 45.0 | EEGAVAAAAASATVMLKC-SA | SerpinB6c (<i>Mus</i> 57%) | SPC | |
| Sjp_0085750 | AF308366 | 45.6 | ESGIEAASVTSPiIVPL-SA | Neuroserpin (<i>Homo</i> 50%) | Elastase-2 | Yan et al, 2005 |
| Sjp_0113720 | | 26.4 | EKGVEAAAAATAIYSLGR-SL | Ovalbumin (<i>Rattus</i> 52%) | KRPs, Thrm, CFc | |
| ShSPI | AAA19730 | 45.9 | ESGIEATTVTSPiIVPF-SA | Ovalbumin (<i>Rattus</i> 48%) | CT, chymase, CatG, CE (Non-inhibitory) | Blanton et al, 1994 |

S. mansoni

S. japonicum

S. haematobium

Table 1. 3: Number of clones of Sm1a, Sm1b, and Sm1c isolated during different developmental life stages of *S. mansoni*.

| | <u>Late Sporocysts</u> | <u>Cercariae</u> | <u>Schistosomula</u> | <u>Adult</u> | <i>Total</i> |
|--------------|------------------------|------------------|----------------------|--------------|--------------|
| Sm1a | 0 | 0 | 8 | 2 | 10 |
| Sm1b | 2 | 0 | 2 | 2 | 6 |
| Sm1c | 7 | 16 | 2 | 9 | 34 |
| <i>Total</i> | 9 | 16 | 12 | 13 | 50 |

Table 1.4: Comparison of the predicted and empirical amino acid sequence of Sm1a, Sm1b, and Sm1c. Listed are the amino acid positions where there was a discrepancy between the predicted sequence and the cDNA sequence. Sequence and structural positions are derived from the predicted results seen in Figure 1.4 and Figure 1.1.

| Sequence position | Amino acid variation | Sm1a | Sm1b | Sm1c | Notes |
|-------------------|----------------------|------|------|-------|-----------------------|
| 9 (hA) | N or S | N | N | N | |
| 86 (s2A) | K or Q | K/Q | K | K | |
| 96 (s2A) | L or F | L/F | L | L | |
| 134 (hF) | S or N | N | N | S/N | Unpredicted variation |
| 152 (s3A) | I or L | I | I | L/I | |
| 154 (s3A) | P or C | P | P | C/H | |
| 197 (s3C) | M or L | M/L | M/L | L | |
| 200 (s3C) | E or K | K | E/K | E | |
| 266-7 (s2C) | NT or IM | IM | NT | TT/NT | |
| 268 (s2C) | E or K | K | K | E/K | Unpredicted variation |
| 270 (s2C) | N or R | K | N | N/K | |
| 284 (s6C) | A or T | A | T | A | Unpredicted variation |
| 288 (hI) | D or N | D | D/N | N | |
| 326-9 (s3A) | FEVD or AGTH | FEVD | FEVD | FEVD | |
| 355 (s4B) | V or I | I | V | V | Unpredicted variation |
| 357 (s4B) | E or Q | Q | E | E | Unpredicted variation |

Chapter 2

*SmSrpQ:
An Endogenous Inhibitor of Cercarial Elastase*

Abstract

The larvae of *Schistosoma mansoni* invade their mammalian host by utilizing a serine protease, cercarial elastase (SmCE), to degrade macromolecular proteins in host skin.

The catalytic activity of serine and cysteine proteases can be regulated after activation by serpins. SmSrpQ, one of two *S. mansoni* serpins found in larval secretions [35, 37, 67, 68], is only expressed during larval development and in the early stages of mammalian infection. *In vitro*, ³⁵S-SmSrpQ was able to form an SDS-stable complex with a component of the larval lysate but no complex was detected when ³⁵S-SmSrpQ was incubated with several mammalian host proteases. Formation of a complex was sensitive to the protease active site inhibitors PMSF, Z-AAPF-CMK, and Z-AAPL-CMK.

Western blot analysis of parasite lysates from different life stages showed that when active SmCE was present, a complex of comparable size to SmCE bound to SmSrpQ was detected. SmSrpQ and SmCE are located in adjacent but discrete compartments in the secretion glands of the parasite. Fluorescent immunohistochemical analysis of simulated infection showed co-localization of SmCE and SmSrpQ in host tissue suggesting a post release regulation of parasite protease activity during skin transversal. The results of this study suggest that cercarial elastase degradation of skin tissue is carefully regulated by the invading larvae.

Introduction

Mammalian *S. mansoni* infection begins with larval degradation of extracellular matrix and cell-cell contacts in the dermis and epidermis, respectively. It is then followed by breach of the vascular endothelium, migration of schistosomula to the lungs, prolonged

residence of adults in the hepatic portal system, and egg passage through the intestinal wall (Figure 2a). Proteomic analyses of *S. mansoni* larval secretions have identified several parasite proteins that could function in host immune evasion and/or promotion of parasite survival [37, 68-70]. Using antisera raised against proteins in larval secretions, Harrop et al. published the partial sequence of a serpin (clone 8, AAB86571) with homology to leukocyte elastase inhibitor [67]. The biological function of this schistosome serpin remains principally speculative. Here data are presented that show the complete clone 8 protein, hereafter called SmSrpQ (Smp_062080), is a serpin involved in regulating the activity of a parasite-derived protease within the host.

Experimental Procedures

Parasite material. *S. mansoni* (Puerto Rican isolate) were maintained in the laboratory by using *Biomphalaria glabrata* as the intermediate snail host and golden hamsters (*Mesocricetus auratus*) as the mammalian host. Cercariae were harvested from *B. glabrata* by light induction and washed according to a previously published protocol [71]. Cercariae used for schistosomula production were washed twice in RPMI and mechanically sheared using a 22-gauge needle to remove their tails. They were then cultured for 24-48 hours in Basch *Schistosoma* culture medium 169 (SCM) with 10% fetal calf serum and penicillin/ streptomycin to produce schistosomula. Lung schistosomula were dissected from hamster lungs and adult worms were perfused from hamster livers three days and 6 weeks post infection, respectively. Cercarial/ adult/ snail hepatopancreatic lysates were prepared by freeze/thawing parasites or snail tissue once in an ethanol/ dry ice bath followed by homogenization and sonication using the Sonifier

250 (Branson, USA) at 30% output for 30 seconds. Lysates were centrifuged at 16,000g for 15 minutes in the Centrifuge 5415D (Eppendorf, Germany) and supernatants were collected.

Northern blots and qPCR. Total RNA samples were collected by homogenizing and sonicating tissue in Trizol (Invitrogen) according to manufacturer's instructions. RNA was resuspended in water, and treated with 5 units of DNase I (New England Biolabs) for 1 hour at 37°C. Samples were then heat-inactivated and cleaned using the RNeasy Mini Kit (Qiagen). Concentrations of final total RNA samples were determined using NanoDrop 3300 (Thermo Scientific). For quantitative PCRs and cloning, cDNA was synthesized using SuperScript III Kit (Invitrogen) according to manufacturer's instruction using oligo-dT. A control reaction containing no reverse transcriptase was also carried out. All qPCR reactions were carried out using Roche Light Cycler 480 SYBR green master mix and the Applied Biosystems 7300 Real-Time PCR System. Primers were designed to amplify a 250bp fragment with an amplification program 95°C for 10 min, 45 cycles of 95°C for 30 sec, 55°C for 60 sec and 30 sec at 72°C (forward primer: 5'-GGT TTT ATG GAG ATA TAG TAG AAG AAA AAC AGA GTC ATT CG-3'; reverse primer: 5'-GGT TGA TAG TGA TTG AGA CGA AAA GAG TTC TTG ATT TTT TC-3'). Reactions were carried out in triplicate with cytochrome oxidase (forward primer: 5'-TAC GGT TGG TGG TGT CAC AG-3'; reverse primer: 5'-ACG GCC ATC ACC ATA CTA GC-3') as an internal standard. For northern blots, 5µg of total RNA were denatured in formaldehyde and formamide then loaded onto a 1.1% agarose/formaldehyde gel and run for 90 minutes at 72V. After electrophoresis, RNA was

transferred to polyvinylidene membrane (Bio-Rad) and crosslinked to the membrane using Stratalinker (Stratagene). ^{32}P labeled DNA probes were generated using RediPrime II DNA labeling kit (GE LifeScience) according to the manufacturers instruction. Blots were hybridized overnight at 42°C in 50% formamide, 5X SSC, 4X Denhardt solution, 0.1% SDS, and 0.1% sodium pyrophosphate.

Recombinant protein expression and antibody production. cDNA from cercariae, prepared as described above, was used to subclone SmSrpQ into pET28a+ for *E. coli* over-expression using forward primer 5'-GAG CTC ATG GAT GTA TTA CAA TCC CTT AAA AC-3' and reverse primer 5'-GCG GCC GCT TAA TAT TGA TCT ATT GGA TTT G-3'. The amplicon was first cloned into TOPO-TA pCR2.1 (Invitrogen), digested with *SacI* and *NotI*, and directionally ligated into pET28a+ (Novagen). Plasmids were transformed into Xjb (DE3) autolysing *E. coli* strain (Zymo Research) and induction was carried out according to the manufacturer's instruction. Inclusion bodies were collected and solubilized in 6M guanidine solution (6M guanidine, 100mM Tris, 500mM NaCl, 20 mM imidazole, pH 8.0). Hexa-His-tagged SmSrpQ was bound to Ni^{2+} IMAC agarose beads, washed with 8M urea buffer (8M urea, 100mM Tris, 500mM NaCl, 25mM imidazole) and eluted with 8M urea solution with 500mM imidazole. Purified protein was excised from SDS-PAGE gel and analyzed by mass spectrometry or used for the immunization of 8 week old BALB/c mice. Pre-bleeds were collected and mice received two boosts every 4 weeks. Excised protein gel slices were homogenized in PBS and TiterMax Gold (Sigma-Aldrich) was used as an adjuvant. Rabbit anti-SmCE antibodies were previously generated [36].

Western blots. 10 μ g of crude lysates were incubated at room temperature for 10 minutes in 20mM Tris (pH 7.5) and 25mM NaCl. Samples were boiled under reducing conditions, resolved by SDS-PAGE analysis, and transferred to PVDF membranes. Blots were blocked overnight with 5% milk in TBS-T (Tris buffered saline with 0.25% Tween 20). Blots were incubated for 1 hour at room temperature with mouse anti-SmSrpQ antibodies (1:2000) or rabbit anti-SmCE antibodies (1:2000), washed with TBS-T and then incubated for 1 hour with horseradish peroxidase conjugated IgG (GE Lifescience) (1:2000). Membranes were extensively washed and visualized with ECL western detection reagents (GE Lifescience). Protein concentrations were determined by Bradford assay [72] using Bio-Rad Protein Assay (BioRad, USA) and BSA as a standard. Readings were done using Spectramax Plus 384 (Molecular Devices, USA).

Collection of material from newly transformed schistosomula. Freshly collected cercaria were transformed into schistosomula in RPMI by passing the larvae through a 22 gauge needle 10 times and tails were removed. Schistosomula were cultured in 4 mls of schistosomula culture media containing 2% bovine serum albumin at 37°C. After each incubation period the parasites were removed washed, gently centrifuged, transferred into fresh media, and visually inspected under a microscope to insure viability and intact morphology. At each time point all media was collected including the wash media. Plates were scraped as previously described [68] to remove any adherent secreted granules which were then collected and pooled with the media. 1mM PMSF was added to prevent proteolytic cleavage of proteins. Samples were lyophilized and resuspended in

water for western blot analysis.

Confocal imaging. Parasites were fixed overnight in cold acetone at -20°C then air dried as previously described [73] prior to blocking overnight in blocking buffer (PBS, 0.5% Triton X-100, 5% BSA, and 5% milk). Primary antibody was diluted 1:2000 in blocking buffer and incubated overnight at 4.0°C, followed by three 4hr washes in wash buffer (PBS, 0.5% Triton X-100); secondary antibody (Invitrogen, Alexa Fluor) was diluted 1:2000 in blocking buffer, incubated overnight and washed extensively. Images were taken using the Zeiss LSM 510 Confocal Microscope. All confocal images were taken with the gain and offset values set from negative controls using pre-bleed serum to ensure a low background signal.

Ex vivo skin invasion and immunohistochemistry. Human skin sections were removed from the abdomen of a recently deceased human male in accordance with IRB approved necroscopy practices. Skin samples were washed with RPMI and the subcutaneous fat removed. Cercarial infection was carried out by placing skin sections over warm RPMI filled wells as previously described [71]. After a two-hour incubation at 37°C, skin sections were removed and fixed in 10% phosphate-buffered Formalin (Fisher Scientific), embedded in paraffin, and sectioned. Fluorescent staining was carried out by blocking the sections in 20% normal goat serum in PBS with 0.5% Triton X-100. Antibodies were diluted in PBS with 2% normal goat serum and 0.5% Triton. Primary antibodies were diluted 1:100 and incubated for 2 hours. Secondary antibodies (AlexaFluor, Invitrogen)

were diluted 1:250 and incubated for 1 hour. Slides were mounted in Vectamount with DAPI (Vectashield). Images were taken using the Zeiss LSM 510 Confocal Microscope.

³⁵S-labeled in vitro cell free SmSrpQ expression and inhibitor assays. Reactions were carried out using the TNT Quick Coupled Transcription/ Translation System (Promega, WI) according to the manufacturers instruction. Briefly, the pET28a+SmSrpQ plasmid was linearized downstream of the SmSrpQ ORF using NotI and the transcription/ translation reaction was incubated at 30°C for 90 minutes. All inhibition reactions were performed in 20mM Tris, 25mM NaCl, pH 8.0 at room temperature. Cercarial lysate was incubated for 10 min at room temperature with Z-AAPF-CMK, Z-AAPL-CMK, Z-AAPV-CMK, E-64, or PMSF prior to incubation with ³⁵S-SmSrpQ for 10 minutes at room temperature. CMK inhibitors were purchased from Bachem (Torrence, CA) while PMSF was purchased from Sigma-Aldrich (St Louis, MO).

Transverse urea gels (TUGs). Transverse urea gels were pored as previously described [74]. Briefly, 7.5 % non-denaturing PAGE gels containing a urea gradient were created by making two volumes of gel mixture. One contained 8M of the denaturant urea and the other contained no urea. Gels were slowly pored using a gradient maker. After solidification, gels were turned 90° such that the urea gradient ran horizontal to the path of the electric field (Figure 2. 1b). Radiolabeled sample of SmSrpQ was mixed with native loading buffer (Invitrogen) and evenly distributed across the top of the gel. Electrophoresis was carried out at 75V for 2 hours using Tris-Glycine-SDS (Bio-Rad)

running buffer. SDS was added to the buffer do to difficulties with the sample entering the gel matrix.

RESULTS

qPCR and northern blot analysis of SmSrpQ transcript levels. The full-length amino acid sequence of clone 8 was completed and renamed SmSrpQ. The predicted P1-P1' RCL specificity was determined to be Leu-Ser (Figure 2. 1a). qPCR analysis revealed that SmSrpQ is expressed in the late schistosome sporocysts when cercariae are completing development in the intermediate snail host, and in aquatic free-swimming cercariae. Transcript levels remained high in cercariae-derived schistosomula after 24 hours of *in vitro* culturing (Figure 2. 2b). These life stages correspond to the early skin invasion stages of infection (Figure 2. 2a). Peak mRNA transcript levels were seen in the cercarial stage. There was less transcript signal in early daughter sporocysts. To verify this expression profile in the life stages where snail RNA might mask the qPCR signal of schistosome transcripts, northern blot analysis was performed (Figure 2. 2c). DNA probes detected peak transcripts in late sporocysts. Transcripts were also detected in daughter sporocysts when cercarial development commences and in cercariae. SmSrpQ was not detected in adult worms. Northern blot analysis also did not detect any expression in egg/ miracidia total RNA extracts.

Functional expression of SmSrpQ. The amino acid sequence of SmSrpQ contains all the components necessary to function as an inhibitory serpin [75]. To confirm its ability to act as a suicide substrate inhibitor and form a complex with proteases, radiolabeled

6X-His tagged SmSrpQ (Figure 2. 1a) was produced using a cell free transcription/translation reaction. The reaction yielded the expected 49 kDa serpin protein (Figure 2. 3a) in which half of the ^{35}S -SmSrpQ was in the inhibitory conformational fold and the remaining in the latent conformation (Figure 2. 1c). The recombinant serpin formed a complex with a component of the cercarial lysate, producing a product of approximately 68 kDa (Figure 2. 3a, black arrow). A lower molecular weight band was also detected consistent with the cleaved serpin (Figure 2. 3a, double arrow). ^{35}S -SmSrpQ only bound to a protease species found in the late sporocyst and cercaria stages. ^{35}S -SmSrpQ did not bind to any components of the lysate from early daughter sporocysts, uninfected snail or adult worms (Figure 2. 3b). ^{35}S -SmSrpQ was not able to form a complex with neutrophil elastase, chymotrypsin (Figure 2. 3c), pancreatic elastase, or recombinant human chymase (data not shown). To confirm that the serpin-protease complex was formed via the enzyme active site, the crude cercarial lysate was preincubated with PMSF, a small molecule chemical inhibitor that irreversibly modifies the active site serine of serine hydrolases (Figure 2. 4). At 400, 200, and 100 μM of PMSF, uncleaved ^{35}S -SmSrpQ (double arrow, lane 3, 4, and 5 respectively) was detected. In the methanol control (lane 2) both cleaved and complexed ^{35}S -SmSrpQ are seen, the presence of uncleaved serpin correlated with a corresponding decrease in amount of complex detected (black arrow) as evidenced by a decrease in band intensity.

To examine the active site P1 specificity of the serpin-targeted protease, the lysate was preincubated with tetrapeptide chloromethylketone (CMK) inhibitors and the formation of the serpin-protease complex was assessed. Complex formation was highly sensitive to

Z-AAPF-CMK. 25 μ M Z-AAPF-CMK decreased complex formation by 39% when compared to the DMSO control reaction (Figure 2. 5a). Z-AAPL-CMK also had an effect at 200 μ M and 100 μ M while preincubation with Z-AAPV-CMK had no effect on complex formation (Figure 2. 5b).

Western blots of SmSrpQ and SmCE during early life stages. The predicted specificity of the RCL of SmSrpQ, the sensitivity to PMSF, and the specific effects of the CMK inhibitors were all consistent with the previously reported biochemical characteristics of SmCE [38]; SmCE is the major protease found in larval stages. To confirm the presence of a protein complex between endogenous SmCE and SmSrpQ, western blots were performed on the crude lysates from different life stages. The lysates were incubated at 25°C for 10 minutes to allow a complex to form. Western blots of uninfected snails and adults detected no SmSrpQ (Figure 2.6a, lane 1 and 5 respectively). Although, SmSrpQ protein (double arrow) was detected in the daughter sporocysts, no complex (black arrow) was seen. Late sporocysts and cercarial lysates contained both unbound SmSrpQ and complexed serpin (Figure 2. 6a, lane 3 and 4 respectively). The size of the complex was approximately the same size and in the same life stages as the 68 kDa complex detected with the *in vitro* translated ³⁵S-SmSrpQ. Protein levels of SmSrpQ were higher in the cercarial stage than in late sporocysts. Active SmCE protein (Figure 2. 6b, open arrow head) was found in the lysates of late sporocysts and cercariae. Daughter sporocysts exclusively contained the higher molecular weight, inactive zymogen (Figure 2. 6b, black star). The higher molecular weight band corresponding to a complex

between SmCE and SmSrpQ was detected in late sporocysts and cercarial lysate (Figure 2. 6b, black arrow).

Localization of SmSrpQ within the parasite. Given that SmCE and SmSrpQ are produced by the parasite at similar time points and SmCE appears to be active in late sporocysts and cercariae the question was raised: does SmSrpQ prevent parasitic tissue damage from SmCE activity within the parasite? To address this question, localization studies of the SmSprQ and SmCE in cercariae, 24hr schistosomula, and three day old lung stage schistosomula were performed to identify the location and any interaction of SmSrpQ and SmCE. *S. mansoni* larvae contain several secretory glands that release material onto and into the host during skin invasion: the post-acetabular glands, the pre-acetabular glands, and the head glands (Figure I. 3). Factors needed for parasite binding and penetration are packaged in acetabular secretory granules and exit from extended cellular processes called ducts. These cell processes extend along the body of the larva to allow release of secretions into the environment at the head of the parasite [76]. Confocal images show that SmSrpQ was located in the post-acetabular glands and their corresponding ducts, in one set of pre-acetabular glands, and the head gland of the cercaria (Figure 2. 7a, red). In 24 hour schistosomula residual SmSrpQ is seen in similar regions of the parasite (Figure 2. 7b, red) except that no serpin protein was detected in the head gland. In the cercaria, SmCE was located in a separate set of pre-acetabular glands and their corresponding ducts (Figure 2. 7a, blue). In the 24hr schistosomula, SmCE is found as residual protein in the pre-acetabular glands (Figure 2. 7b, blue). SmCE was neither detected in the head gland nor in the post-acetabular glands. Lung stage

schistosomula isolated from infected hamsters had virtually no SmSrpQ and SmCE (Figure 2. 7c). The tegument and other cells of the larvae were free of SmSrpQ and SmCE at all three time points.

SmSrpQ and SmCE release and ex vivo skin co-localization. Lacking co-localization on the tegument and within the parasite, it was asked if regulation of SmCE activity by SmSrpQ occurred outside of the parasite and if release of these two proteins was temporally regulated. Newly transformed schistosomula were placed in SCM with 2% BSA and incubated at 37°C. Their secretions were collected at 30 minute to 1 hour intervals and analyzed by western blot. Release of SmSrpQ (Figure 2. 7a) and SmCE (Figure 2. 8b) was greatest after 30 minutes incubation. The remaining time points show a similar waxing and waning pattern of release for both proteins.

To localize SmSrpQ and SmCE during infection, a skin infection was simulated by exposing human skin sections to cercariae for two hours. SmCE and SmSrpQ co-localized in human skin in zones of tissue degradation both in the dermis and superficial epidermis (Figure 2. 9b, section 6, magenta). Some SmSrpQ remained within the parasite (Figure 2. 9b, black star) but none localized to the tegument or other cells of the organism.

DISCUSSION

SmSrpQ is a serpin originally identified in the secreted products of invading *S. mansoni* larvae (cercariae). Northern blot and qPCR analysis showed that SmSrpQ is expressed

from the initiation of cercarial development in daughter sporocysts until 24-hour schistosomula. This suggests that SmSrpQ plays a role in the early stages of infection when cercariae and schistosomula invade host skin to enter dermal blood vessels. No transcripts were found in adult worms or the egg/ miracidium stage nor was SmSrpQ protein detected in lung stage schistosomula. Recombinant SmSrpQ was unable to bind host proteases, namely, neutrophil elastase (Figure 2. 3c) and cathepsin G (data not shown) but was able to complex with a component of the larval lysate. PMSF, a serine protease inhibitor, blocked serpin-protease complex formation (Figure 2. 4).

Invasion of human skin by *S. mansoni* requires the disruption of the epidermal cell layer, the basement membrane, and the extracellular matrix of the dermis. Host desmosome proteins, complement factors, immunoglobulin, as well as epidermal cell lysis products are examples of protein degradation produced in the wake of larval invasion [35]. Extracellular matrix and cell-cell junction degradation has been attributed to serine protease activity, particularly to SmCE [36, 38, 77, 78]. SmCE is one of the most abundant proteins in cercarial secretions [37]. A synthetic tetrapeptide library screen of purified native SmCE showed that the S1 pocket of the protease prefers a Leu, Phe, or Met substrate sidechain [36]. The primary sequence of SmSrpQ predicts a Leu-Ser in the P1-P1' position in the reactive center loop (Figure 2. 1a).

Z-AAPF-CMK is an effective inhibitor of cercarial invasion and a known inhibitor of SmCE [71]. When cercarial lysates were preincubated with Z-AAPF-CMK a marked reduction in complex formation with SmSrpQ was observed (Figure 2. 5a). This is in

contrast to the complete lack of effect on complex formation following preincubation of the lysate with Z-AAPV-CMK (Figure 2. 5b), which does not inhibit SmCE but does inhibit neutrophil elastase [79]. Western blots of lysates confirmed that complex formation only occurs when active SmCE -was present (Figure 2. 6). In early daughter sporocyst lysates, where only the SmCE zymogen form was present, no complex with SmSrpQ was detected.

One potential role for SmSrpQ, as a cytosolic serpin maybe to prevent parasite tissue damage in the event of accidental SmCE release. This would be similar to monocyte/neutrophil elastase inhibitor (MNEI), which is an intracellular serpin of cells of the myeloid lineage [80]. This potent inhibitor of neutrophil elastase, cathepsin G, and chymase [81], lacks a signal sequence, and functions to protect granulocytes from intracellular release of protease found in azurophilic granules [81]. Localization of SmSrpQ versus SmCE (Figure 2.7a) suggests it is unlikely that SmSrpQ interacts with SmCE inside the parasite given SmSrpQ is in the head gland, post acetabular, and disparate set of pre-acetabular glands, while SmCE resides in the adjacent set of pre-acetabular glands. The complex formation seen by western blots (Figure 2. 6) is likely due to the break down of this spatial/cellular barrier between these two proteins upon lysis of the parasite. Electron-micrograph localization in frozen thin sections showed SmCE in both pre- and post acetabular glands [77] but subsequent studies using confocal imaging have not detected SmCE in the post-acetabular glands [82].

The co-localization of SmSrpQ and SmCE (Figure 2. 9b) in human skin invasion assays suggests that the parasite is regulating the ECM degrading activity of SmCE in the host. This role for SmSrpQ is similar to that of α 1-antitrypsin in lung tissue. Patients with an α 1-antitrypsin deficiency suffer from severe early onset emphysema. This condition results from an imbalance in neutrophil elastase proteolytic activity in bronchial and alveolar tissue [83]. During inflammation leukocytes release ECM degrading enzymes, such as neutrophil elastase, that may inadvertently cause tissue damage [84]. α 1-Antitrypsin and to a lesser extent α 2-macroglobulin regulates elastase activity and limits the ECM damage in the lung. Like schistosome cercariae, inflammatory cells such as macrophages and monocytes secrete both protease and the corresponding inhibitors [84].

Inflammatory damage to host skin tissue, called cercarial dermatitis, can be observed with the accidental infections of humans by avian schistosomes, such as *Trichobilharzia regenti*, that are not adapted to a human host. Initial infection with *T. regenti* larvae causes an acute inflammatory response characterized by edema, thickening of the skin, and a large infiltration of mast cells, neutrophils, and other leukocytes [85] leading to the killing of most parasites within the dermal tissue. *S. mansoni* is a schistosome more adapted to the human host. Infection experiments using human skin [86] or a mouse model [41] have shown a limited immune response to invading larvae with no significant parasite killing, resulting in parasites being able to enter the host blood vessels.

Dermatitis can occur after a heavy exposure to cercariae, but symptoms subside after 48 hours and the rare cases are confined to non-sensitized individuals e.g. tourists [87].

S. mansoni effectively invades intact skin and has developed multiple mechanisms to evade the host immune response and establish an infection that can debilitate but not kill the host. The tight post-translational regulation of SmCE by SmSrpQ may represent an adaptation to limit host tissue damage to the region of larval invasion and minimize any ensuing innate immune response. Concomitant release of SmSrpQ and SmCE in human skin may be an adaptation to prevent severe inflammation due to excessive or uncontrolled damage to host cells/ tissue.

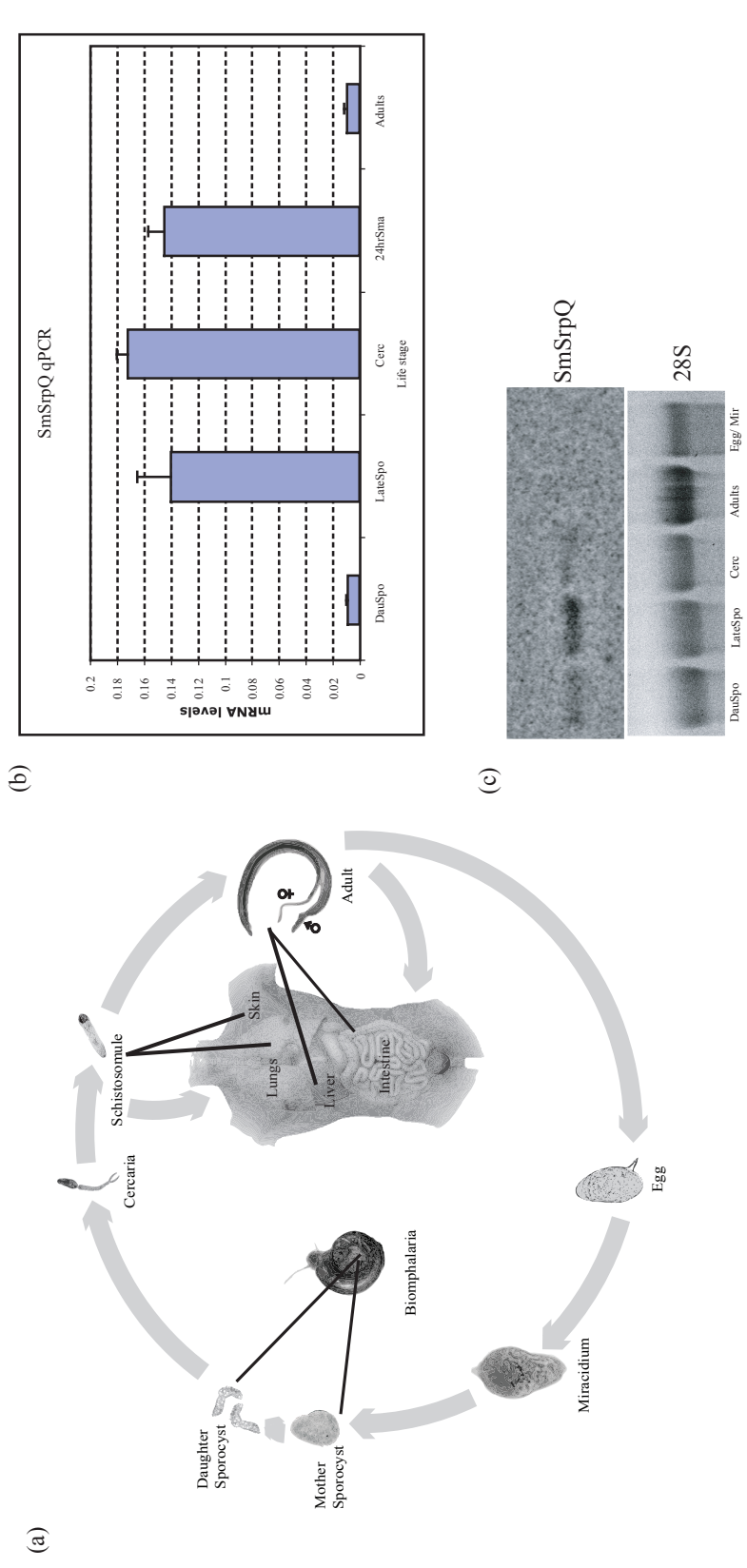


Figure 2. 2: *SmSrpQ* mRNA levels during *S. mansoni* developmental life cycle. (a) The life cycle of *S. mansoni*. In addition to the free swimming miracidium and cercaria, shown are the stages in the molluscan intermediate host: mother sporocysts, daughter sporocysts (early and late) which give rise to cercariae (late sporocysts contain unreleased cercariae and differentiating sporocysts); the mammalian stages: schistosomula and adults. (b) PCR of *SmSrpQ* during the parasitic life cycle: early daughter sporocysts (35 days post snail infection), late sporocysts (8 weeks post infection), free swimming cercariae (after exiting the snail), transformed cercariae after 24hr incubation at 37°C (schistosomula, Sma), and fully matured paired worms removed from hamster host. Reactions were performed in triplicate and normalized to *S. mansoni* cytochrome oxidase expression. (c) Northern blot analysis of mRNA. In addition to daughter sporocysts, late sporocysts, cercaria, and adults, shown are the egg/miracidium stage not shown in the qPCRs. 28S RNA was used as a loading control.

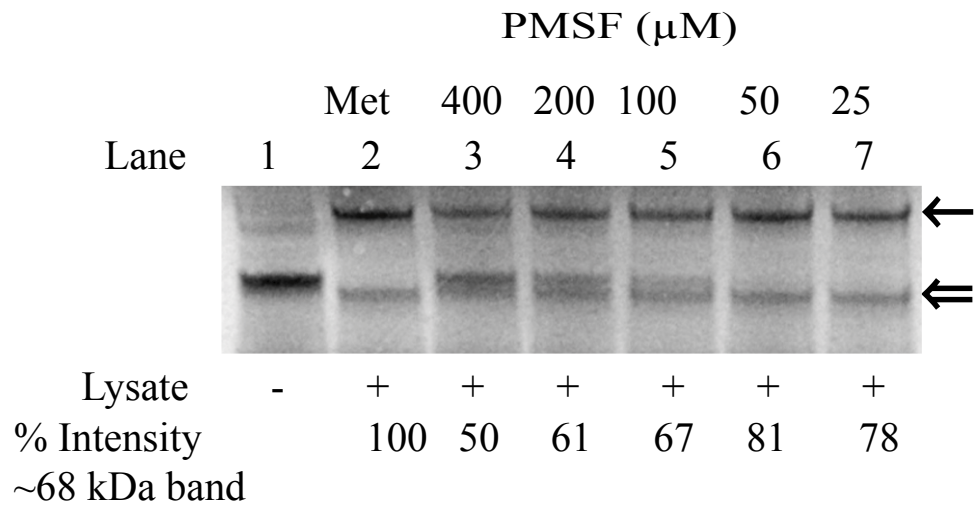


Figure 2. 4: Effect of active site inhibitor PMSF on complex formation. Cercarial lysate was preincubated with small molecule inhibitors for 10 min at RT, followed by incubation with ^{35}S -labeled SmSrpQ. Lysates were incubated with decreasing concentration of PMSF (lane 3-7) or methanol (lane 2). The effect of PMSF was measured by comparing the band intensity of the complex (black arrow) to the methanol control. The double arrow denotes the presence of cleaved as well as uncleaved serpin.

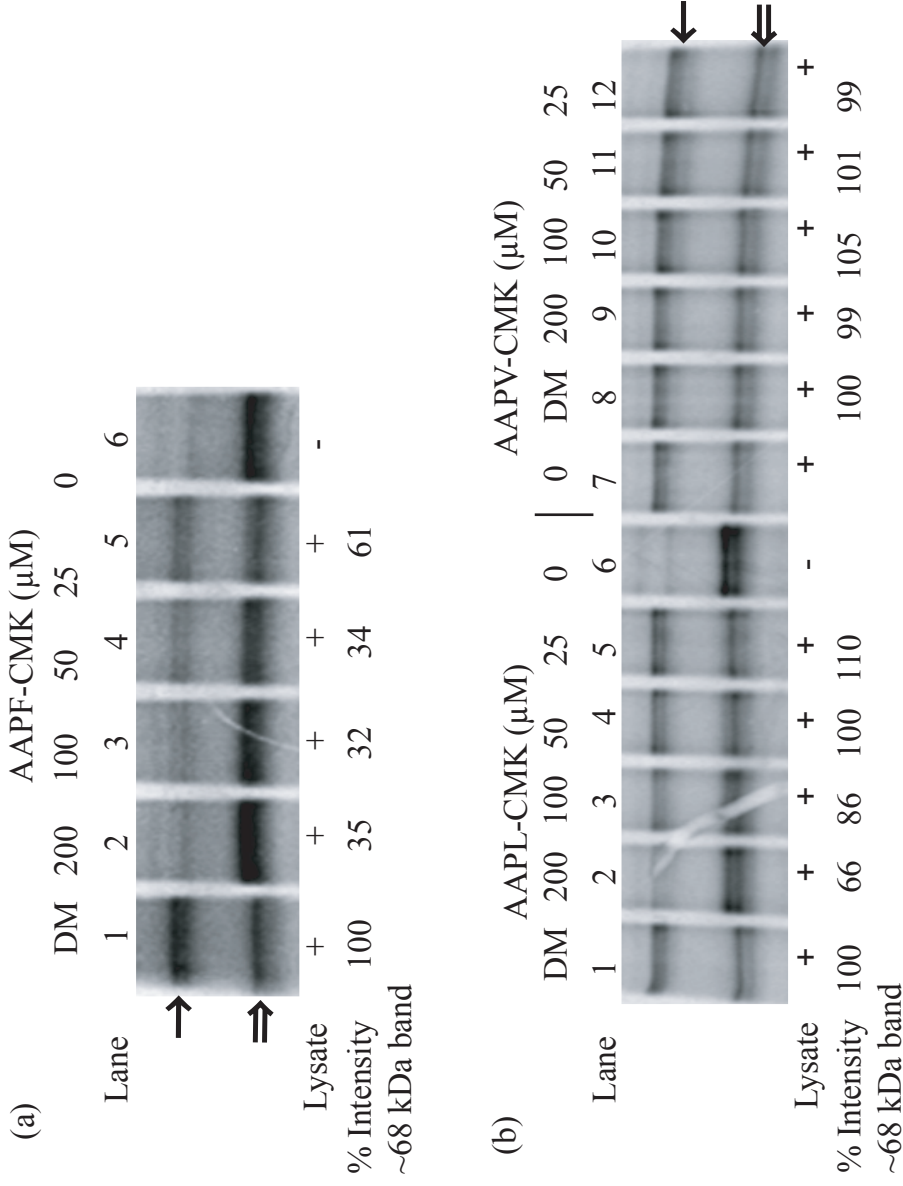


Figure 2. 5: Effect of chloromethyl ketone inhibitors on complex formation. Cercarial lysates were preincubated with small molecule inhibitors for 10 min at RT, followed by incubation with 35 S-labeled SmSrpQ. Lysates were incubated with decreasing concentration of (a) AAPF-CMK and (b) AAPL-CMK and AAPV-CMK. DM represents the DMSO control. E64, calpain inhibitor I and II, calcium, and EDTA had no effect (data not shown).

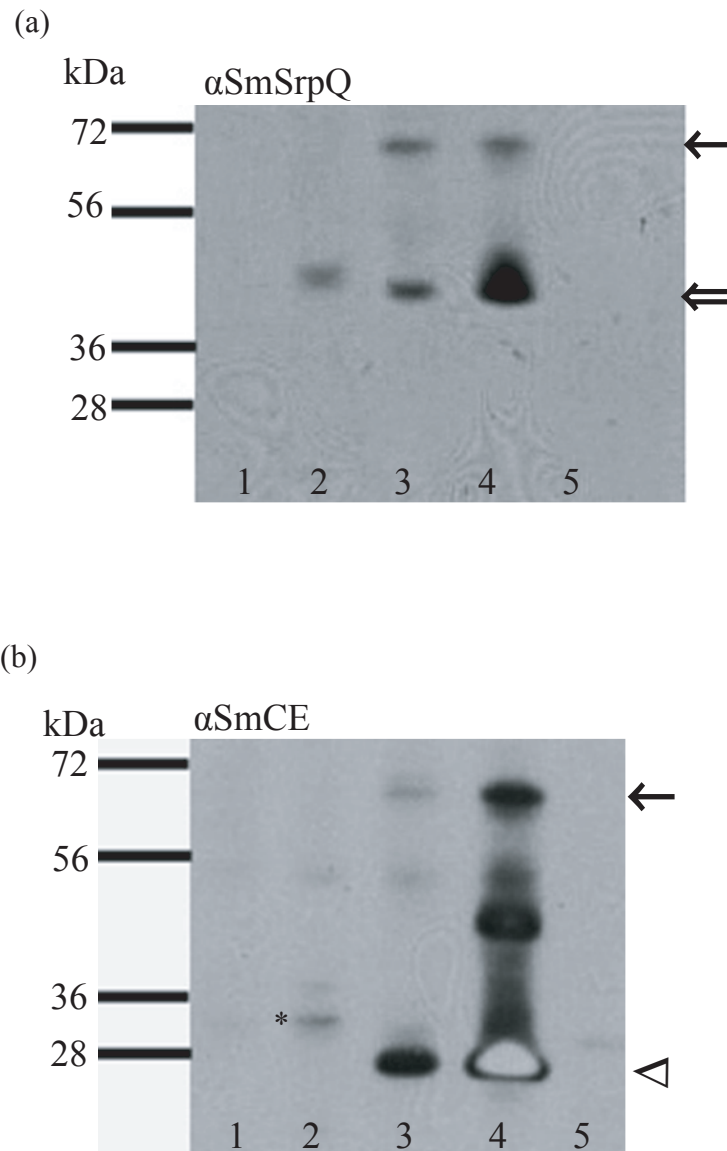


Figure 2. 6: *Life cycle western blot analysis.* Western blot analysis of (a) SmSrpQ and (b) SmCE protein levels during early parasite development. Primary antibodies were diluted 1:2000. Approximately 5 μ gs of each lysate was used. Lane 1: noninfected snails; lane 2: snail lysate 35 days post infection (daughter sporocysts); lane 3: snail lysate 8 weeks post infection (late sporocysts); lane 4: cercarial lysate; and lane 5: adult lysate. Upper band is marked by black arrow, uncomplexed SmSrpQ is marked by double arrow, open arrowhead denotes active SmCE, and SmCE zymogen is marked by a black star.

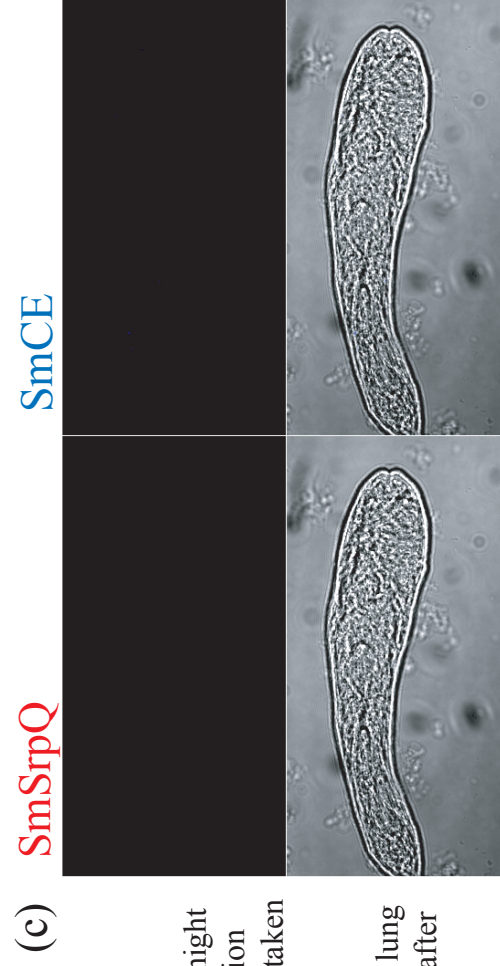
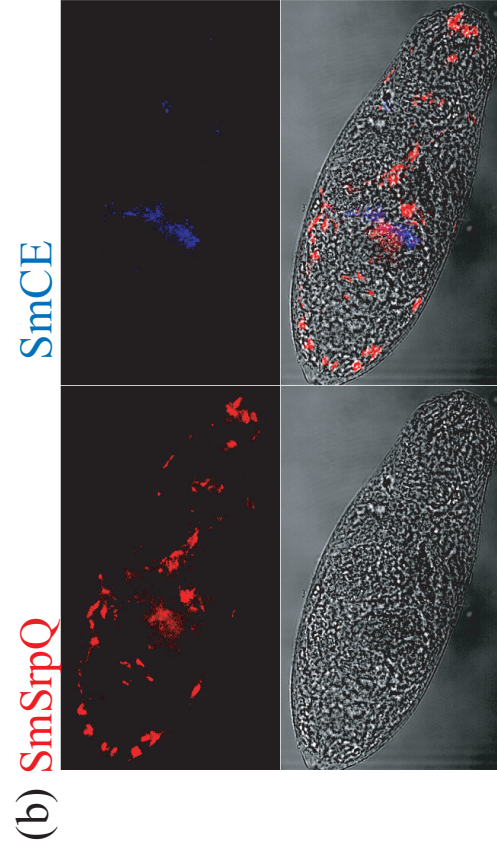
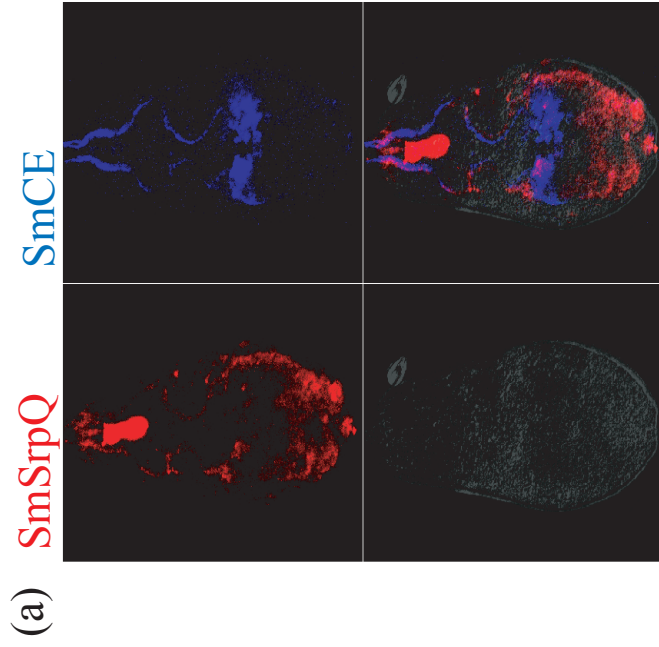


Figure 2. 7: Localization of SmSrpQ and SmCE. Parasites were fixed with cold acetone, incubated overnight with primary antibodies followed by overnight incubation with the Alexa-fluor secondary antibody. Images were taken of (a) recently shed cercariae prior to transformation to schistosomula, (b) cercariae that are transformed into schistosomula and incubated for 24hrs at 37°C, and (c) lung stage schistosomula isolated from the hamsters 3 days after infection.

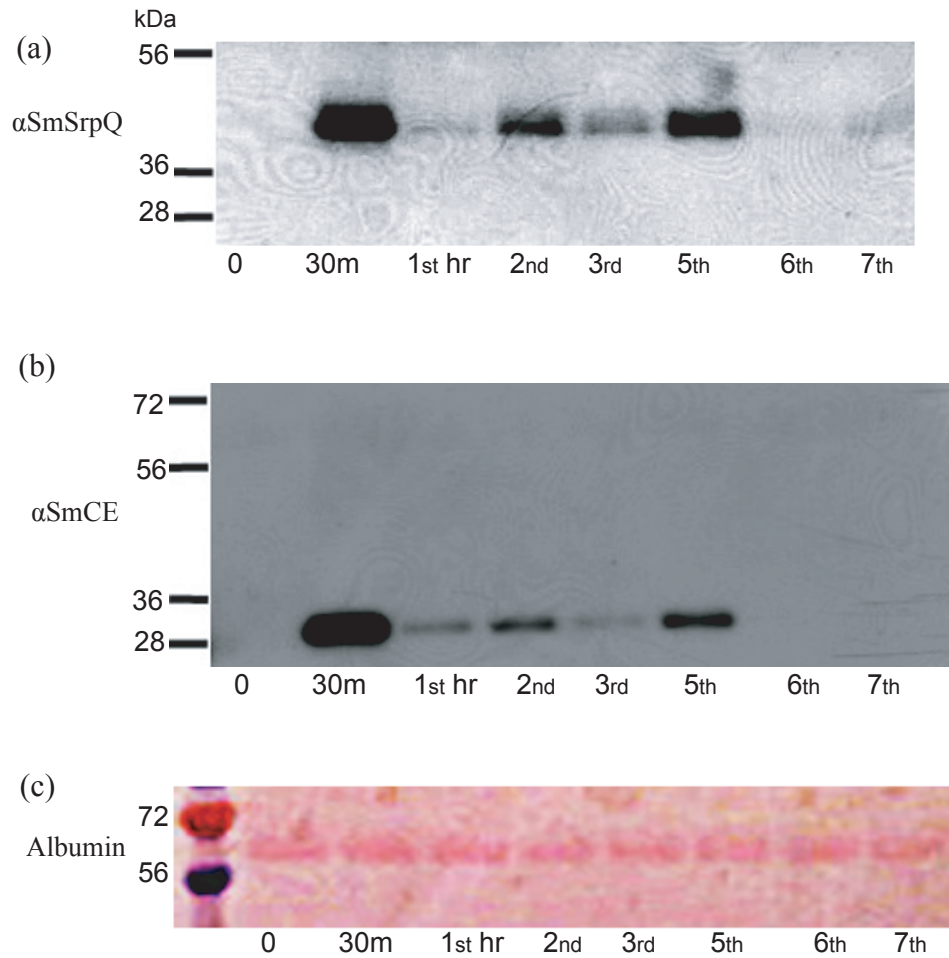
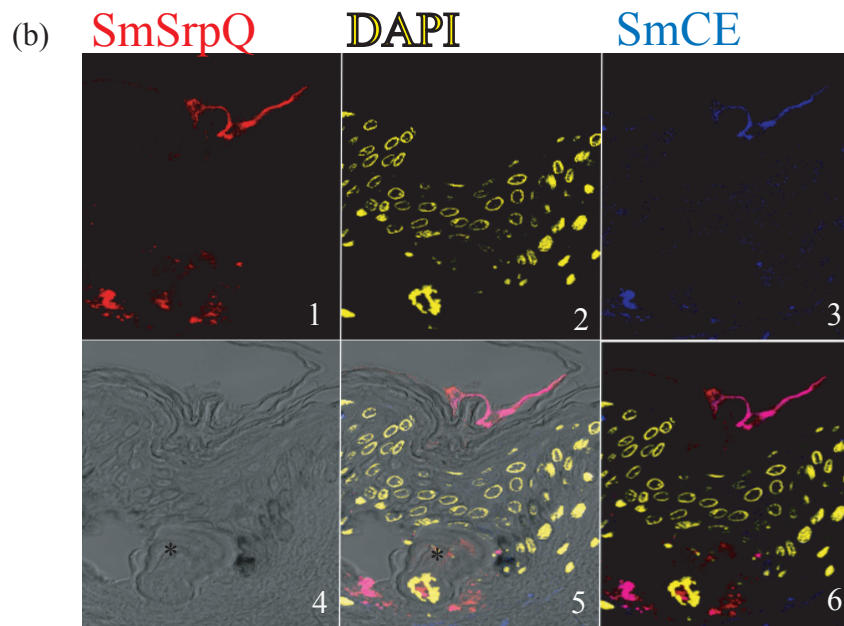
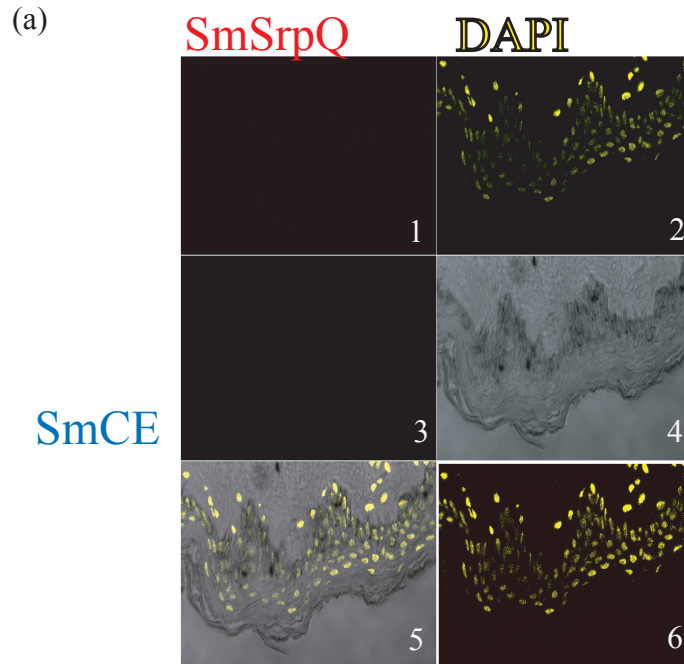


Figure 2. 8: *Secretion of SmSrpQ and SmCE by schistosomula.* The proteins released from newly transformed schistosomula were collected over time. 10 µgs were loaded and western blots were performed probing for SmSrpQ (a), SmCE (b). Blots were ponceau stained and shown is the BSA used as a loading control (c).



Co-localization

Figure 2. 9: Immunolocalization of SmSrpQ and SmCE during a mock infection. The release of SmSrpQ and SmCE during a simulated infection of human skin tissue was visualized using the red channel for SmSrpQ (panel 1), blue channel for SmCE (panel 3), yellow channel is for DAPI which stains the nuclei of epidermal and parasite cells (panel 2), co-localization is shown in magenta (panel 5, 6).

Chapter 3

Expression and Purification of SmSrpQ & SmSerp_C

Abstract

SmSrpQ and SmSerp_Q are released by the *S. mansoni* larvae during skin penetration. To further understand their biological role and biochemical properties, both of these proteins were recombinantly expressed. SmSrpQ was expressed in *S. cerevisiae*. High levels of rSmSrpQ were achieved by fusing the serpin to the human ubiquitin protein and placing expression under the control of the GAPDH promoter rather than the ADH2 promoter. The expression of rSmSerp_C was achieved using *E. coli* and pET28a+. Furthermore, radio-labeled SmSerp_C was able to complex with trypsin, human plasma kallikrein, and a molluscan tryptic serine protease, most likely a *B. glabrata* trypsin. SmSrpQ inhibition of SmCE, shown previously in Chapter 2, and SmSerp_C inhibition of kallikrein and a snail protease indicate the inhibitory nature of these serpins and their potential role in the pathogenesis/ biology of the parasite.

Introduction

Heterologous expression of serpins has been achieved in many expression systems. Which system works best will depend on the individual composition of the serpin. Unlike recombinant expression of other proteins, each expression system carries the added risk of endogenous proteases cleaving the reactive center loop or forming a complex with the recombinant serpin, rendering an unusable serpin protein. Of the serpins from *S. mansoni*, SmSrpQ and SmSerp_C, were expressed in the early stages of larval development (Figure 1. 2) and have been isolated from the secreted content of the invading larva [37, 67]. Thus, these two serpins appear to play a role in pathogenesis.

Heterologous expression of SmSrpQ and SmSerp_C would be instrumental in understanding early parasite invasion of the human skin.

Producing the schistosome serpin of interest in sufficient quantities is necessary for carrying out kinetic analysis of enzyme inactivation, antibody production, and for obtaining crystal structures among other experiments. In the case of SmSrpQ, several expression systems failed to produce active serpin protein (unpublished data). *E. coli* expression yielded cleaved serpin and the majority of the recombinant protein produced was found in inclusion bodies. Even though human plasminogen activator inhibitor-1 [88] and α 1-antitrysin [89] have been successfully refolded from inclusion bodies, this was not the case with SmSrpQ. The baculovirus expression system has also lead to successful serpin expression [90, 91] but insect cells only produced inactive full length SmSrpQ (data not shown). Intracellular yeast expression using *Saccharomyces cerevisiae* is a system that yielded high levels of active serpin in several cases [rev in 92] and was used to express SmSrpQ.

Unlike bacterial expression of SmSrpQ, high level of soluble protein was obtained of rSmSerp_C using *E. coli* strain BL21(DE3). Here we present work cloning, expressing, and purifying SmSerp_C and SmSrpQ using two expression systems.

Experimental Procedures

Construction *S. cerevisiae* expression plasmids. For intracellular yeast expression two plasmids were constructed: pBS24.1SmSrpQ and pBS24.1GapSmSrpQ2. Cloning of

SmSrpQ into pBS24.1 involved the removal of an internal *Bam*HI site SmSrpQ using internal primers (reverse: 5'-CAG CAT CTT CGG GGT CCA TCT GAA ACG CCA CAG ATT C-3'; forward: 5'-CTG TGG CGT TTC AGA TGG ACC CC-3'). The primer at the 5' end incorporated a *Xba*I restriction site and a 6X-His tag (5'-TCT AGA ATG GAT CAT CAC CAT CAC CAT CAC GAT GTA TTA CAA TC-3'). A *Sal*I restriction site was incorporated at the 5' end of SmSrpQ (reverse primer: 5'-GTC GAC TTA ATA TTG ATC TAT TGG ATT TGT AAC ATG TCC-3'). SmSrpQ was amplified from cercarial cDNA and cloned into TOPO-vector pCR2.1 (Invitrogen). *Sal*I and *Xba*I sites were used to clone the SmSerpQ insert from pCR2.1 into the yeast shuttle vector pAB125 creating a fusion gene containing the alcohol dehydrogenase 2 promoter (ADH2p) upstream of SmSrpQ. This fusion gene was cloned into the expression vector pBS24.1 using *Bam*HI and *Sal*I restriction site (Figure 3. 1a). pBS24.1 contained with URA3 and LEU2d genes needed for auxotrophic selection of recombinant yeast clones. For the construction of pBS24.1GapSmSrpQ2 (Figure 3. 1b), the codon for SmSrpQ was resynthesized to favor the yeast codon usage; a 5' *Sac*II restriction site and 6X-His tag, and a 3' *Sal*I were also added to the resynthesized gene: SmSrpQ2 (Figure 3. 2). Resynthesis was carried out by GenScript (USA). The protein sequence of SmSrpQ remained unchanged. SmSrpQ2 was amplified (F: 5'- CCG CGG TGG TGG TCA TCA TCA TCA TCA TCA T-3' and R: 5'-GTC GAC TCA TCA GTA TTG GTC TAT TGG GTT-3'), cloned into pCR2.1 and digested with *Sac*II and *Sal*I. The insert was ligated to yeast vector pBM100 (courtesy of Phillip Barr) creating a fusion gene containing the human ubiquitin protein under the control of the glyceraldehyde-3-phosphate dehydrogenase (GAPDH) promoter. *Bam*HI and *Sal*I restriction sites were used to clone

the fusion gene into pBS24.1 and thus creating pBS24.1GapSmSrpQ2 (Figure 3. 1b). pBS24.1GapAAT (Figure 3. 1c) contained the resynthesized human α 1-antitrypsin-ubiquitin fusion protein. It was used as a positive control.

Yeast transformations. *S. cerevisiae* strain BJ2168(circle-) was used for all yeast expression (courtesy of Phillip Barr). Yeast cells were grown at 30°C. Yeast were transformed in lithium acetate (LiAc) as previously described [93]. Briefly, overnight cultures of BJ2168 were diluted to OD₆₀₀=0.02 and then grown until OD₆₀₀ was between 1.5 and 2.0 in 50 mls of YPD media. They were then collected and washed twice with water. Cells were resuspended in one ml of water and 100 μ l of cell suspension was used for each transformation. Cells were pelleted and resuspended in 100mM LiAc, 35% PEG, 100 μ g of denature salmon sperm DNA, and concentrated plasmid samples. This transformation mix was incubated for 40-50 minutes in a 42°C water bath. Cells were then washed and resuspended in water. Transformants were plated in fresh SC-Ura. Colonies were streaked in SC-Ura media and single colonies were selected for expression. Transformations were verified by PCR.

Expression of SmSrpQ. Induction of yeast strains containing pBS24.1SmSrpQ were carried out by growing transformants for 72 hours in SC-Ura with 8% glucose followed by 48 hours of growth in YPD. Cells were then washed to remove excess glucose and resuspended in SC-Ura with 8% succinate. After 48 hours, yeast cells were pelleted and lysed using a microfluidizer. Cleared lysate was used for purification. Yeast transformants containing pBS24.1GapSmSrpQ2 were grown in SC-Ura with 8% glucose

for 72 hours and then in YPD for 48 hours. Cells were collected, lysed in nickel binding buffer (100mM Tris, pH 8.0, 750 mM NaCl) and cleared lysates were used for protein purification. Alternatively, when the first step of purification was ion exchange, lysis buffer consisted of 20 mM Tris (pH 8.0) and 25 mM NaCl. All lysates contained 200 μ l of yeast protease inhibitor cocktail (Sigma). Whole lysates were analyzed using SDS-PAGE for initial screenings.

Purification of SmSrpQ. One tablet of EDTA-free protease inhibitor cocktail (Roche) was added to each lysate. When ion exchange was the initial purification step, lysates were passed through 5ml Q-Sepharose HP column (HP-Q, General Electric) using the Acta FPLC (Pharmacia). Protein was eluted using 20 mM Tris (pH 8.0) and 1M NaCl. Pooled eluted HP-Q samples or the initial lysates were incubated with nickel agarose beads for 2 hours. Beads were then washed overnight at 4.0°C followed by two more washes with nickel wash buffer (100mM Tris, pH 8.0, 750 mM NaCl, 25 mM imidazole). Recombinant protein was eluted in 100mM Tris (pH 8.0), 750 mM NaCl, 500 mM imidazole. Protein samples were analyzed by SDS-PAGE and western blots.

Cloning and expression of SmSerp_C. SmSerp_C was amplified from late sporocyst cDNA using forward primer: 5'- GAG CTC ATG GGT TTC ACA ACT AAT G-3' and reverse primer: 5'-GTC GAC TCA TTT ATT GTT CGT TAA AG-3'. *SacI* and *SalI* restriction sites were incorporated to the 5' and 3' end, respectively. PCR product was gel purified and cloned into TOPO-TA plasmid pCR4.0 (Invitrogen). The clones were digested with *SacI* and *SalI* and ligated to pET28a+ (Novagen) (Figure 3. 1d). *E. coli*

strain BL21(DE3) chemically competent cells (Stratagene) were transformed with pET28aSerp_C plasmids according to the manufacture's instructions. Colony PCRs were used to verify the presence of SmSerp_C in bacterial transformants. Inductions were carried out by diluting overnight cultures 1/100 in luria broth (with kanamycin). Cells were grown for 3 hours and they were then split. Half of the cells were induced with 0.5mM IPTG (Roche) and the other half was left without IPTG. Cell were then grown for 3 hours and then pelleted and washed.

Ion exchange and nickel purification of SmSerp_C. Initial colony screening was conducted by collecting cells and resuspending them in water and SDS-loading buffer (Invitrogen) with DTT. Samples were boiled for 10 minutes and 10 μ l were loaded on 4-12% Bis-Tris SDS gels (Invitrogen). Crude nickel purifications for screening purposes were conducted by denaturing whole cells in 6M Guanidine-HCl. The mixture was spun at 13000g for 15 minutes. His-tagged SmSerp_C was purified using Qiagen nickel spin columns and purification was done per manufacturer's recommendation under denaturing conditions. Large scale purification of soluble *E. coli* lysate was carried out by resuspending cell pellets in 50 mM sodium phosphate buffer (pH 7.0) and one tablet of protease inhibitor cocktail (Roche). A microfluidizer was used to lyse the bacterial cells. Cell lysate was spun for 40 minutes at 25000g. The supernatant (soluble fraction, SF) was loaded onto a SP-sepharose FF (General Electric) column and purification of positively charged proteins was conducted using an Acta Purifier FPLC (Pharmacia). Eluted proteins were incubated with nickel agarose beads (Qiagen) for 2 hours. Beads were then washed overnight at 4.0°C followed by two more washes with nickel wash buffer (100ml

Tris, pH 8.0, 750 mM NaCl, 25 mM imidazole). Recombinant protein was eluted in 100mM Tris (pH 8.0), 750 mM NaCl, 500 mM imidazole. Protein samples were analyzed on SDS-PAGE gels. Mass spectrometry analysis was conducted by the UCSF Mass Spectrometry Facility (San Francisco, California)

In vitro translation of ³⁵S- SmSerp_C and complex formation assays. Reactions were carried out using the TNT Quick Coupled Transcription/ Translation System (Promega, WI) according to the manufacturers instruction. This system required the use of an expression plasmid under the T7 promoter. Briefly, the pET28aSmSerp_C plasmid was linearized downstream of the SmSerp_C ORF using *XhoI* and the transcription/ translation reaction was incubated at 30°C for 90 minutes. Complex formation assays with SmSerp_C and trypsin (Sigma), plasma kallikrein, cercarial lysates, and snail lysates were carried out at 30°C for 8-10 mins in 20mM Tris (pH 8.0) and 25 mM NaCl. Thrombin (Sigma) assays were for 10 mins at 30°C in 100 mM NaCl, 25 mM CaCl₂, 0.1 units of heparin. Coagulation Factor Xa was incubated with SmSerp_C in 20 mM Tris (pH 7.4), 700 mM NaCl, and 25 mM CaCl₂ for 10 min at 30°C. Assays were analyzed with SDS-PAGE. Gels were dried and visualized with phosphoimage screens (General Electric) and the Typhoon Trio (GE Lifesciences).

Results

Expression and purification of rSmSrpQ. Expression of SmSrpQ using the pBS24.1SmSrpQ construct was under the ADH2 promoter region (Figure 3. 1a).

Because this promoter is repressed 100 fold by the presence of glucose [94], induction

was conducted with an alternate non-fermentable carbon source. Out of the alternative carbon sources tested (Figure 3. 10), 8% succinate (lane 10), 8% galactose (lane 5), and 8% mannitol (lane 8) induced the highest amount of rSmSrpQ (Figure 3. 10b, arrow). For large-scale expression 8% succinate was used. After ion exchange and batch nickel purification very little rSmSrpQ was isolated (Figure 3. 4a). The presence of rSmSrpQ was only visible in western blots (Figure 3. 4b) and not seen with Coomassie blue staining. Western blots showed a clean doublet band in the nickel elutions (Figure 3. 4, lane 5-8). Some rSmSrpQ was in the nickel bead flowthrough.

To increase the expression levels, SmSrpQ was fused to ubiquitin. The conserved ubiquitin cleavage site of Arg-Gly-Gly was placed before the 6X-His tag on rSmSrpQ. The fusion protein was placed under the constitutive GAPDH promoter. Expression under the GAPDHp, when compared to the previous expression attempts (Figure 3. 4b), nearly doubled in some clones (Figure 3. 5b, lanes 3, 4, 8). Yet, the expression levels obtained with the positive control, α 1-antitrypsin (Figure 3. 5a, lane 10 and 11), were high enough to detect the α 1-antitrypsin protein in crude lysate (Figure 3. 5a, red arrow) and the cleaved ubiquitin protein (black arrow). The codon usage for α 1-antitrypsin was reengineered to favor the yeast codon usage. No ubiquitin protein was detected in the rSmSrpQ clones (Figure 3. 5a, lanes 1-8). Once SmSrpQ was resynthesized (Figure 3. 2) the ubiquitin protein was detectible in the crude lysates (Figure 3. 5c, black arrow) and the band at the corresponding rSmSrpQ2 molecular weight was thicker (Figure 3. 5c, red arrow) compared to the negative control (Figure 3.5c, lane 4). Nickel purification of

SmSrpQ2 showed Coomassie levels of protein of the expected molecular weight of rSmSrpQ2 (Figure 3. 6, lanes 4-6, black arrow).

Expression and purification of rSmSerp_C. *E. coli* BL21(DE3) was used for the expression of rSmSerp_C using the pET28a+ plasmid. Although the initial screening for expression on whole lysate bacterial lysate showed no difference between induced (Figure 3. 7a, lanes 2-6) and uninduced (lane 7), nickel purification of denatured lysates showed a band in the eluant of the expected molecular weight (Figure 3. 7b, lanes 3, 6, 8). This band was not seen in the purified uninduced control (Figure 3. 7b, lane 2). The clone in lane 7/8 was used for large-scale induction and purification. Cation exchange chromatography followed by nickel batch purification of the pooled eluant yielded high levels of SmSerp_C (Figure 3. 8a, lanes 5-8 and lanes 11-13). Mass spectrometric analysis of the protein corresponding the molecular weight of SmSerp_C showed 85% peptide coverage of Smp_003300 (the Sm genome database designated name of SmSerp_C) (Figure 3. 8b).

SmSerp_C complex formation assays. *In vitro* translation of SmSerp_C using the pET28a+ vector yielded doublet bands of the expected molecular weight of approximately 49 kDa of uncleaved ³⁵S-SmSerp_C and the cleaved form (Figure 3. 9a). After an 8-minute incubation with trypsin, a higher molecular weight band is detected (Figure 3. 9b, red arrow) as well as a lower molecular weight band (arrow head). A higher molecular weight band(s) was also detected when ³⁵S-SmSerp_C was incubated with uninfected snail lysate (Figure 3. 9e, lane 1) and human plasma kallikrein (lanes 5-

8). No higher molecular weight band was detected following incubation with thrombin (Figure 3. 9c), Factor Xa (Figure 3. 9d), and cercarial lysate (Figure 3. 9e, lane 3).

Discussion

SmSerp_C and SmSrpQ are serpins released by the *S. mansoni* cercaria/ schistosomulum upon invasion of the host skin. These two serpins are of the same length (388 amino acids) and molecular weight but vary greatly in their protease specificity (Figure 3. 3). The Leu-P1 of SmSrpQ is a preferred residue of the S1 pocket of chymotrypsin like serine proteases while the Arg-P1 of SmSerp_C is favored by trypsin like proteases. Heterologous expression of these two serpins provide an important tool for verification of their inhibitory properties. *E. coli* proved not to be an ideal expression system for the production of rSmSrpQ but *S. cerevisiae* was a more successful source of rSmSrpQ. Bacterial BL21(DE3) cells, however, were able to produce large quantities of uncleaved soluble rSmSerp_C.

Initial yeast production of rSmSrpQ resulted in small quantities of rSmSrpQ (Figure 3. 5) even though the expression vector used, pBS24.1, had been successfully in producing recombinant protein from Chagas' disease insect vector *Triatoma protracta* [95]. To improve the level of expression, the ADH2 promoter was replaced with the non-glucose repressible GAPDH promoter. This construct was then ligated to the human ubiquitin gene that was shown to increase the production of foreign genes in yeast by more than a hundred fold [96]. Both of these alterations nearly double the amount of rSmSrpQ found in the soluble yeast lysates (Figure 3. 6b, lanes 1-8) as compared to the un-ubiquitinated

rSmSrpQ expression (Figure 3. 5b, lane 1). Yet, expression in the α 1-antitrypsin control was significantly higher. Expression was high enough to detect, in the crude lysates, the cleaved ubiquitin protein (Figure 3. 6a, black arrow) and α 1-antitrypsin (red arrow). A key difference between the α 1-antitrypsin and rSmSrpQ was the re-engineering of the coding region of α 1-antitrypsin to favor the *S. cerevisiae* codon usage. Once SmSrpQ was resynthesized (Figure 3. 2), expression levels matched the positive control (Figure 3. 6c). Ni⁺⁺-agarose batch purification of rSmSrpQ yielded several milligrams of protein per liter of cells. The activity of the recombinant product remains to be tested.

Evidence of the activity of inhibitory activity of SmSrpQ against SmCE has been presented in the previous chapter, there is, however, no information on the activity of SmSerp_C. To verify the predicted inhibitory nature of SmSerp_C in that it was capable of forming a complex with trypsin-like proteases, a radiolabeled recombinant protein under the T7 promoter was produced (Figure 3. 10a). ³⁵S-SmSerp_C was able to form a complex with trypsin, plasma kallikrein, and a component of the snail lysate (Figure 3. 10, red arrows) but not with thrombin or Factor Xa. In multiple cases a lower molecular weight band was detected (Figure 3. 10, black arrow head). The pET28aSmSerp_C construct contains a thrombin cleavage site that would remove the N-terminal His-tag from the recombinant protein. Cleavage at this N-terminal site and at the RCL by a tryptic protease would account for the observed drop in molecular weight.

Parasitic inhibition of plasma kallikrein and a trypsin-like protease in snail lysate suggests several important biological functions of SmSerp_C. Human plasma kallikrein,

is a trypsin-like serine protease involved in the cleavage of high molecular weight kininogen into bradykinin which controls vascular permeability [97] and plasma kallikrein is involved in the coagulation contact activation pathway [98]. Incubating plasma kallikrein with ^{35}S -SmSerp_C resulted in multiple bands (3. 10e, lanes 5-8), which correspond, to several glycosylated species of kallikrein [99] previously seen in human plasma purified kallikrein [100]. The early release of SmSerp_C from the larva [37] and expression profile (Figure 1. 2) suggests the serpin could function earlier during infection, before the parasite reaches the blood vessel. Tryptic kallikrein-like protease 5, 7, and 14 have been isolated in various levels of the epidermis [101], their function in the skin is largely unknown. Studying the biological role of SmSerp_C in the skin could also elucidate the functions of kallikrein and tryptic kallikrein-like proteases in the skin if, indeed, these are the targeted proteases.

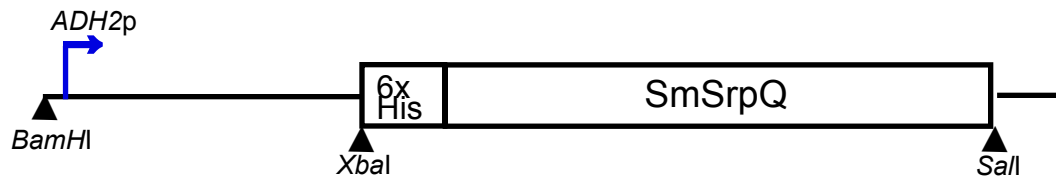
^{35}S -SmSerp_C also formed an SDS-stable complex with a tryptic serine protease in the snail lysate (Figure 3. 10e, lane 1-2, red arrow). A previous study isolated two tryptases from the snail host of schistosomes: BgSP- α and BgSP- β [38]. The infected snail produced a less intense higher molecular weight band perhaps do to competition with the endogenous SmSerp_C or because parasitic infection causes a reduction in the levels of snail tryptases. This complex was not detected in snail-tissue free larval lysate (Figure 3. 10e, lane 3).

As a proof of principle, the pET28aSmSerp_C was used for recombinant expression in *E. coli*. Although bacterial expression of rSmSrpQ yielded either cleaved or insoluble

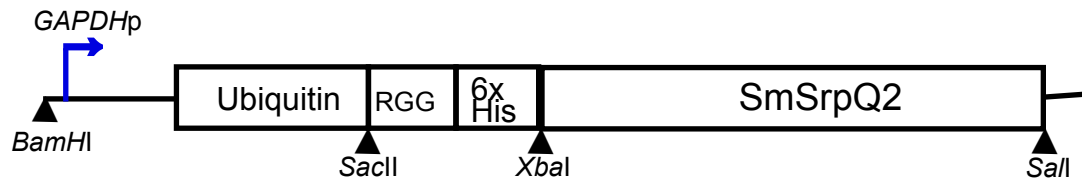
protein, expression of rSmSerp_C resulted in high levels of soluble protein (Figure 3. 9a). Mass spectrometry showed an intact recombinant protein, complete with its RCL (Figure 3. 9b, black line). Removal of the thrombin cleavage site would be ideal for kinetic analysis but the recombinant protein can still be used to verify complex formation with tryptic proteases.

The purification of recombinant SmSrpQ and SmSerp_C is a step forward in uncovering the biochemical properties that govern the inhibitory activity of these serpins. The conformational state of the recombinant proteins remains to be verified. ³⁵S-SmSerp_C appears to have inhibitory activity against trypsin, snail tryptases, and human plasma kallikrein while SmSrpQ behaves as an autoregulator of SmCE. The recombinant proteins would allow for a more comprehensive understanding of the nature of the inhibition of these proteases.

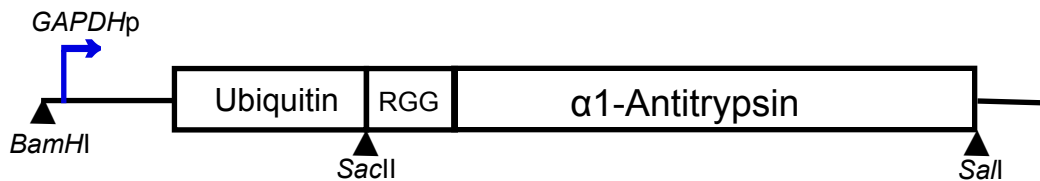
(a) pBS24.1SmSrpQ



(b) pBS24.1GapSmSerpQ2



(c) pBS24.1GapAAT



(d) pET28SmSerp_C

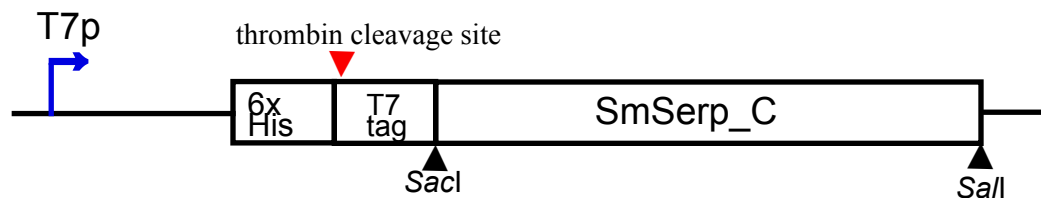


Figure 3. 1: Expression vector constructs. (a) pBS24.1SmSrpQ *S. cerevisiae* expression vector under the ADH2 promoter region. (b) pBS24.1GapSmSerpQ2 yeast expression vector using the constitutive GAPDH promoter. SmSrpQ was resynthesized to favor the *Saccharomyces* codon usage and fused with the ubiquitin protein. The construct also contains a 6X His-tag and the Arg-Gly-Gly motif needed for endopeptidase cleavage of ubiquitin. (c) Positive expression control vector pBS24.1GapAAT features the resynthesized α 1-antitrypsin gene fused with ubiquitin.

SmSrpQ MDVLSLKNFSGR**F**YGD IVEEKQSHSENTFL**S**PFNV**V**Y**T**AL**G**MI**S**.**G**SEM**N**T**K**AE**I**M**K**V**M**H**L**SN**C**L**E**H**H**A**I**H**Y**G**I**S**G****L**L
SmSerpC MGFTTNEPR**Y**N**V**.**F**ARD**L**LDISATGINDYLS**S**PIS**V**ELL**L**T**L**L**G**SG**G**PK**G**NT**K**V**Q**I**A**E**A**L**L**DD**T**K**E**Y**Q**KL**A**SR**T**F**A**L**L**

SmSrpQ FD..C**S**E**R**G**E**G**V**E**I**M.F**G**N**G**L**F**TAEDVN**V**K**E**D**Y**Q**N**T**L**K**S**Y**N**AQ**T**E**S**V**A**F**Q**M**D**P**E**D**A**G**K**R**I**N**Q**A**S**L**T**K**G**K**I**Q**E**L**F**S**S**Q
SmSerpC YHNL**T**N**E**K**I**E**G**K**Q**V**I**S**I**C**N**G**M**F**L**Q**N**E**T**K**I**K**P**H**F**L**T**R**M**K**N**I**F**H**N**D**V**F**N**V**D**F**T**K.A**E**D**A**R**K**N**I**E**W**V**S**N**K**T**S**H**L**I**P**T**V**L**K**.**E**

SmSrpQ SLSTD**I**SVLV**I**T**T**Y**F**E**G**M**D**LL**P**F**L**Q**G**S**S**H**E**SD**F**F**K**LD**G**S**T**M**N**V**K**I**M**Y**M**N**S**F**D**M**T**S**L**P**D**L**K**S**R**A**I**K**I**P**F**K**N**P**K**F**S**L**L**I**V**
SmSerpC P**L**PP**T**LL**G**LI**N**T**I**Y**F**K**G**K**W**K**K**P**F**S**N**H**S**T**T**E**G**E**F**K**P**N**N**Q**P**I**I**K**I**P**M**H**I**M**D**S**I**E**Y**G**L**F**P**K**Y**K**I**H**M**I**S**K**S**F**M**N**P**R**F**S**F**I**V**I

SmSrpQ LPNAND**G**L**L**EL**L**D**A**L**H**R**D**DD**G**ISS**I**L**S**SN**F**K**D**T**S**L**H**I**Y**L**P**K**F**K**I**KE**G**NA**I**S**L**V**D**C**L**Q**K**M**G**M**K**E**A**F**H**P**G**S**A**N**F**T**M**S**E**S**S**N**F**
SmSerpC LP**T**.EP**G**K**L**E**Y**AD**N**V**L**R**G**E**I**K**L**PH**L**V**S**K**L**E**S**K**Q**VA**L**S**L**P**K**F**L**DF..S**I**D**L**I**E**T**L**K**N**M**Y**I**T**D**L**F**D**SA**K**A**D**LR**G**I**T**D**S**K**V**H

SmSrpQ CIR**D**IL**E**K**A**I**L**E**V**N**E**Q**G**V**A**A**A**A**S**S**V**E**V**V**Q**L**S**A**P**L**L**P**E**F**S**D**E**E**F**R**V**N**H**S**F**F**V**S**I**W**K**D.S**V**P**I**F**L**G**H**V**T**N**P**I**D**Q**Y**...
SmSerpC V**Q**V**L**Q**H**S**V**A**L**K**V**N**E**D**G**V**E**A**A**A**A**T**V**M**G**I**G**L**R**S**A**R**P**P..S**I**R**F**D**V**N**E**S**F**I**C**Y**V**Y**D**K**I**L**K**T**S**L**F**A**G**R**I**I**K**P**V**P**L**T**N**N**K**

RCL

| | Length (amino acids) | MW (kDa) | pI | P2-P1' | Target Protease |
|-----------------|----------------------|----------|------|--------|-------------------|
| SmSrpQ | 388 | 4.33 | 5.0 | QL-S | Chymotrypsin-like |
| SmSerp_C | 388 | 4.37 | 9.21 | LR-S | Trypsin-like |

Figure 3. 3: Comparison of SmSrpQ and SmSerp_C. The two serpins were aligned using Multalin. Exactly matched residues are highlighted in red and residues of similar properties are boxed in blue. The RCL is underlined. The table denotes the biochemical properties of SmSerp_C and SmSrpQ.

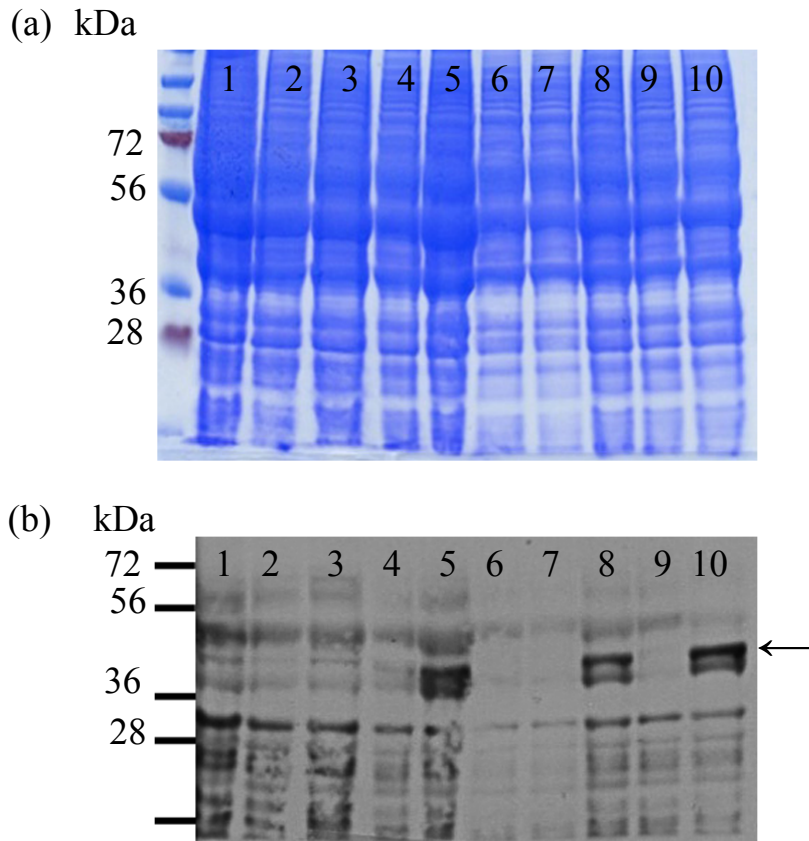


Figure 3. 4: Comparison of non-fermentable carbon sources. Yeast cells (WT BJ2165 and pBS24.1SmSrpQ transformants) were first grown in SC-Ura with 8% glucose then the glucose was replaced with non-fermentable carbon sources. WT cells (lanes 1-3) were grown in lane 1: 8% galactose; lane 2: 8% mannitol; lane 3: 8% succinate. pBS24.1SmSrpQ transformants were grown in lane 4: 8% arabinose; lane 5: 8% galactose; lane 6: 1% glucose; lane 7: 8% glycerol; lane 8: 8% mannitol; lane 9: 8% raffinose; lane 10: 8% succinate. (a) Coomassie Blue stained SDS-PAGE. (b) immunoblot.

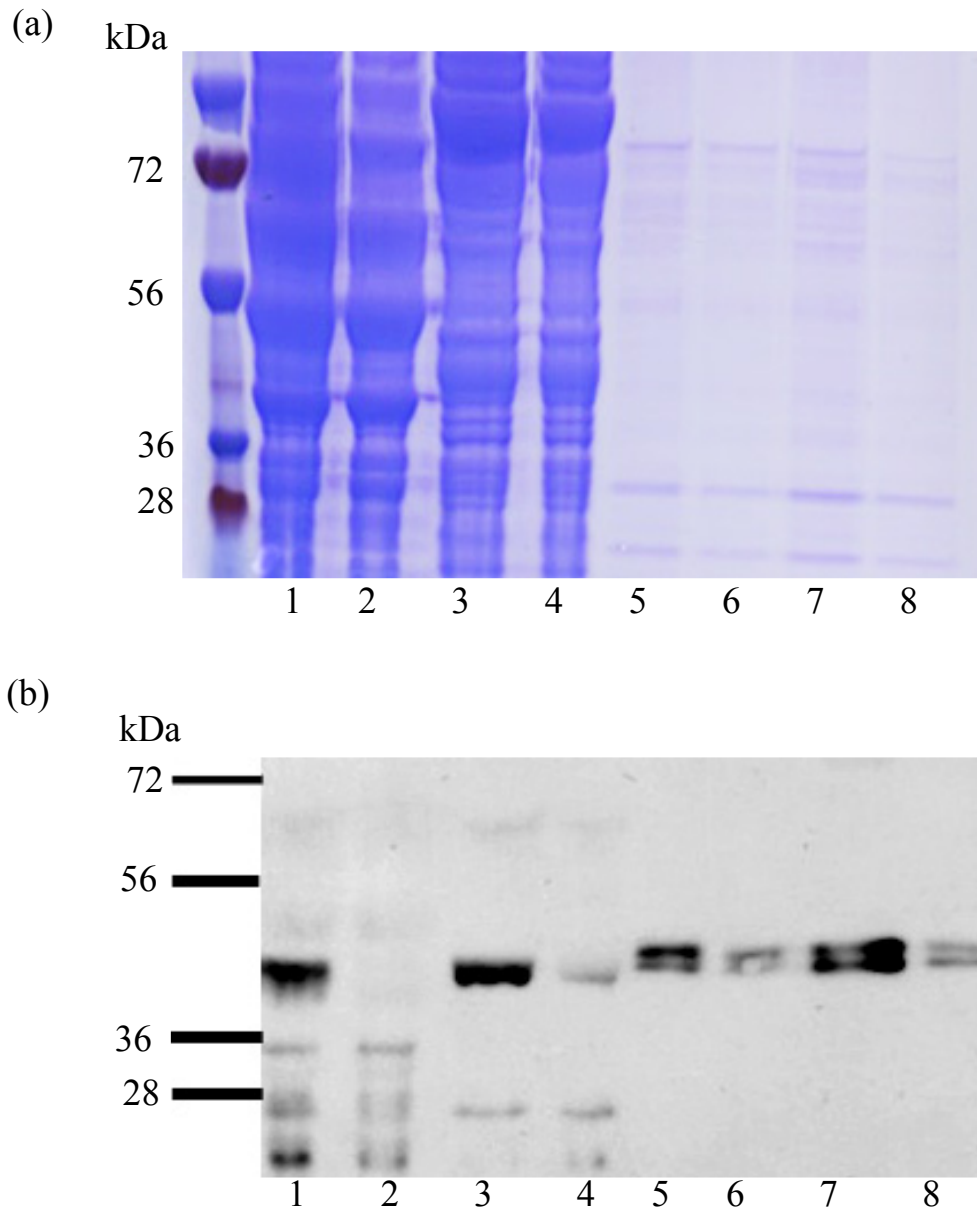


Figure 3. 5: *rSmSrpQ* purification. *rSmSrpQ* was purified from the soluble fraction of yeast lysate. After passage through a Q-Sepharose FF column, samples were incubated with Ni⁺⁺-agarose beads and proteins were eluted with 500mM imidazole. (1) soluble fraction; (2) Q-sepharose flowthrough; (3) pooled Q-sepharose eluant; (4) Ni⁺⁺-agarose flowthrough; (5-8) Ni⁺⁺-agarose elutions 1-4. (a) SDS-PAGE; (b) western immunoblot.

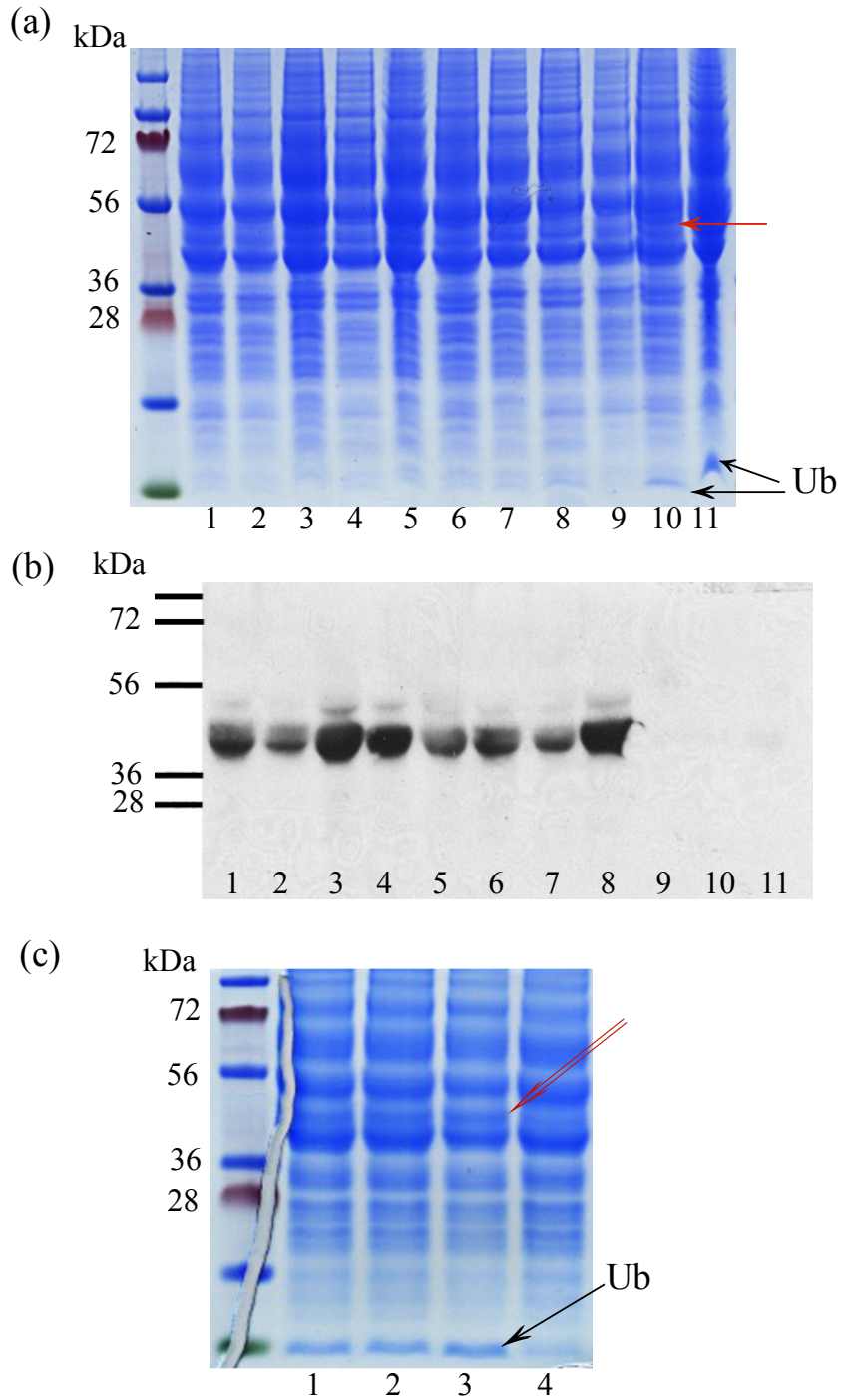


Figure 3. 6: Ubiquitin-*SmSrpQ* expression using *ADH2p* and *GAPDHp*.
 (a) Crude lysate SDS-PAGE analysis of: lanes 1-8: *SmSrpQ*-ubiquitin; lane 9: WT BJ26128; lane 10 and 11: α 1-antitrypsin-ubiquitin. Red arrow in lane 10 points to α 1-antitrypsin protein band and the black arrow shows cleaved ubiquitin (Ub) protein in α 1-antitrypsin samples. (b) Western immunoblots of (a) samples. (c) Crude lysate SDS-PAGE analysis of r*SmSrpQ2*-Ub after *SmSrpQ* was resynthesized. Lane 1-3: *SmSrpQ2*-Ub clones; lane 4: negative control.

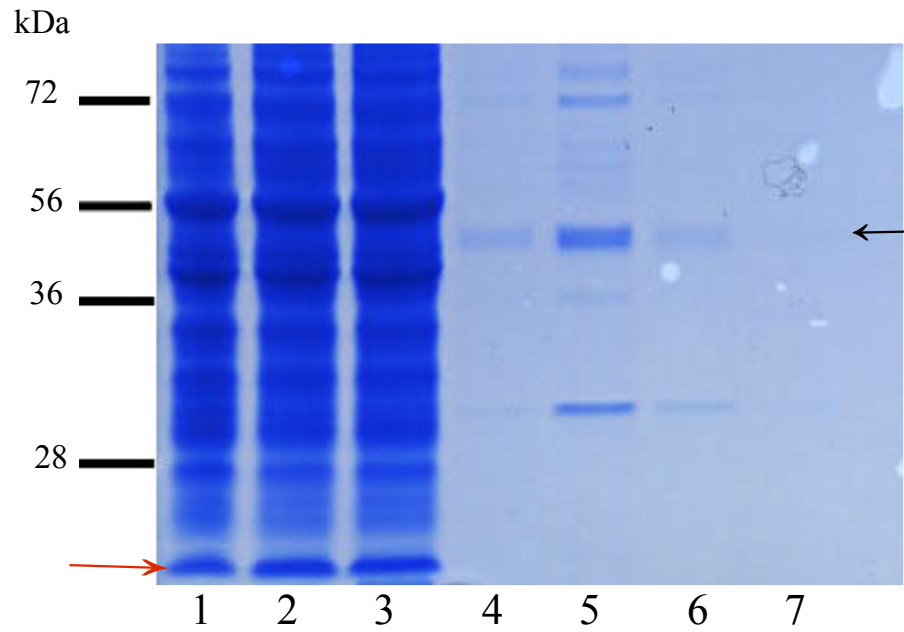


Figure 3. 7: *rSmSrpQ2* purification. rSmSrpQ2 was isolated using Ni⁺⁺-agarose beads. Lane 1: soluble fraction of α 1-antitrypsin clones; lane 2: soluble fraction of rSmSrpQ2 clones; lane 3: Ni⁺⁺ purification flowthrough; lane 4-7 rSmSrpQ2 elutions.

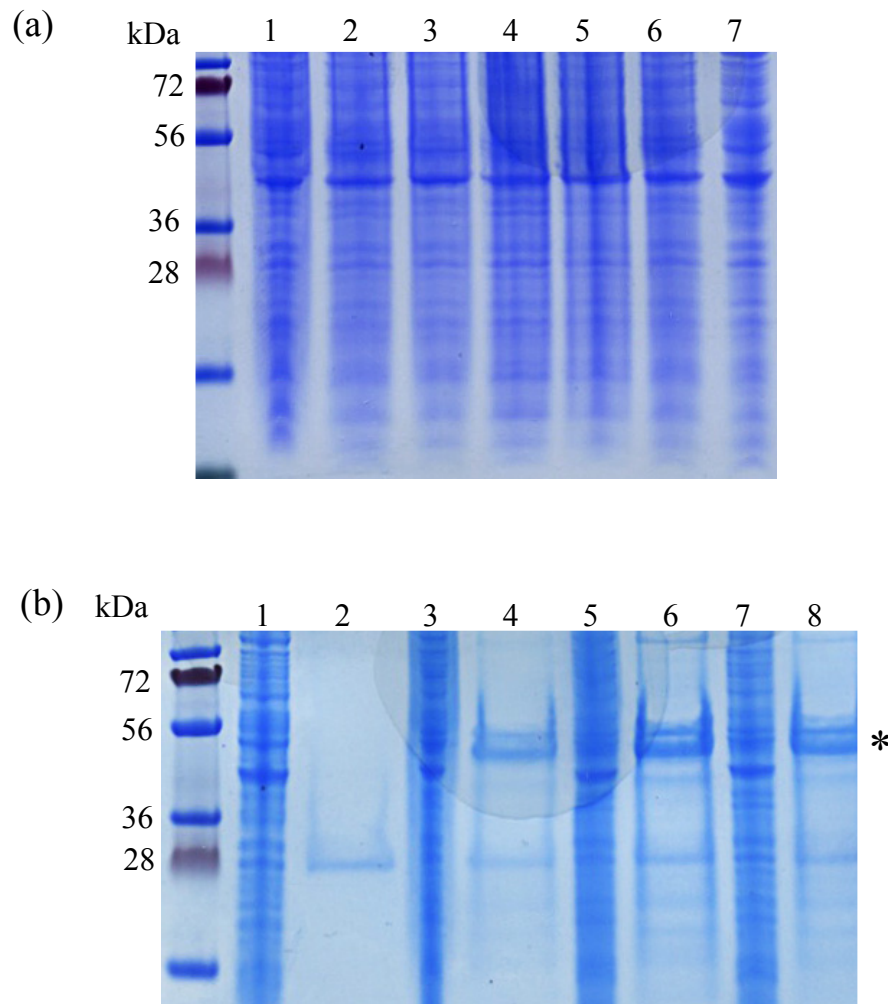
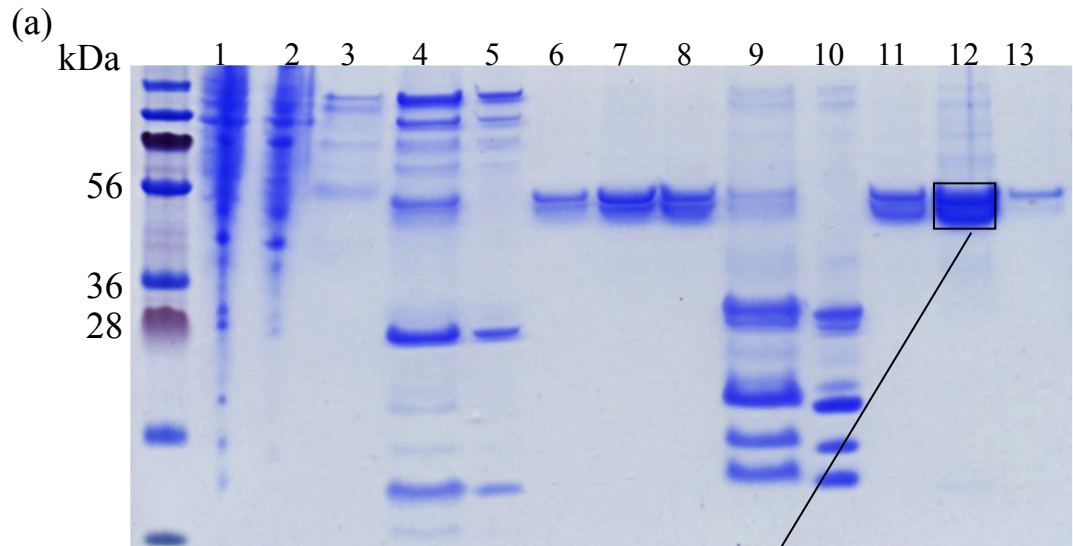


Figure 3. 8: *rSmSerp_C* colony screening. (a) SDS-PAGE analysis of *E. coli* BL21 lysates. Lane 1: empty vector; lane 2-6: induced *SmSerp_C* clones; lane 7: uninduced *rSmSerp_C* clone. (b) Gel analysis of clones after Ni⁺⁺-agarose spin column purification under denaturing conditions. Uninduced sample (lane 1: soluble fraction; lane 2: purified samples); three induced clones (lanes 3, 5, and 7: soluble fractions; lanes 4, 6, and 8: purified samples).



(b)

1 Acc. #: [Smp_003300](#) Species: SCHISTOSOMA MANSONI Name: serine protease inhibitors, 29046.m002665, 29046.t000051

Protein MW: 43776.2 **Protein pI:** 9.2 **Protein Length:** 388

1 MGFTTNEPRY NVFARDLLDI SATGTNDYLS SPISVFLLLT TLLGSGGPKG NTKVQIAEAL ELDDTKEYQK LASRTFALLY
 81 HNLTKIEIG KQVISIGNGM FLQNETKIKP HFLTRMKNIF HNDVFNVDFT KAEDARKNIN EWVSNKTSHL IPTVLKEPLP
 161 PTTLLGLINT LYFKGKWKKP FSNHSTTEGE FKPNNQPIIK IPMMHIMDSI EYGLFPKYKI HMISKFMNP RFSFIVILPT
 241 EPGKLEYADN VLRGEIKLPH LVSKLESKQV ALSLPKPRLD FSIDLIELTK NMYITDLFDS AKADLRGITD SKVHVQVLQH
 321 SVALKVNEDG VEAAAATVMG IGLRSARPPP SIRFDVNESF ICYVYDKILK TSLFAGRIIK PVPLTNNK

Figure 3. 9: *rSmSerp_C* purification. Bacterial lysates from two clones, clone 1 (lanes 1-8) and clone 2 (lanes 9-13), were purified using SP-Sepharose columns followed by Ni⁺⁺-agarose batch purification. Lane 1: soluble fraction; 2: SP-Sepharose flowthrough; 4 and 9: SP-Sepharose pooled elutions; 5 and 10: Ni⁺⁺-agarose flowthrough; 6-8 and 11-13: Ni⁺⁺-agarose elutions. (b) Mass spectrometry results of nickel eluted protein. Results indicate 85% peptide coverage of Smp_003300, the database name of SmSerp_C.

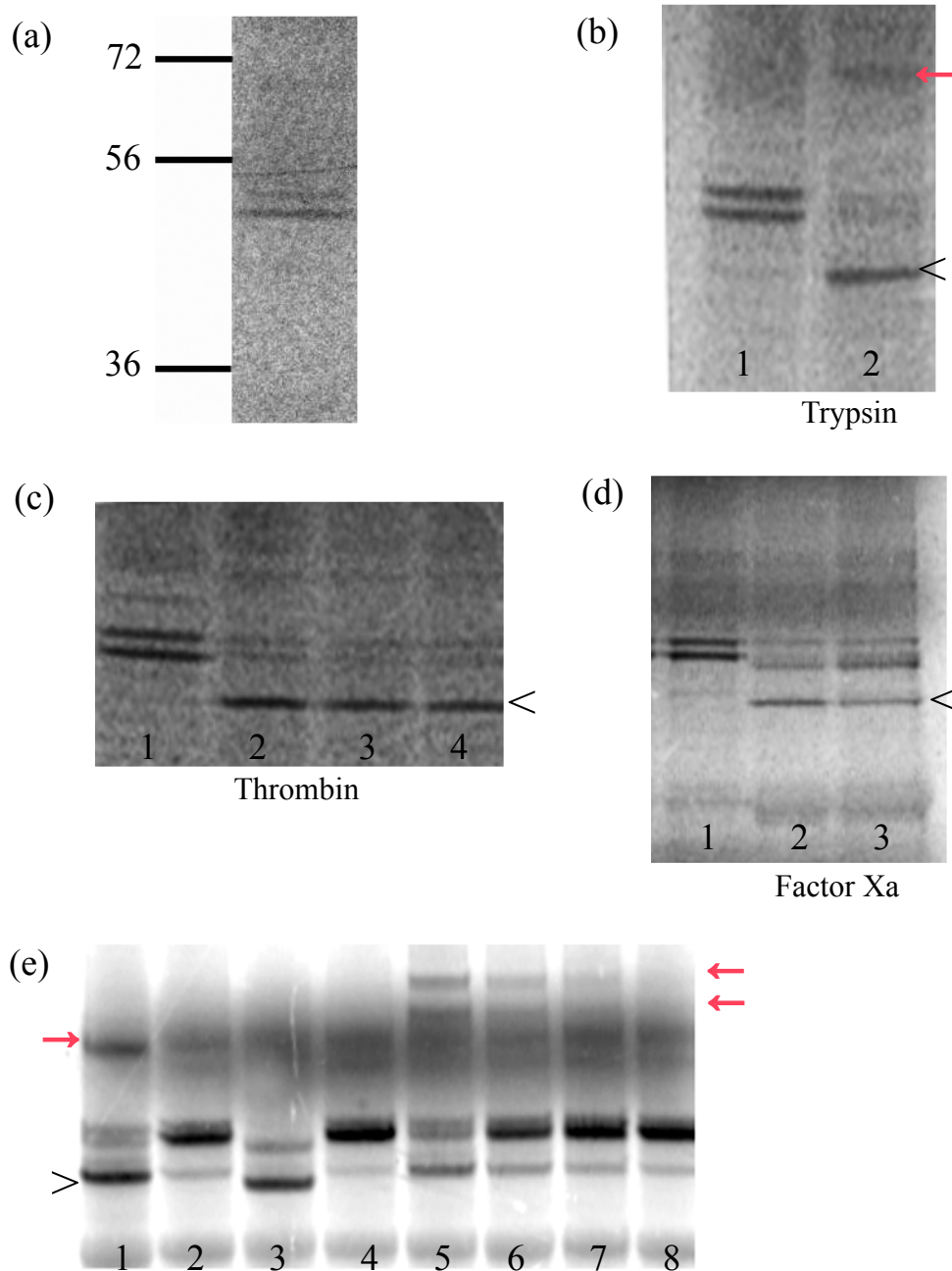


Figure 3.10: ^{35}S -*SmSerp_C* complex formation assays. (a) In vitro translation resulted in a product approximately 49 kDa in mass. ^{35}S -*SmSerp_C* incubated with (b) trypsin; (c) decreasing concentrations of thrombin; (d) factor Xa; (e) uninfected *B. glabrata* lysate (lane 1), 10 week infected snail (lane 2), *S. mansoni* cercarial lysate (lane 3), decreasing concentrations of human plasma kallikrein (lanes 5-8). Red arrows indicate potential serpin-protease complex and open arrows denote un-His tagged cleaved protein.

Chapter 4

Concluding Remarks

From complement activation, coagulation, and fibrinolysis to vascular permeability, many mammalian proteolytic cascades are carefully regulated by serpins. Several of these proteinaceous inhibitors retain the tertiary structure common to the protein family yet perform non-inhibitory functions. For example, transport of hormones thyroxine and cortisol is serpin mediated [102]. With all the biological functions mediated by serpins, little information exists on the regulatory (and non-inhibitory) roles of the numerous serpins identified in human parasites. In this dissertation, I not only identified the serpins found in the trematode parasites *S. mansoni* and *S. japonicum* but also provided empirical information on the likely function of two of these serpins.

Many questions remain as to the exact role of all of the 13 schistosome serpins. With the progress of the *S. haematobium* genome annotation, more schistosome serpins are likely to be identified. Because genetic manipulation of the nuclear genome of schistosomes is not yet possible, RNA interference remains one possible way to assess the biological role of the schistosome serpins. In adults, RNAi has been used to knock-down proteolytic activity in the worm gut [103] but not all genes are amenable to transcriptional knock-down by RNAi [104]. In *S. mansoni*, only the Sm1a-c serpins are present in the adult worms (Figure 1. 2). In contrast, all the serpins are expressed in the daughter and late sporocysts. RNAi results in sporocysts has been reported [105, 106], but these experiments were performed on primary (mother) sporocysts transformed *in vitro* from miracidia. A recent proof of principle study demonstrated that by adding polytheleneimine to the dsRNA soaking mixture, it was possible to successfully deliver dsRNA or siRNA constructs to the hepatopancreas of uninfected *B. glabrata* [107]. If

this delivery method can effectively and reliably knock-down transcripts within the sporocysts of an infected snail for a prolonged period of time, it would be a step forward in understanding the function of parasite serpins.

Although RNAi knock-down cannot be reliably achieved in all schistosome developmental life stages, biochemical and structural characterization of many schistosome serpins can still be carried out. Two *S. mansoni* serpins, SmSrpQ and SmSerp_C, were expressed and purified using three different expression systems: rabbit reticulolysate-T7 cell free system, *S. cerevisiae*, and *E. coli*. SmSrpQ and SmSerp_C are phylogenetically (Figure 1. 3) and biochemically (Figure 3. 3) disparate from each other yet early data suggest that both are involved in how the parasite interacts with its hosts. The production of properly folded recombinant protein will allow calculation of the kinetic constants that govern serpin-protease interactions. Furthermore, the effects of cofactors can be explored. Does the level of degraded ECM play a role in the interaction of SmSrpQ and SmCE? SmSerp_C is able bind to both human plasma kallikrein and molluscan protease(s). If one or both of these proteases are the true target, what pivotal role do these proteases play in the host response to the parasite such that the parasite has developed a method to subvert their activity?

Purification of recombinant protein will also assist in understanding what effects the amino acid changes in the otherwise identical Sm1a, Sm1b, and Sm1c proteins have on protease specificity and/ or allosteric control. The amino acid changes found in the “gate” region of β -sheet C and “breach” region β -sheet A of the Sm1a-c could affect the

conformational state of the serpin and, therefore, how each serpin behaves *in vivo*.

Recombinant expression and crystallization of schistosome serpins can also clarify the nature of the 9-16 amino acid extension of helix D.

Schistosome research in the post-genomic era promises a greater understanding of the dynamic relationship these parasites possess with their hosts. It is hoped that new lines of inquiry building from the findings of this body of work will lead to the recognition of new drug targets and vaccine candidates against the schistosome. Schistosome serpins may play important roles in both post-translational regulation of schistosome-derived proteases as well as parasite defense mechanisms against the action of host proteases.

Abbreviations & References

Abbreviations

AAPF-CMK: Z-Ala-Ala-Pro-Phe- chloromethylketone
AAPL-CMK: Z-Ala-Ala-Pro-Leu- chloromethylketone
AAPV-CMK: Z-Ala-Ala-Pro-Val- chloromethylketone
ADH2p: alcohol dehydrogenase 2 promoter
BLAST: Basic local alignment search tool
DALYs: disability adjusted life years
DCs: dendritic cells
DMSO: dimethyl sulfoxide
ECM: extracellular matrix
GAPDHp: glyceraldehyde-3-phosphate dehydrogenase promoter
ICAM: inter-cellular adhesion molecule
IMAC: immobilized metal affinity chromatography
MNEI: monocyte/ neutrophil elastase inhibitor
PAI-1: plasminogen activator inhibitor 1
PAMPs: pathogen-associated-molecular patterns
PAR: protease activated receptor
PBS: phosphate buffered saline
PGE: prostaglandin E
PMSF: phenylmethylsulphonyl fluoride
RCL: reactive center loop
RT: room temperature
SCM: Schistosoma culture media
Serp: serine/ cysteine protease inhibitor
SmCE: *S. mansoni* cercarial elastase
SmSerp_C: *S. mansoni* serpin C
SmSrpQ: *S. mansoni* serpin Q
TLR: Toll-like receptor
TNF- α : tumor necrosis factor α
VCAM: vascular cell adhesion molecule

References

1. WHO, *Schistosomiasis Fact Sheet #115*. Programmes and Projects, ed. W.H. Organization. Vol. 115. 2010. 3.
2. King, C.H., *Parasites and poverty: the case of schistosomiasis*. Acta Trop. **113**(2): p. 95-104.
3. Chitsulo, L., et al., *The global status of schistosomiasis and its control*. Acta Trop, 2000. **77**(1): p. 41-51.
4. King, C.H., K. Dickman, and D.J. Tisch, *Reassessment of the cost of chronic helminthic infection: a meta-analysis of disability-related outcomes in endemic schistosomiasis*. Lancet, 2005. **365**(9470): p. 1561-9.
5. WHO, *World Health Report*. World Health Organization, 2001.
6. Pearce, E.J. and A.S. MacDonald, *The immunobiology of schistosomiasis*. Nat Rev Immunol, 2002. **2**(7): p. 499-511.
7. Abdulla, M.H., et al., *Drug discovery for schistosomiasis: hit and lead compounds identified in a library of known drugs by medium-throughput phenotypic screening*. PLoS Negl Trop Dis, 2009. **3**(7): p. e478.
8. McManus, D.P. and A. Loukas, *Current status of vaccines for schistosomiasis*. Clin Microbiol Rev, 2008. **21**(1): p. 225-42.
9. Tran, M.H., et al., *Tetraspanins on the surface of Schistosoma mansoni are protective antigens against schistosomiasis*. Nat Med, 2006. **12**(7): p. 835-40.
10. Cardoso, F.C., et al., *Schistosoma mansoni tegument protein Sm29 is able to induce a Th1-type of immune response and protection against parasite infection*. PLoS Negl Trop Dis, 2008. **2**(10): p. e308.
11. Cardoso, F.C., et al., *Human antibody responses of patients living in endemic areas for schistosomiasis to the tegumental protein Sm29 identified through genomic studies*. Clin Exp Immunol, 2006. **144**(3): p. 382-91.
12. Lu, D.B., et al., *Transmission of Schistosoma japonicum in marshland and hilly regions of China: parasite population genetic and sibship structure*. PLoS Negl Trop Dis. **4**(8): p. e781.
13. Blazova, K. and P. Horak, *Trichobilharzia regenti: the developmental differences in natural and abnormal hosts*. Parasitol Int, 2005. **54**(3): p. 167-72.
14. Horak, P. and L. Kolarova, *Molluscan and vertebrate immune responses to bird schistosomes*. Parasite Immunol, 2005. **27**(7-8): p. 247-55.
15. Amiri, P., et al., *The Schistosomatium douthitti cercarial elastase is biochemically and structurally distinct from that of Schistosoma mansoni*. Mol Biochem Parasitol, 1988. **28**(2): p. 113-20.
16. Shiff, C.J., et al., *The influence of human skin lipids on the cercarial penetration responses of Schistosoma haematobium and Schistosoma mansoni*. J Parasitol, 1972. **58**(3): p. 476-80.
17. He, Y.X., B. Salafsky, and K. Ramaswamy, *Comparison of skin invasion among three major species of Schistosoma*. Trends Parasitol, 2005. **21**(5): p. 201-3.
18. Loverde, P.T. and L. Chen, *Schistosome female reproductive development*. Parasitol Today, 1991. **7**(11): p. 303-8.

19. Cheever, A.W., et al., *Kinetics of egg production and egg excretion by Schistosoma mansoni and S. japonicum in mice infected with a single pair of worms*. Am J Trop Med Hyg, 1994. **50**(3): p. 281-95.
20. Zaidi, Z. and S.W. Lanigan, *Chapter 1. Dermatology in Clinical Practice*. 2010, London: Springer- Verlag.
21. Shaw, A.S. and Y. Huang, *Immunology. CAR'ing for the skin*. Science. **329**(5996): p. 1154-5.
22. Streilein, J.W., *Skin-associated lymphoid tissues (SALT): origins and functions*. J Invest Dermatol, 1983. **80 Suppl**: p. 12s-16s.
23. Miller, L.S. and R.L. Modlin, *Human keratinocyte Toll-like receptors promote distinct immune responses*. J Invest Dermatol, 2007. **127**(2): p. 262-3.
24. Nestle, F.O., et al., *Skin immune sentinels in health and disease*. Nat Rev Immunol, 2009. **9**(10): p. 679-91.
25. Kambe, N., et al., *The inflammasome, an innate immunity guardian, participates in skin urticarial reactions and contact hypersensitivity*. Allergol Int. **59**(2): p. 105-13.
26. Macleod, A.S. and W.L. Havran, *Functions of skin-resident gammadelta T cells*. Cell Mol Life Sci. **68**(14): p. 2399-408.
27. Foster, C.A., et al., *Human epidermal T cells predominantly belong to the lineage expressing alpha/beta T cell receptor*. J Exp Med, 1990. **171**(4): p. 997-1013.
28. Hunger, R.E., et al., *Langerhans cells utilize CD1a and langerin to efficiently present nonpeptide antigens to T cells*. J Clin Invest, 2004. **113**(5): p. 701-8.
29. Bedoui, S., et al., *Cross-presentation of viral and self antigens by skin-derived CD103+ dendritic cells*. Nat Immunol, 2009. **10**(5): p. 488-95.
30. Guttman-Yassky, E., et al., *Major differences in inflammatory dendritic cells and their products distinguish atopic dermatitis from psoriasis*. J Allergy Clin Immunol, 2007. **119**(5): p. 1210-7.
31. Zahn, S., et al., *Human primary dendritic cell subsets differ in their IL-12 release in response to Leishmania major infection*. Exp Dermatol. **19**(10): p. 924-6.
32. Fukunaga, A., et al., *Dermal dendritic cells, and not Langerhans cells, play an essential role in inducing an immune response*. J Immunol, 2008. **180**(5): p. 3057-64.
33. Miller, H.R. and A.D. Pemberton, *Tissue-specific expression of mast cell granule serine proteinases and their role in inflammation in the lung and gut*. Immunology, 2002. **105**(4): p. 375-90.
34. Pham, C.T., *Neutrophil serine proteases: specific regulators of inflammation*. Nat Rev Immunol, 2006. **6**(7): p. 541-50.
35. Hansell, E., et al., *Proteomic analysis of skin invasion by blood fluke larvae*. PLoS Negl Trop Dis, 2008. **2**(7): p. e262.
36. Salter, J.P., et al., *Cercarial elastase is encoded by a functionally conserved gene family across multiple species of schistosomes*. J Biol Chem, 2002. **277**(27): p. 24618-24.
37. Curwen, R.S., et al., *Identification of novel proteases and immunomodulators in the secretions of schistosome cercariae that facilitate host entry*. Mol Cell Proteomics, 2006. **5**(5): p. 835-44.

38. Salter, J.P., et al., *Schistosome invasion of human skin and degradation of dermal elastin are mediated by a single serine protease*. J Biol Chem, 2000. **275**(49): p. 38667-73.
39. Angeli, V., et al., *Role of the parasite-derived prostaglandin D2 in the inhibition of epidermal Langerhans cell migration during schistosomiasis infection*. J Exp Med, 2001. **193**(10): p. 1135-47.
40. Ramaswamy, K., P. Kumar, and Y.X. He, *A role for parasite-induced PGE2 in IL-10-mediated host immunoregulation by skin stage schistosomula of Schistosoma mansoni*. J Immunol, 2000. **165**(8): p. 4567-74.
41. Incani, R.N. and D.J. McLaren, *Histopathological and ultrastructural studies of cutaneous reactions elicited in naive and chronically infected mice by invading schistosomula of Schistosoma mansoni*. Int J Parasitol, 1984. **14**(3): p. 259-76.
42. Machado, D.C., et al., *Potential allergens stimulate the release of mediators of the allergic response from cells of mast cell lineage in the absence of sensitization with antigen-specific IgE*. Eur J Immunol, 1996. **26**(12): p. 2972-80.
43. Gettins, P.G., *Serpin structure, mechanism, and function*. Chem Rev, 2002. **102**(12): p. 4751-804.
44. Law, R.H., et al., *An overview of the serpin superfamily*. Genome Biol, 2006. **7**(5): p. 216.
45. Silverman, G.A., et al., *The serpins are an expanding superfamily of structurally similar but functionally diverse proteins. Evolution, mechanism of inhibition, novel functions, and a revised nomenclature*. J Biol Chem, 2001. **276**(36): p. 33293-6.
46. Crowther, D.C., D.L. Evans, and R.W. Carrell, *Serpins: implications of a mobile reactive centre*. Curr Opin Biotechnol, 1992. **3**(4): p. 399-407.
47. Whisstock, J., R. Skinner, and A.M. Lesk, *An atlas of serpin conformations*. Trends Biochem Sci, 1998. **23**(2): p. 63-7.
48. Yi, J.Y. and H. Im, *Structural factors affecting the choice between latency transition and polymerization in inhibitory serpins*. Protein Sci, 2007. **16**(5): p. 833-41.
49. Huntington, J.A., R.J. Read, and R.W. Carrell, *Structure of a serpin-protease complex shows inhibition by deformation*. Nature, 2000. **407**(6806): p. 923-6.
50. Luke, C.J., et al., *An intracellular serpin regulates necrosis by inhibiting the induction and sequelae of lysosomal injury*. Cell, 2007. **130**(6): p. 1108-19.
51. Levashina, E.A., et al., *Constitutive activation of toll-mediated antifungal defense in serpin-deficient Drosophila*. Science, 1999. **285**(5435): p. 1917-9.
52. Abraham, E.G., et al., *An immune-responsive serpin, SRPN6, mediates mosquito defense against malaria parasites*. Proc Natl Acad Sci U S A, 2005. **102**(45): p. 16327-32.
53. Zhang, M., et al., *Maspin plays an important role in mammary gland development*. Dev Biol, 1999. **215**(2): p. 278-87.
54. Zou, Z., et al., *Maspin, a serpin with tumor-suppressing activity in human mammary epithelial cells*. Science, 1994. **263**(5146): p. 526-9.
55. Sheng, S., et al., *Maspin acts at the cell membrane to inhibit invasion and motility of mammary and prostatic cancer cells*. Proc Natl Acad Sci U S A, 1996. **93**(21): p. 11669-74.

56. Quinsey, N.S., et al., *Antithrombin: in control of coagulation*. Int J Biochem Cell Biol, 2004. **36**(3): p. 386-9.
57. Ishiguro, K., et al., *Complete antithrombin deficiency in mice results in embryonic lethality*. J Clin Invest, 2000. **106**(7): p. 873-8.
58. Rau, J.C., et al., *Serpins in thrombosis, hemostasis and fibrinolysis*. J Thromb Haemost, 2007. **5 Suppl 1**: p. 102-15.
59. Yamasaki, M., et al., *Crystal structure of a stable dimer reveals the molecular basis of serpin polymerization*. Nature, 2008. **455**(7217): p. 1255-8.
60. Cugno, M., et al., *Haemostasis contact system and fibrinolysis in hereditary angioedema (C1-inhibitor deficiency)*. J Clin Chem Clin Biochem, 1988. **26**(7): p. 423-7.
61. Ray, C.A., et al., *Viral inhibition of inflammation: cowpox virus encodes an inhibitor of the interleukin-1 beta converting enzyme*. Cell, 1992. **69**(4): p. 597-604.
62. Quan, L.T., et al., *Granzyme B is inhibited by the cowpox virus serpin cytokine response modifier A*. J Biol Chem, 1995. **270**(18): p. 10377-9.
63. Yenbutr, P. and A.L. Scott, *Molecular cloning of a serine proteinase inhibitor from Brugia malayi*. Infect Immun, 1995. **63**(5): p. 1745-53.
64. Zang, X., et al., *A novel serpin expressed by blood-borne microfilariae of the parasitic nematode Brugia malayi inhibits human neutrophil serine proteinases*. Blood, 1999. **94**(4): p. 1418-28.
65. Stanley, P. and P.E. Stein, *BmSPN2, a serpin secreted by the filarial nematode Brugia malayi, does not inhibit human neutrophil proteinases but plays a noninhibitory role*. Biochemistry, 2003. **42**(20): p. 6241-8.
66. Ford, L., et al., *Characterization of a novel filarial serine protease inhibitor, Ov-SPI-1, from Onchocerca volvulus, with potential multifunctional roles during development of the parasite*. J Biol Chem, 2005. **280**(49): p. 40845-56.
67. Harrop, R., et al., *Characterization, cloning and immunogenicity of antigens released by transforming cercariae of Schistosoma mansoni*. Parasitology, 2000. **121 (Pt 4)**: p. 385-94.
68. Knudsen, G.M., et al., *Proteomic analysis of Schistosoma mansoni cercarial secretions*. Mol Cell Proteomics, 2005. **4**(12): p. 1862-75.
69. Lacleste, J.P., et al., *Paramyosin inhibits complement C1*. J Immunol, 1992. **148**(1): p. 124-8.
70. Chen, L., et al., *Skin-stage schistosomula of Schistosoma mansoni produce an apoptosis-inducing factor that can cause apoptosis of T cells*. J Biol Chem, 2002. **277**(37): p. 34329-35.
71. Lim, K.C., et al., *Blockage of skin invasion by schistosome cercariae by serine protease inhibitors*. Am J Trop Med Hyg, 1999. **60**(3): p. 487-92.
72. Bradford, M.M., *A rapid and sensitive method for the quantitation of microgram quantities of protein utilizing the principle of protein-dye binding*. Anal Biochem, 1976. **72**: p. 248-54.
73. Skelly, P.J. and C.B. Shoemaker, *Schistosoma mansoni proteases Sm31 (cathepsin B) and Sm32 (legumain) are expressed in the cecum and protonephridia of cercariae*. J Parasitol, 2001. **87**(5): p. 1218-21.

74. Dafforn, T.R., R.N. Pike, and S.P. Bottomley, *Physical characterization of serpin conformations*. *Methods*, 2004. **32**(2): p. 150-8.
75. Quezada, L.A. and J.H. McKerrow, *Schistosome serine protease inhibitors: parasite defense or homeostasis?* *An Acad Bras Cienc.* **83**(2): p. 663-72.
76. Dorsey, C.H., et al., *Ultrastructure of the Schistosoma mansoni cercaria*. *Micron*, 2002. **33**(3): p. 279-323.
77. Fishelson, Z., et al., *Schistosoma mansoni: cell-specific expression and secretion of a serine protease during development of cercariae*. *Exp Parasitol*, 1992. **75**(1): p. 87-98.
78. McKerrow, J.H., et al., *Purification and characterization of an elastolytic proteinase secreted by cercariae of Schistosoma mansoni*. *J Biol Chem*, 1985. **260**(6): p. 3703-7.
79. Campbell, E.J., et al., *Proteolysis by neutrophils. Relative importance of cell-substrate contact and oxidative inactivation of proteinase inhibitors in vitro*. *J Clin Invest*, 1982. **70**(4): p. 845-52.
80. Remold-O'Donnell, E., J. Chin, and M. Alberts, *Sequence and molecular characterization of human monocyte/neutrophil elastase inhibitor*. *Proc Natl Acad Sci U S A*, 1992. **89**(12): p. 5635-9.
81. Cooley, J., et al., *The serpin MNEI inhibits elastase-like and chymotrypsin-like serine proteases through efficient reactions at two active sites*. *Biochemistry*, 2001. **40**(51): p. 15762-70.
82. Dvorak, J., et al., *Differential use of protease families for invasion by schistosome cercariae*. *Biochimie*, 2008. **90**(2): p. 345-58.
83. Ekeowa, U.I., et al., *alpha1-Antitrypsin deficiency, chronic obstructive pulmonary disease and the serpinopathies*. *Clin Sci (Lond)*, 2009. **116**(12): p. 837-50.
84. Campbell, E.J., R.M. Senior, and H.G. Welgus, *Extracellular matrix injury during lung inflammation*. *Chest*, 1987. **92**(1): p. 161-7.
85. Kourilova, P., et al., *Cercarial dermatitis caused by bird schistosomes comprises both immediate and late phase cutaneous hypersensitivity reactions*. *J Immunol*, 2004. **172**(6): p. 3766-74.
86. He, Y.X., L. Chen, and K. Ramaswamy, *Schistosoma mansoni, S. haematobium, and S. japonicum: early events associated with penetration and migration of schistosomula through human skin*. *Exp Parasitol*, 2002. **102**(2): p. 99-108.
87. Ross, A.G., et al., *Katayama syndrome*. *Lancet Infect Dis*, 2007. **7**(3): p. 218-24.
88. Lee, H.J. and H. Im, *Purification of recombinant plasminogen activator inhibitor-1 in the active conformation by refolding from inclusion bodies*. *Protein Expr Purif*, 2003. **31**(1): p. 99-107.
89. Kwon, K.S., S. Lee, and M.H. Yu, *Refolding of alpha 1-antitrypsin expressed as inclusion bodies in Escherichia coli: characterization of aggregation*. *Biochim Biophys Acta*, 1995. **1247**(2): p. 179-84.
90. Jayakumar, A., et al., *Production of serpins using baculovirus expression systems*. *Methods*, 2004. **32**(2): p. 177-84.
91. Brandt, K.S., et al., *Isolation, characterization, and recombinant expression of multiple serpins from the cat flea, Ctenocephalides felis*. *Arch Insect Biochem Physiol*, 2004. **55**(4): p. 200-14.


92. Pemberton, P.A. and P.I. Bird, *Production of serpins using yeast expression systems*. Methods, 2004. **32**(2): p. 185-90.
93. Gietz, R.D. and R.H. Schiestl, *High-efficiency yeast transformation using the LiAc/SS carrier DNA/PEG method*. Nat Protoc, 2007. **2**(1): p. 31-4.
94. Price, V.L., et al., *Expression of heterologous proteins in Saccharomyces cerevisiae using the ADH2 promoter*. Methods Enzymol, 1990. **185**: p. 308-18.
95. Paddock, C.D., et al., *Identification, cloning, and recombinant expression of procalin, a major triatomine allergen*. J Immunol, 2001. **167**(5): p. 2694-9.
96. Ecker, D.J., et al., *Increasing gene expression in yeast by fusion to ubiquitin*. J Biol Chem, 1989. **264**(13): p. 7715-9.
97. Kaplan, A.P. and K. Joseph, *The bradykinin-forming cascade and its role in hereditary angioedema*. Ann Allergy Asthma Immunol. **104**(3): p. 193-204.
98. Griffin, J.H. and C.G. Cochrane, *Human factor XII (Hageman factor)*. Methods Enzymol, 1976. **45**: p. 56-65.
99. Veloso, D., et al., *Structure, kinetics, and function of human and rhesus plasma prekallikreins are similar*. Thromb Haemost, 1992. **68**(5): p. 526-33.
100. Nagase, H. and A.J. Barrett, *Human plasma kallikrein. A rapid purification method with high yield*. Biochem J, 1981. **193**(1): p. 187-92.
101. Ovaere, P., et al., *The emerging roles of serine protease cascades in the epidermis*. Trends Biochem Sci, 2009. **34**(9): p. 453-63.
102. Pemberton, P.A., et al., *Hormone binding globulins undergo serpin conformational change in inflammation*. Nature, 1988. **336**(6196): p. 257-8.
103. Delcroix, M., et al., *A multienzyme network functions in intestinal protein digestion by a platyhelminth parasite*. J Biol Chem, 2006. **281**(51): p. 39316-29.
104. Geldhof, P., et al., *RNA interference in parasitic helminths: current situation, potential pitfalls and future prospects*. Parasitology, 2007. **134**(Pt 5): p. 609-19.
105. Mourao, M.M., et al., *Phenotypic screen of early-developing larvae of the blood fluke, schistosoma mansoni, using RNA interference*. PLoS Negl Trop Dis, 2009. **3**(8): p. e502.
106. Boyle, J.P., et al., *Using RNA interference to manipulate endogenous gene expression in Schistosoma mansoni sporocysts*. Mol Biochem Parasitol, 2003. **128**(2): p. 205-15.
107. Knight, M., et al., *Polyethyleneimine (PEI) Mediated siRNA Gene Silencing in the Schistosoma mansoni Snail Host, Biomphalaria glabrata*. PLoS Negl Trop Dis. **5**(7): p. e1212.

Publishing Agreement

It is the policy of the University to encourage the distribution of all theses, dissertations, and manuscripts. Copies of all UCSF theses, dissertations, and manuscripts will be routed to the library via the Graduate Division. The library will make all theses, dissertations, and manuscripts accessible to the public and will preserve these to the best of their abilities, in perpetuity.

Please sign the following statement:

I hereby grant permission to the Graduate Division of the University of California, San Francisco to release copies of my thesis, dissertation, or manuscript to the Campus Library to provide access and preservation, in whole or in part, in perpetuity.


Author Signature

09.01.11
Date